MAY 2018

Ph.D in Electrical and Electronics Engineering

RAGHAD GHALIB ALSULTAN

UNIVERSITY OF GAZİANTEP

GRADUATE SCHOOL OF

NATURAL & APPLIED SCIENCES

DESIGN OF MIMO MICROSTRIP ANTENNA SYSTEM

Ph. D. THESIS

IN

ELECTRICAL AND ELECTRONICS ENGINEERING

BY

RAGHAD GHALIB ALSULTAN

MAY 2018

Design of MIMO Microstrip Antenna System

Ph. D. Thesis

in

Electrical and Electronics Engineering

University of Gaziantep

Supervisor

Prof. Dr. Gölge ÖGÜCÜ YETKIN

by

Raghad Ghalib ALSULTAN

May 2018

REPUBLIC OF TURKEY
UNIVERSITY OF GAZİANTEP
GRADUATE SCHOOL OF NATURAL & APPLIED SCIENCES
ELECTRICAL AND ELECTRONICS ENGINEERING

Name of the thesis: Design of MIMO Microstrip Antenna System

Name of the student: Raghad Ghalib ALSULTAN

Exam date: 14-05-2018

Approval of the Graduate School of Natural and Applied Sciences

Prof. Dr. A. Necmeddin YAZICI
Director

I certify that this thesis satisfies all the requirements as a thesis for the degree of Doctor of Philosophy.

Prof. Dr. Ergun ERÇELEBİ
Head of Department

This is to certify that we have read this thesis and that in our consensus opinion it is fully adequate, in scope and quality, as a thesis for the degree of Doctor of Philosophy.

Prof. Dr. Gölge ÖGÜCÜ YETKIN
Supervisor

Examining Committee Members:	Signature
Prof. Dr. Savaş UÇKUN	.....
Prof. Dr. Uğur Cem HASAR	.....
Prof. Dr. Gölge ÖGÜCÜ YETKIN	.....
Assoc. Prof. Dr. Kemal DELIHACIOĞLU	.....
Assoc. Prof. Dr. Muharrem KARAASLAN	.....

I hereby declare that all information in this document has been obtained and presented in accordance with academic rules and ethical conduct. I also declare that, as required by these rules and conduct, I have fully cited and referenced all material and results that are not original to this work.

Raghad Ghalib ALSULTAN

ABSTRACT

DESIGN OF MIMO MICROSTRIP ANTENNA SYSTEM

ALSULTAN, Raghad Ghalib
Ph.D. in Electrical and Electronics Eng.
Supervisor: Prof. Dr. Gölge ÖGÜCÜ YETKIN
May 2018
87 page

This study presents five different configurations of microstrip antenna array with various innovative decoupling structures to reduce the mutual coupling between closely elements antenna system. The first design is comprised of two E-shaped antennas that are placed parallel and orthogonal to each other. The 2x3 matrix of C-Shaped Resonator (CSR) is proposed and placed between the antenna elements over the substrate, to reduce the mutual coupling and enhance the isolation between the antennas. The second design consists of a novel ladder-shaped conducting wall structure (LSCW) placed between two closely antennas. The proposed multiple-input multiple-output (MIMO) system is a dual band system operating at 4.45 GHz or 10.3 GHz frequencies depending on the dimensions of LSCW structure. The third design introduces defected ground structure (DGS) composed of spiral square slots etched from the extending ground plane. The fourth one is a dual-band systematic design of two planar MIMO monopole antennas predicated on the concept of metamaterials (MTMs). In this design, the MTM resonator is placed in the space between the antenna elements. The last one presents two-element microstrip array with three periodic T- Shaped DGS etched in the ground plane. The basic parameters of the MIMO array such as mutual coupling, surface current distribution, VSWR, ECC, DG, and the total efficiency have been simulated to verify the reliability and the validity of the MIMO systems. The results of simulation and measurements are presented, and the results are compatible with each other.

Key Words: MIMO antenna, Mutual coupling, defected ground structure (DGS), Diversity gain, Correlation coefficient, Metamaterials.

ÖZET

MIMO MIKROŞERIT ANTEN SISTEM DIZAYNI

ALSULTAN, Raghad Ghalib
Doktora Tezi, Elektrik-Elektronik Müh. Bölümü
Tez Yöneticisi: Prof. Dr. Gölge ÖGÜCÜ YETKIN
Mayıs 2018
87 sayfa

Bu çalışma, anten sistemlerinin yakın elemanları arasındaki karşılıklı kuplajı azaltmak için çeşitli yenilikçi dekuplaj yapılarına sahip mikroşerit anten dizisinin beş farklı konfigürasyonunu sunmaktadır. İlk tasarım, birbirine paralel ve ortogonal yerleştirilmiş iki E-şekilli antenden oluşur. Karşılıklı kuplajı azaltmak ve antenler arasındaki yalıtımı geliştirmek için 2x3 C-Şekilli Rezonatör (CSR) matrisi önerilmiştir ve alttaşın üzerindeki anten elemanları arasına yerleştirilmiştir. İkinci tasarım, birbirine yakın iki anten arasına yerleştirilmiş yeni bir merdiven şekilli iletken duvar yapısından (LCSW) oluşmaktadır. Önerilen çok-girişli çok-çıkışlı (MIMO) sistemi, LSCW yapısının boyutlarına bağlı olarak 4,45 GHz veya 10,3 GHz frekanslarında çalışan çift bartlı sistemdir. Üçüncü tasarım, yer düzleminden çıkarılar sarmal kare yarıklardan oluşan defekli yer yapısını (DGS) sunmaktadir. Dördüncüsü, metamalzemeler (MTMs) kavramı üzerine kurulu iki düzlemsel MIMO monopol antenin çift bantlı sistematik bir tasarımıdır. Bu tasarımıda MTM rezonatör anten elemanları arasındaki boşluğa yerleştirilmiştir. Son tasarım, yer düzleminden çıkarılar üç periyodik T-Şekilli DGS'yle iki-elemanlı mikroşerit diziyi sunmaktadır. MIMO sistemlerinin güvenilirliğini ve geçerliliğini doğrulamak için MIMO dizisinin karşılıklı eşleme, yüzey akım dağılımı, VSWR, ECC, DG ve toplam verim gibi temel parametreleri simüle edilmiştir. Simülasyon ve ölçüm sonuçları sunulmuş ve sonuçlar birbirleriyle uyumludur.

Anahtar Kelimeler: MIMO anteni, Karşılıklı kuplaj, hatalı zemin yapısı (DGS), Çeşitlilik kazancı, Korelasyon katsayısı, Metamaterials.

To my parents and to my beloved husband, for their love and support

ACKNOWLEDGEMENTS

Thanks to ALLAH, for giving me the strength and capability in achieving my study and helping me out at difficult times.

First of all, I extend my thanks and gratitude to my beloved country, Iraq, for their confidence and trust in my abilities to allow me to study in one of the finest educational institutions.

I also would like to express my sincere gratitude to my advisor Prof. Dr. Gölge Ögücü Yetkin for her continuous support to my Ph.D. study and related research, for her patience, motivation, and immense knowledge. Her guidance helped me a lot in all the time of research and writing of this thesis. I could not imagine having a better advisor and mentor than her.

My deepest gratitude towards Dr. Muharrem Karaaslan and his team for kindly helping in the fabrication of the antennas and doing the experiments in the laboratories of İskenderun Technical University, Turkey.

Special thanks to the Scientific and Technological Research Council of Turkey (TÜBİTAK) for their support under project no. 114E495 for CST simulation in this dissertation.

I would like to express my deepest sense of gratitude to my great husband who offered his continuous advice and encouragement throughout my study. I thank him for his absolute support to present my dissertation and encouragement whenever I was in need.

A special thanks to my parents wherever words cannot express how grateful I am to them for all their sacrifices that they made on my behalf; their prayers for me were what sustained me thus far. I hope that I have achieved their bequest to get Ph.D. and I dedicate this dissertation to them.

I would like to thank my family; my brothers and sister for supporting me spiritually throughout writing this thesis and my life in general.

TABLE OF CONTENTS

Page

LIST OF TABLES

Page

LIST OF FIGURES

Page

LIST OF ABREVIATIONS

AAS	Adaptive Antenna System
BW	Bandwidth
CDF	Cumulative distribution function
CSR	C-Shaped Resonator
CSRR	Complementary split ring resonator
DE	Differential evolution
DG	Diversity Gain
DGS	Defected ground structure
DNG	Double-negative
DPS	Double-positive
EBG	Electromagnetic band gap
EM	Electromagnetic
ENG	Epsilon-negative
FDGS	Fractal defected ground structure
FDTD	Finite-Difference Time-Domain
FIT	Finite integration technique
GP	Ground plane
GPS	Global positioning system
LH	Left-handed
LHM	Left-handed material
LoS	Line of Sight
MEG	Mean Effective Gain
MIMO	Multiple Input Multiple Output

MPA	Microstrip patch antenna
MSA	Microstrip antenna
MTM	Metamaterial
NRI	Negative refractive index
PDGS	Periodic defected ground structure
QoS	Quality of Service
RH	Right-handed
SD	Spatial Diversity
SISO	Single Input Single Output
SM	Spatial Multiplexing
SNR	Signal to noise ratio
SRR	Split ring resonator
SW	Surface waves

LIST OF SYMBOLS

ρ_c	Correlation coefficient
ρ_e	Envelop Correlation coefficient
d	Distance between antennas
f	Frequency
f_c	Center frequency
f_r	Resonant frequency
n	Refractive index
P_H	Horizontal polarization
P_V	Vertical polarization
h	Thikness of the substrate
XPR	Cross-polarization power
ε_r	Relative permittivity
λ_o	Free space wavelength
μ_r	Relative permeability

CHAPTER 1

INTRODUCTION

This chapter consists of a concise introduction. The literature review is one of the leading approaches to understanding the development of the microstrip MIMO antenna. The related literature reviews are accomplished by reference books and published papers covering the survey of literature starting from single microstrip antenna to the development of microstrip MIMO antenna systems. This chapter also highlights the objectives, problem statement, the arrangement of the thesis and the scope of research.

1.1 Literature Review

The antenna is one of the essential elements in the Radio Frequency (RF) system for transmitting and receiving signals from as well as through the air as a transport medium [1]. Also, without an appropriate and efficient design of the antenna, there will be no signal propagation because the signal produced by the RF system will not be transmitted, and no signal can be identified on the receiver part.

Antenna design is a dynamic and creative field in the communication systems for future evolution. A lot of the sorts of the antenna were made to apt by multiple communication applications. One of the most important types is the microstrip antenna (MSA). The basic concept of antenna of microstrip geometries was initially examined in the 1950's [1]. It was developed in 1953 by Déschamps, the incipient known realization of a microstrip line antenna that integrated with the microstrip transmission line, but it acquired the considerable importance only in 1970 [2, 3].

MSAs occupies a large area of research and became amongst the most imaginative and inventive topics in antenna theory and design. The essential thought of microstrip antenna originated from using integrated circuit technique not just for the circuit components and transmission lines, but even for the radiating elements of an electronic communication system.

In general, the simplest configuration of MSA formed from a rectangular patch (or other shapes such as triangular, circular) mounted on the top side of a substrate which is upheld by a ground plane. Microstrip patch antenna due to its simplicity, conformal nature and ability to combine with the rest of the printed circuit plays an essential role in modern communications systems. Despite these features, the MSA suffering from some disadvantages such as narrow bandwidth, poor polarization, excitation of surface waves and space waves, spurious feed radiation, limited power capacity, and tolerance difficulty [4, 5, 6]. Over the years, many of research and investigations have been made to defeat the defects that associated with these types of antennas. In that respect, different techniques are used to support the bandwidth, one trend to rise the bandwidth that has been done by either decreasing the dielectric constant or increasing the height of the dielectric. Increasing the height of the substrate is inappropriate for low profile structures. In addition, to decrease the dielectric constant causes fringing fields [7, 8, 9]. The second serious factor which decreases the performance of MSA is the gain that describes the directional property of antennas. To accomplish improved performance over that of a single antenna, a large number of individual antenna elements has been used. By forming a set of radioactive elements in an electrical and geometrical arrangement, new antenna design has been presented, created by multi-elements, is known as an antenna array [10, 11], where multiple transmit and multiple receive antennas are required.

Arrays of antennas are used to direct radiated power towards the desired direction. The radiation of all the antenna elements sums up, to form the radiation beam, which leads to increase the overall gain, high directivity, and better performance, with minimum power wastage.

Multiple Input Multiple Output (MIMO) array technology became a revolution in modern communication systems. Recently, the designers of microstrip antenna have employed MIMO technology, where at least two or more radiating patches were utilized in the design for transmission and reception. In communication systems, MIMO arrays improve the effectiveness of the antenna such as increasing the gain, provide diversity reception and other features which are hard to get with a single component [12, 13]. As MIMO systems employed multiple antenna elements, they demand a high level of decoupling between antenna elements. Therefor, the whole performance of antenna array tends to deteriorate due to the strong mutual coupling interaction among the array elements which also influences on antenna

efficiency. Because of that, in the design of MSA arrays, the mutual coupling or the separation between the radiating elements is a significant problem to must be addressed [14, 15]. Various antenna designs and different decoupling techniques have been introduced to reduce the mutual coupling influence in MIMO systems. Choosing the proper design and configurations of antenna, considering one of the simplest decoupling technologies that can be used to improve isolation [16, 17]. In [18] parasitic elements, adding a double-coupling path is presented, it can generate an opposite coupling path to suppress the mutual coupling. Techniques to modify ground structure are presented in [19, 20].

In the recent years, metamaterials (MTMs) as artificial structures exhibit electromagnetic characteristics that are unusual or hard to get in nature; works as isolation walls between the array elements. This property has been exploited to minify the mutual coupling between the elements in MIMO arrays. Various sorts of MTMs like Electromagnetic Band Gab (EBG) substrate, Defected Ground Structure (DGS), Split Ring Resonator (SRR), Complementary Split Ring Resonator (CSRR), etc. have been used to suppress the mutual coupling of a closely spaced antenna [21-34].

From the perspective of EBG material, mushroom like EBG structure is realized by a parallel LC resonator. It comprises of the connecting vias and metallic patches. Together, they are acting as inductors, and the gap between these patches behaves like a capacitor. Its band gap features are represented in two ways, one by suppression of surface wave propagation and other by the in-phase reflection coefficient [21, 22]. In [23] the structure of miniaturized two-layer EBG is given to mitigating the electromagnetic coupling between closely spaced planar monopoles. Both of the arrays are printed on both sides of a substrate layer that is fragile with a rotation between the elements to give the maximum coupling due to miniaturize. The structure of the proposed EBG contains a footprint that is small in addition to provide a satisfactory reduction of the mutual coupling through the operating frequency band. In [24], the dual-band MIMO antenna using double-size EBG is proposed. The EBG structure which uses H shape on the patch and H shape with the bridge on the ground plane one makes the size of EBG cell much more compact. Using this structure leads to decreases the mutual coupling between the antenna elements of 20 dB and improves the antenna gain. Especially at the lower band. In [25] spiral shape for EBG is presented for 2 × 2 element microstrip patch array antenna with slot feed. Suppression of surface waves using EBG has improved the gain about 1.2 dB.

Plenty of investigations have been presented to estimate the performance of arrays when specific shapes were etched from the ground plane. Thus, it was noticed that defects increase the effective capacitance and inductance of the microstrip transmission line. Due to the defects, the current distribution is changed as well. The characteristics of the transmission line will change. This technique is called DGS. The substrate with DGS is recognized as MTM substrate when the both relative permittivity ε_r and permeability μ_r are negative. These properties have been exploited to enhance the isolation as well as to reduce mutual coupling [26, 27]. In [28] S-shaped periodic PDGS is proposed. The elements of the coplanar placed antenna operate at the same frequency band in addition to center frequency 2.57 GHz. The PDGS comprised of three S-shaped of DGS placed between the MSA elements. When the proposed PDGS structure has been employed, more than 40 dB mutual coupling reduction between the MSA elements is achieved. In [29] a compressed patch antenna array with dual resonant frequencies is presented. The mutual coupling can be decreased at two resonant frequencies by embedding a simple C-shaped resonator in the middle of the two radiating patches at the same time etching an inverted C-shaped slot DGS on the ground plane. The measurement results display that the isolation between the antenna ports has been enhanced about 10 dB and 18 dB at the two operating frequencies with the presence of the proposed DGS and resonator structure. In [30] presented a fractal (FDGS) between coplanar spaced MSA elements. The bandgap property of second and third iterative FDGS is obtained and used to suppress the mutual coupling between antenna elements. More than 35 dB mutual coupling reduction is achieved when using the third repeated of FDGS.

Various geometrical configurations in the class of MTM can be given. The reason to enhance magnetic properties as well as the coupling will be reduced by suppressing the ground current that flowed between the radiating elements. The SRR, the modified SRR, and CSRR are the configurations, are the few popular configurations between them.

SRR is widely used; it has a permeability that is negative within a frequency band that considered very near in terms of the frequency band of the single SRR. It is used in a wide manner to create left handed MTM. It can be manufactured when we use the technology of the printed circuit [31, 32]. In [33] CSRR is used to suppress surface waves (SW) between the elements of a MSA array. The technique of the given decoupling is investigated by putting the meta structure between antennas on the top

of the patch layer besides to etch it in the ground plane. It enhances the isolation about 14.6 dB, at the time of the meta structure is presented on both sides (top and bottom) of the antenna array. In [34] the 2 × 3 matrix of the C-shaped resonator (CSR) is proposed and placed between the antenna elements over the substrate, to suppress the mutual coupling and improve the isolation between the antennas.

In this thesis, different configurations of two-elements MIMO antenna system with varying decoupling structures and mechanisms to enhance the isolation and to decrease the mutual coupling between antenna elements have been designed, five major MIMO antenna designs have been presented and analyzed separately for their isolation, correlation and diversity performance. Fabrication of the prototypes was made to test the validity of the simulation outcomes.

1.2 Problem Statement

Future communication systems have to fulfill the requirements of high data rates and flexible interfaces for different communication system standards. The employment of multiple antennas at both the transmitter side as well as the receiver side are to form a MIMO antenna. It is an emerging technology that was prepared in building the networks of high data rate wireless a reality.

The priority was given to microstrip antenna arrays according to its attractive features like the low profile, lightweight, and low production cost. Simultaneously, a critical phenomenon in microstrip antennas leads to reduced radiation efficiency because of excitation of surface waves across the substrate layer. Surface waves have a substantial effect on the mutual coupling between the array elements. This effect can be considered from the possible sources that cause performance decline of an array which involves increased side-lobe level, the impedance mismatching, decreased gain, the deviation of the radiation from the desired one due to the excitation of the surface wave. In MIMO arrays, when the receiving antenna as well as transmitting antenna are put in a tight manner side by side, the transmitting energy may even block the receiver. Because of that, the mutual coupling of MIMO antenna is a critical feature that should be taken into consideration in the design process, as it can lead to a significant regression in the general performance.

1.3 Aim of Dissertation

Microstrip antenna array plays an essential role in modern communication system technology. Design and implementation MIMO antenna array with high-performance that satisfies the demands of modern communication and provides good diversity performance is the main goal of our research. The mutual coupling is a significant problem that declines the performance of the microstrip MIMO systems and limits their various applications in modern high data rate wireless systems. The mutual coupling arises due to the small distance between the antenna elements. This investigation addresses the following inquiries: (a) what is the best MIMO antenna array configuration to achieve the optimal performance? And (b) what is the best extra proper design placed between the two MIMO elements to mitigate the mutual coupling impact and enhance the isolation to accomplish the goal of the thesis.

The objectives of this dissertation are:

I. Design and simulate different configurations of the microstrip printed MIMO antenna array,
II. Investigate several kinds of innovative decoupling structures. Without appropriate approach, the design of such structures is based on the trial-and-error concept,
III. Study the effect of decoupling structures such as mutual coupling, isolation, current distribution when placed in the space between the array elements on the performance of the MIMO antenna,
IV. Fabricate the models to verifying the simulation results, then compare the performance of the modified and traditional antennas.

1.4 Scope of This Dissertation

The dissertation is divided into several stages as follows:

- Understanding the basic theory of microstrip antenna array MSAs, including the characteristics of the MSAs and explain the fundamental parameters that affecting on it,
- Many geometries of two element microstrip printed antenna arrays without and with different decoupling structures between the antenna elements have been examined by reducing the coupling that is mutual and improving the isolation,

- The antennas with and without decoupling structures have been fabricated to support the simulation results and examined by using Vector Network Analyzer.

1.5 Organization of Dissertation

The outline of this thesis is organized into five chapters.

- **The first chapter** is an introduction that provides a brief literature survey for MIMO antennas, the scope of the project, objective and layout of the thesis.
- **The second chapter** demonstrates the evolution of the MIMO array, beginning from the conventional microstrip antenna, by discussing the features, advantages, and limitations of this antenna. Then it highlights the MIMO antenna with mentioning the parameters required to characterize its performance. Also, it presents a concise of the fundamental parameters should be taken into consideration when designing the MIMO antenna because through of it the antenna performance is evaluated.
- **The third chapter** discusses the concept of the mutual coupling and its effect on a MIMO antenna array's performance. From the perspective of MTM, it includes the illustration of the different types of MTMs structures such as EBG, DGS, that are proposed to suppress the mutual coupling in the middle of closely spaced antenna elements in the array.
- **The fourth chapter** describes the antenna design methodology that is used for implementing this study. It presents different types of microstrip MIMO antenna array with five types of innovative decoupling structures that are inserted in the space between the two antenna elements to suppress the mutual coupling and enhancement the isolation. Finally, to certify the validity of designs, all models have been fabricated, then the outcomes have been analyzed and compared.
- **The fifth chapter** provides a conclusion to this research work. Also, recommendations for possible future work of this research.

CHAPTER 2

MIMO MICROSTRIP ANTENNA SYSTEMS

This research focuses on the microstrip antenna array. To understand this type of antenna, it is necessary to start off by illustrating the architecture of microstrip antenna as well as its characteristics and features. Digital communication systems that are employed the MIMO system has begun as a quantum leap in the modern communications world.

In this chapter, the parameters are required by characterizing the performance of MIMO antennas are also highlighted a brief explanation of the most important parameters that should be considered while designing MIMO antennas, is presented.

2.1 Microstrip Antenna

Microstrip patch antenna (MPA) generally comprised of four main parts (radiating patch, substrate layer, ground plane layer, and the feeding part). The radiating patch is a very thinning metallic layer ($t << \lambda_o$, where λ_o is the free space wavelength), with length L and width W printed on one side of a substrate with relative permittivity ($\varepsilon_r < 10$), of thickness h, which has a ground plane (same metal of the patch) located on the reverse side of the substrate, as explained in Figure 2.1.

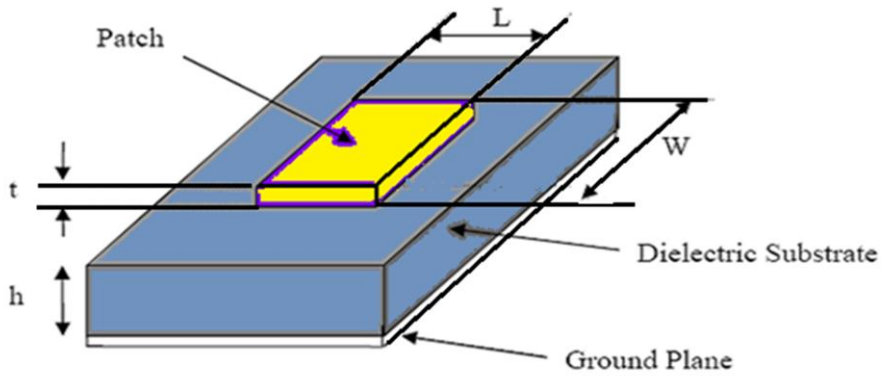

Figure 2.1 Microstrip patch antenna

The patch conductors are usually made of copper, gold, tin, or nickel, and they can assume virtually any shape for instance circle, rectangular, square, triangle, but regular shapes is usually utilized for simplifying the analysis and performance foretelling. Figure 2.2 shows different shapes and sizes of the patch. Ideally, the ε_r of the substrate should be low ($\varepsilon_r < 2.5$), to improve the fringing fields that cause the radiation. It is also can be used with high dielectric constant material to load the patch and reduce its size, but the high value of the dielectric constant substrate may or may not be available to fabricate.

In general, according to dielectric constant ε_r, the substrate materials can be classified into three types [6]:

1. Materials with a ε_r in the range of (1.0-2.0). This kind of material can be air, polystyrene foam, or dielectric honeycomb,
2. Materials with ε_r in the range of (2.0-4.0) such as fiberglass reinforced, teflon,
3. Materials with ε_r in the range of (4-10), like ceramic, quartz, or alumina.

In antenna design, it is essential to choose an appropriate substrate. There are factors taken into consideration such as temperature, humidity and other environmental ranges of operation. The thickness of the substrate layer *h* has a significant impact on the resonant frequency f_r and bandwidth *BW* of the antenna. The *BW* of the MPA will increase with increasing substrate thickness h, but as the substrate thickness increases, surface waves increase too, which normally are not a desirable phenomenon [35, 36].

From other hand, the antenna is radiating mainly from one side of the substrate because of that it is easy to feed it from the other side (the ground plane), or from the bottom of the element. Generally, the antenna feeding mechanism can be divided into two collections; contacting and non-contacting. The four most common feed mechanisms that used in patch antenna are the microstrip line, coaxial probe (both contacting schemes), aperture coupling and proximity coupling (both non-contacting). For maximum transfer of power (matching of the feed line with the input impedance of the antenna), feeding is considered as the most important factor to be observed. Many good designs have been neglected due to their poor feeding. The antenna design can be valid with functional characteristics and good radiation parameter, but when feeding is inadequate, the total performance could be reduced to a low level; as a result, the whole system to be rejected.

Microstrip line and coaxial probe feed techniques to feed the MIMO array systems has been selected for this research due to their beneficial features as below:

- Simple to design and easy to fabricate.
- Allow planar feeding,
- Easy to obtain input match,
- The feed can be etched on the same substrate to give a planar structure without the need for any extra matching element.

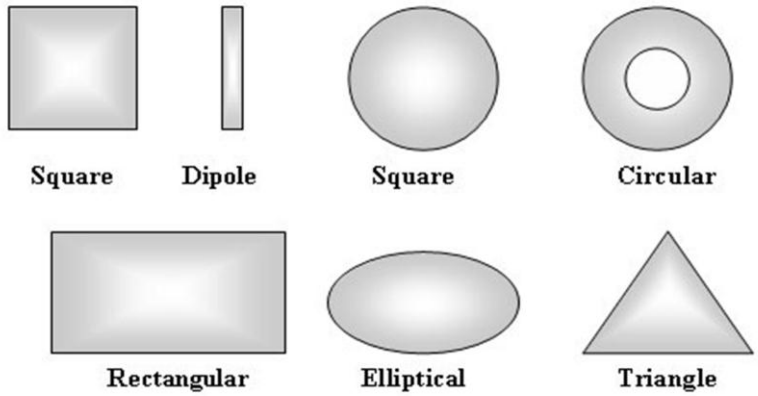

Figure 2.2 Different shapes and sizes of patch[2]

2.2 Advantage, Disadvantage, and Application

MPAs possessed numerous benefits when it compared to other microwave antennas, and as a result, a lot of applications can cover the broad frequency range between 100 MHz to 100 GHz. A portion of the essential benefits of MSAs that compared with customary microwave antennas are [1-5]:

- Low size and light weight,
- Profile planar configuration is low which efficiently can be compatible with host surface,
- It can be produced in substantial quantities. As a result, it has low fabrication cost,
- Both circular, as well as linear polarizations, are easy to get with simple feed,
- The antennas of dual polarization and dual frequency can be done in an easy manner,
- Can be integrated with microwave integrated circuits,
- It is mechanically and is stable when mounted on a surface can be rigid.

MPAs are suffering from drawbacks comparison with conventional antennas. Some of their significant disadvantages are given below [1-5]:

- Narrow bandwidth,
- Surface wave excitation,
- Low efficiency,
- Low gain,
- Superfluous radiation from feeds and junctions.

Applications

MPAs occupies a large area in applications of communication systems because of its advantages that distinguish it from other kinds of antennas. Some of these applications are [1-5]:

- Telemetry and missiles,
- Mobile radio (pagers, telephones, manpack systems),
- Direct broadcast services and satellite communication,
- Doppler and radars,
- Intruder alarms and biomedical radiators.

2.3 Method of Analysis

There are many methods of microstrip antenna analysis; the most popular are transmission line (in which we assume that the patch is a transmission line or a part of a transmission line). The second method is the cavity mode (here we assume that the patch is a dielectric loaded cavity). The transmission line method is the easiest way of studying the microstrip patch antennas.

2.3.1 Transmission Line Model

The transmission line method is the easiest way to study the microstrip antenna. In this method the transmission line model represents the microstrip patch antenna by two slots, separated by a low-impedance transmission line of length (L). The results we get are not the best accurate compared with other methods, but it is good enough to design the antenna. To analyze the theory of a microstrip transmission line we have two different cases:

- **W/h < 1** (narrow strip line) and this is not what we are interested in.
- **W/h >>1** and ε_r >1 (wider transmission line) this will help us to build a good idea to study the antenna, as shown in Figure 2.3.

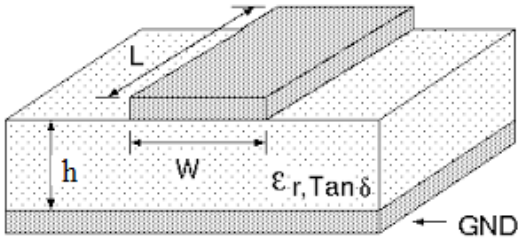

Figure 2.3 Microstrip line

The first approximation we make is to assume that the thickness of the conductor (t) that forms the line has no effect on our calculations, because it is very thin comparing with the substrate h, (h >> t), hence, the microstrip line dimensions: the width W, the length L, the height h, and the dielectric constant ε_r of the substrate.

The characteristic impedance of the microstrip line can be written as [1-5]:

$$Z_o = \frac{120\,\pi}{\sqrt{\varepsilon_{reff}}\left(1.393+\frac{W}{h}+\frac{2}{3}\ln\left(\frac{W}{h}+1.444\right)\right)} \tag{2.1}$$

The width of the microstrip line is given by:

$$W = \frac{1}{2f_r\sqrt{\mu_o\varepsilon_o}}\sqrt{\frac{2}{\varepsilon_r+2}} = \frac{v_o}{2f_r}\sqrt{\frac{2}{\varepsilon_r+1}} \tag{2.2}$$

where v_o is speed if light in free space.

The microstrip patch antenna in Figure 2.4 (a) and (b) looks longer than its physical dimensions because of the effect of fringing. The effective length, therefore, is differing from the physical length by ΔL_{eff}.

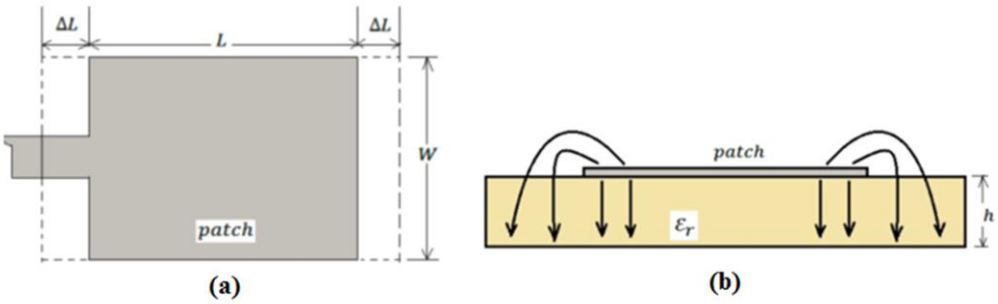

Figure 2.4 a) physical and effective length of a microstrip patch
b) Electric field lines

A very popular approximation to calculate the extension of the length of the patch is given as:

$$\frac{\Delta L_{eff}}{h} = 0412\frac{(\varepsilon_{reff}+0.3)(\frac{W}{h}+0.264)}{(\varepsilon_{reff}-0.58)(\frac{W}{h}+0.8)} \quad (2.3)$$

From equation (2.4) we can see that the extension of the length ΔL is a function of the ratio $\frac{w}{h}$ and ε_{reff}.

To calculate the effective length (L_{eff}), we add the length L to the extension of the length ΔL_{eff} as shown:

$$L_{eff} = (L + 2\Delta L_{eff}) \quad (2.4)$$

To estimate the effective dielectric constant let us consider the radiating patch is embedded into the dielectric as shown in the Figure 2.5.

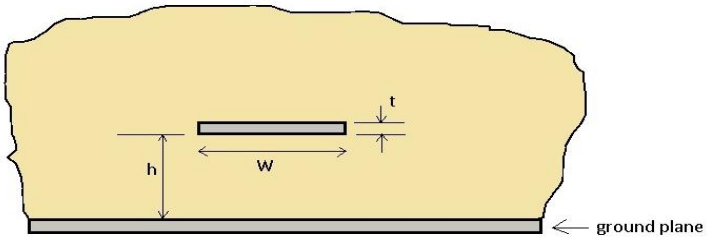

Figure 2.5 Microstrip line embedded into the dielectric

For patch antennas, air is above the substrate, this will lead to $1 < \varepsilon_{reff} < \varepsilon_r$

For $\varepsilon_{reff} >> 1$, ε_{reff} is closer to the actual value of the dielectric constant ε_r of the substrate.

The affective dielectric constant is also a function of frequency f_r as shown:

$$f_r = \frac{v_o}{2\sqrt{\varepsilon_{reff}(L+2\Delta L_{eff})}} \quad (2.5)$$

The effective dielectric constant ε_{reff} can be calculated from the formula:

$$\varepsilon_{reff} = \frac{\varepsilon_r+1}{2} + \frac{\varepsilon_r-1}{2\sqrt{1+\frac{12h}{W}}} \quad (2.6)$$

2.4 Multiple-Antenna Techniques

Wireless communication systems were used for voice and small data transfers and most of the high-data rate transfer devices employed wired communications. In view of the tremendous revolution in the world of communications, such as cell phones having an integrated camera, emailing capability, a Global Positioning System (GPS), there are more requests for wireless high-speed data transfers, which traditional antennas do not have the capacity of dealing with it due to Co-channel multipath interference [37]. As well as to the requirements for high-speed data transfers, there is also need for quality control, which involves high capacity and low error rate. In order to maintain specific Quality of Service (QoS), the multipath fading effect has to be dealt with. As the signal that can be transmitted, is reflected onto the different targets on its way to the receiver side, the signal may be suffering from distortion and fading. We can call this phenomenon "multipath fading". The interference that is Co-channel alludes to the interference produced by many various signals that utilizing the similar frequency. Therefore, multiple antennas are employed to decrease the error rate as well as to improve the quality and capacity of wireless transmission. By adjusting the radiation according to the traffic condition, directing just the radiation to the signal environment and the intended direction. Generally, most of the multiple antennas are formed of a number of antennas; either at the receiver or the transmitter. A coding technology, as well as developed signal processor are the primary factors in multiple antennas. The techniques of multiple antenna, can be divided into three classes: Spatial Multiplexing (SM), Spatial Diversity (SD), and Adaptive Antenna System (AAS).

2.4.1 Spatial Diversity

It can be defined as a portion of antenna diversity technology in which many antennas are employed to enhance the quality and signal integrity of a wireless link. Generally, in the areas, that are densely populated, the transmission systems utilize various spatial diverse receiving antennas vertically separated on a tower. Because the signals that are transmitted will not suffer from the same level of attenuation as it disperses slowly and propagates along slightly diverse paths. There is no clear Line of Sight (LoS) between the receiver antenna the transmitter. Consequently, the multipath fading impact appears on the transmission path. In spatial diversity, the sum of receiving and transmitting antennas are placed in a space close to each other. Hence, if one antenna a fade, another one will have a LoS or an integrity signal. The basic concept of it is depicted in Figure 2.6.

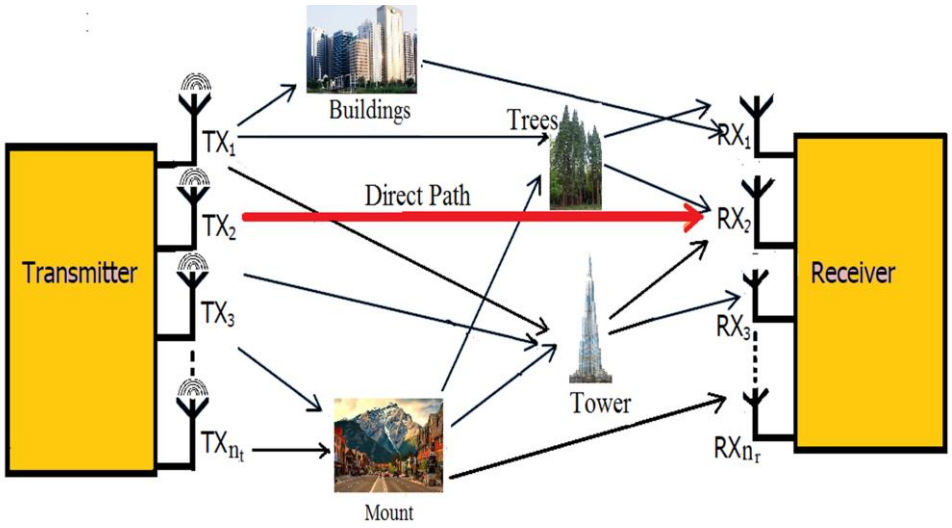

Figure 2.6 Spatial Diversity

2.4.2 Spatial Multiplexing

Spatial multiplexing used to give extra data bandwidth in multipath systems. The basic concept of multiplexing is the divide (multiplex) transmit the data stream to several branches and transmit via several (independent) channels. In other words, the systems of multiple antenna, through different antennas, can establish parallel data streams to enhance the data transfer rate [37].

The bit influx which is to be transmitted is distributed or demultiplexed into the variety of data segments. These divided segments transmitted across different antennas at the same time. The bit rate increases in a rapid manner without the need for further transmission or bandwidth power. The signal that arrived at the receiving antenna is a mixture of all individual data segments are separated at the receiver side by using an interference decoding technique.

2.4.3 Adaptive Antenna System

AAS is formed of multiple antenna elements at the receiving or transmitting side of the communication system, whose signals are, in an adaptive manner, processed due to the advantages of the spatial dimension of the channel of mobile radio. The system of AAS can focus on its transmit power towards a receiver, and it can focus on its power towards the transmitter whereas receiving. Accordingly, the adaptive antenna system can improve the link quality by employing multiple data streams from the various antennas and combines the impacts of multipath propagation.

2.5 MIMO Technique

The MIMO technology exploits multipath to afford a high increase in channel capacity without the requirement for extra bandwidth or transmit the power by using multiple antennas to obtain an improvement in array gain and improve the diversity performance as well. Consequently, enhancing the spectral efficiency and reliability.

A MIMO system with N number of transmitting and receiving antennas is shown in Figure 2.6. The essential thought of this method is to send various data information streams utilizing multiple antennas at the same carrier frequency without extra power. When the data information stream is transmitted through the antenna; it is received at the qth antenna subsequent to going in various paths as appeared in Figure 2.6. This technique for propagation is known as multipath propagation, which happens due to the reflections of the signal of various targets in the channel.

Consider the system in Figure 2.7, the signal that arrived at the receiver can be expressed as follows [38]:

$$x_q(t) = \sum_{p=1}^{N_t} h_{qp}(t) s_p(t) \qquad (2.7)$$

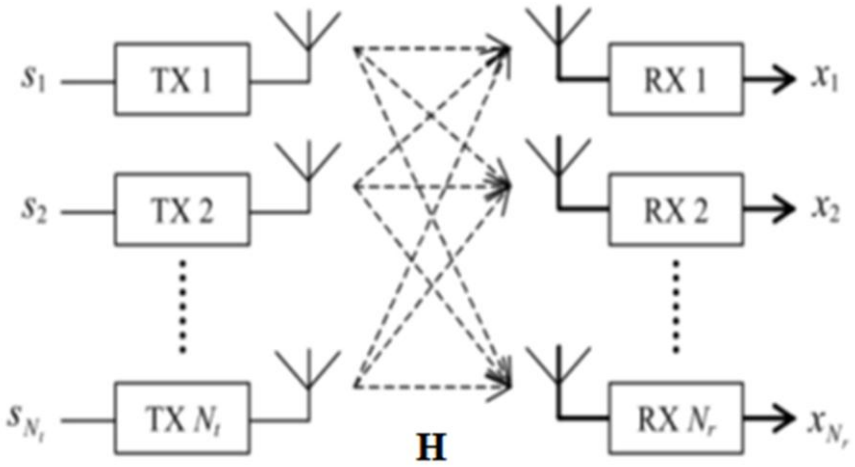

Figure 2.7 A schematic representation of a primary MIMO antenna

where x_q(t) denotes the received data on the qth receiver, s_p(t) expresses the transmitted data on pth transmitter. h_{qp}(t) expresses on the path gain between pth transmitter and qth receiver. In this context, using the matrix approach, the same parameters can be represented as shown below:

$$s(t) = \begin{pmatrix} s_1(t) \\ s_2(t) \\ . \\ . \\ . \\ s_{N_t}(t) \end{pmatrix}, X(t) = \begin{pmatrix} x_1(t) \\ x_2(t) \\ . \\ . \\ . \\ x_{N_r}(t) \end{pmatrix} \quad H(t) = \begin{pmatrix} h_{11}(t) h_{12}(t) & \dots & h_{1N_i}(t) \\ h_{21}(t) h_{22}(t) & \dots & h_{2N_i}(t) \\ . & . & . \\ . & . & . \\ . & . & . \\ h_{N_i1}(t) h_{N_i2}(t) & \dots & h_{N_rN_i}(t) \end{pmatrix} \quad (2.8)$$

The *s(t)* and *x(t)* matrices show transmitted and received data streams, respectively, while, the *H(t)* matrix represents the channel coefficient, as well as the elements of this matrix, describe the path gains from the respective transmitting antenna to the receiving antenna. The *H(t)* matrix includes the mathematical model of the physical transmission path of the transmitted signal that involves both the multipath channel properties of the physical medium and the antenna design. Thus, the communication system performance in a MIMO system will be specified by the multipath channel characteristics and the configuration of the antenna array.

2.6 MIMO Antennas Figure of Merit

There are fundamental parameters must be taken into account when designing the MIMO antennas:

2.6.1 Mutual Coupling and Isolation - For MIMO applications, the signals transmitted by multiple antenna elements are for the most part expected to be uncorrelated or independent. However, in physical existence, the current incited on a single antenna element creates the voltage in the nearby element terminals and is called mutual coupling [1]. It implies there is mutual coupling existing between proximal antenna elements continuously. The results of mutual coupling involve distortions in the radiation pattern and variations in the element gains. For applications of MIMO, the mutual coupling must be kept as minimum as possible. Considering the importance of this phenomenon, we will discuss it in more detail in the next chapter.

They explained the port-to-port isolation as the transmission of signal power between two of the input ports of the multiport antenna under test. It is described by $|S_{21}|$ parameter. The isolation between antenna elements could be defined as [13]:

$$\text{Isolation} = -10 \, \text{Log}_{10} |S_{21}|^2 \quad (2.9)$$

To operate MIMO systems efficiently, the $|S_{21}|$ should be minimized in low values as possible. Moreover, to get maximum signal power radiated by an antenna element, it must be confident that a negligible quantity of transmitting signal power affects the ports of other antenna elements terminated by the matched impedances. Several

studies have been carried out in this direction, where it explains the mutual coupling and its effect on improving the isolation. It should be noted that in most of the literature the term of mutual coupling has been correlated with the term isolation and the two terms became synonymous with each other. In other words, the mutual coupling is characterized by the isolation in most of the times. On the other hand, the isolation is not the accurate portrayal of mutual coupling, as it is possible that the isolation is splendid, but it is not necessary for mutual coupling to be low in this case [14,39,40]. Thus, to investigate the mutual coupling phenomenon; one should not depend only on the isolation, but it is better to take into consideration the surface current distributions on the non-excited radiating element, when the nearby radiating element, is excited.

2.6.2 Mean Effective Gain (MEG) – the effectiveness of MIMO systems can be distinguished by MEG of the multiple antennas. The MEG is an analytical means to estimate of the antenna gain, which are explained as the total mean incident power and the ratio of the mean received power of the antenna. Mathematically, it can be expressed as follows [13,41]:

$$\text{MEG} = \int_0^{2\pi}\int_0^{\pi}\left(\frac{XPR}{1+XPR}G_\theta(\theta,\varphi)P_\theta(\theta,\varphi) + \frac{1}{1+XPR}G_\varphi(\theta,\varphi)P_\emptyset(\theta,\varphi)\right)\sin\theta d\theta d\varphi \qquad (2.10)$$

where P_θ and P_φ are the angular diversity functions of the incident power with respect to θ and φ directions sequentially, G_θ and $G\varphi$ are the gains with respect to θ and φ directions respectively, and XPR denotes to the cross-polarization power which is defined as the ratio of the mean received power in the vertical polarization (P_V) to the mean received power in the horizontal polarization (P_H), mathematically, can be expressed as:

$$XPR = \frac{P_V}{P_H} \qquad (2.11)$$

The XPR varies extremely, relying on the surrounding environment, where there is no direct LoS between the transmitter and receiver, measurements denote that the XPR is almost 0 dB. The amount of XPR is equal 1, when the antenna exists in an absolutely random channel environment [42, 43].

In order to obtain the gain that has high diversity, the MEG ratio between both of the antennas that has to be to the unity or close to it, so as to be the average received power by each antenna is almost equal [44].

2.6.3 Correlation Coefficient – it is a very significant factor for the systems that supplying diversity. The correlation coefficient can be considered statistically as well as mathematical means that can measure the level of identity among the received signals. Its range changes from zero to one. Theoretically, For high diversity systems, need a very low correlation coefficient (zero by default). We have to keep in mind that this parameter is classified according to three types: complex, envelope, and power correlation coefficients. The first one, the complex correlation coefficient, shows the measure of correlation, that is complex, between the received signals at the antennas. It can be written as [42] .

$$\rho_c = \frac{\int_0^{2\pi}\int_0^{\pi}(XPRE_{\theta k}E_{\theta l}(\theta,\varphi)P_{\theta}(\theta,\varphi)+ E_{\emptyset k}(\theta,\varphi)E_{\emptyset l}(\theta,\varphi)P\varphi(\theta,\varphi))\sin\theta d\theta d\emptyset}{\sqrt{\sigma_k^2\sigma_l^2}} \quad (2.12)$$

Where σ_k^2 and σ_l^2 express on the variances of kth and lth branches and can be given as:

$$\rho_c = \int_0^{2\pi}\int_0^{\pi}(XPRG_{\theta k}(\theta,\varphi)P_{\theta}(\theta,\varphi) + G_{\emptyset k}(\theta,\varphi)P_{\emptyset}(\theta,\varphi))d\theta d\emptyset \quad (2.13)$$

Then:

$$G_{\theta k}(\theta,\varphi) = E_{\theta k}(\theta,\varphi)E_{\theta l}(\theta,\varphi) \quad (2.14)$$

$$G_{\emptyset k}(\theta,\varphi) = E_{\varphi k}(\theta,\varphi)E_{\varphi l}(\theta,\varphi) \quad (2.15)$$

where $E_{\theta k}$ and $E_{\theta k}$ can be complex electric fields in the directions θ and φ respectively, for the kth antenna. Similarly, the mathematical analysis is valid for the lth antenna.

The second type of correlation is the envelope correlation coefficient (ECC). Usually, expressed for the evaluation the diverse behavior of MIMO systems. This factor a real number and by definition provides the correlation among the amplitudes of the signals at antennas. The ECC can be given as mentioned below:

$$\rho_e = |\rho_c|^2 \quad (2.16)$$

In fact, it is best to calculate the correlation of the 3D radiation scheme but its somewhat complex way. Nevertheless, On the assumption that the diversity system ought to operate in a uniform multipath condition, the ECC can be determined from S-parameters using the following formula [20]:

$$\rho_e = \left|\frac{S_{11}^*S_{12}+S_{21}^*S_{22}}{\sqrt{1-|S_{11}|^2-|S_{21}|^2}.\sqrt{1-|S_{22}|^2-|S_{12}|^2}}\right|^2 \quad (2.17)$$

It provides a simple approach compared with the radiation pattern, yet it ought to be underlined that this formula is absolutely correct when it meets the next accompanying assumptions [4, 5]:

- The antenna system efficiency should be high, and the mutual losses must be low as possible,
- Load termination of the non-measured (not excited) antenna is 50 Ω. Actually, the radio front-end module does not always obtain this condition, but the 50 Ω evaluation approach is usually acceptable.

It is evident that with all these constraints in real systems the ECC calculated based on the S_{ij} parameters is not providing the exact value. But in spite of that, It gives high-resolution approximate. Furthermore, the ECC must be less than 0.3 to classify the system as a high-efficiency system with good diversity performance [13].

2.6.4 Diversity Gain - DG is a figure of merit that used to quantify the diversity performance scheme or to show that how much the transmission power can be decreased when a diversity scheme is introduced, without a performance loss. The DG is usually expressed in decibels, and sometimes as a power ratio. In other words, the DG can also be defined as the increment of the signal to noise ratio (SNR) at a given probability. Accordingly, DG can be computed through the cumulative distribution function (CDF) curves of the SNR, then comparing the combined SNR using some specific diversity technique with the SNR of a un-coded SISO communication system, can be written mathematically as [42]:

$$DG = \frac{(SNR)_c}{(SNR)_r} \tag{2.18}$$

where the two symbols “c” and “r” are utilized to denote the combined and the reference. Hence, DG can be explained as the difference between a combined CDF compared with a reference CDF at the same scale of CDF.

The DG is also associated with the ECC. The mathematical expression between DG and the ECC can be shown as:

$$\mathrm{DG} = 10 \times \sqrt{1 - |\rho_e|^2} \tag{2.19}$$

It is deduced from the above formula that the minimum correlation coefficient will be the maximum diversity gain. Consequently, to obtain a good DG; the isolation in between the antennas must be high. Conversely, the DG will be small. Moreover, whatever the combining technique is being applied, the maximum value of DG is obtained when the ECC is zero.

CHAPTER 3

MUTUAL COUPLING IN ANTENNA ARRAYS

The multiple compact antennas receive extraordinary attention due to the fast development of the wireless MIMO communication systems. A critical aspect and big challenge in multiple antenna systems are mutual coupling impact between array elements. In this chapter, a summary on mutual coupling in antenna arrays and some techniques that used to suppress it has been presented. Various types of MTM configurations like EBG, DGS, and SRR are depicted along with their operational principles.

3.1 Microstrip Antenna Arrays

The rapid development of the modern wireless communication system requires designing antennas with very directive characteristics to satisfy the demands of long-distance communication such as increasing gain, directivity, compact size and other features that may not be available with a single antenna element. Usually, a single radiating element produces radiation patterns with narrow bandwidth, low efficiency, and low gain. All these and more make the utilization of a single element antenna not recommendable. Accordingly, the usage of antennas in an array configuration conquers these downsides [4].

MSA array is one of the simplest configurations of antenna arrays, consists of a combination of radiating antenna elements, geometrically placed in a proper form, to produce the demanded radiation pattern. Each individual antenna in the array is known as an element. The microstrip antenna array is very versatile and suitable for many applications that required pencil beams, fan beams, and omni-directional coverage. Moreover, it offers a selection between linear polarization and circular polarization[4,5].

3.2 Mutual Coupling

The coupling may exist through the radiation from the multi-surface paths, within the feed structure or from reflections at the antenna terminal because of impedance mismatches. Mainly, mutual coupling occurs in between closely spaced antenna elements, therefore, is defined as the electromagnetic excitation between the antenna elements in an antenna array structure [8]. Antenna to antenna mutual coupling represents energy absorbed by one antenna receiver when a second nearby antenna is excited. Generally, mutual coupling is considered an unacceptable phenomenon because the energy that should be radiated away is absorbed through another closely antenna as shown in Figure 3.1 (a). Similarly, the energy that could have been captured by one antenna is instead absorbed by a neighboring antenna [45] as seen in Figure 3.1(b).

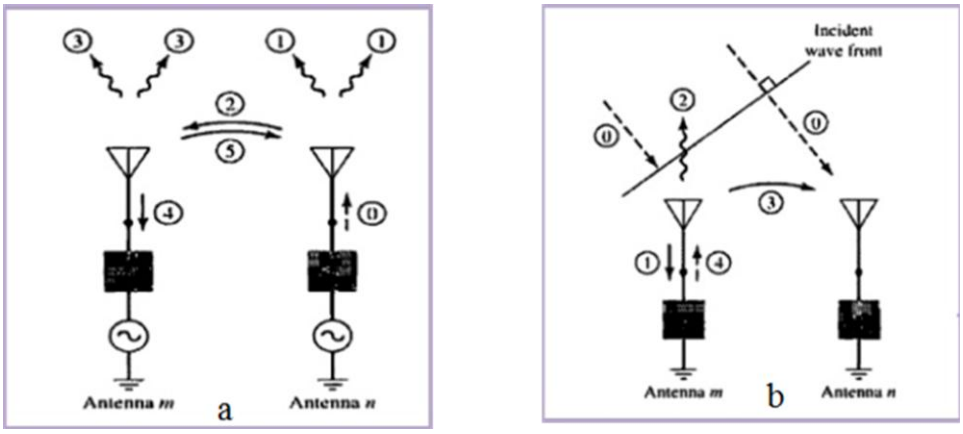

Figure 3.1 Mutual coupling path [45]
(a): Coupling paths between antennas m and n at transmitting mode.
(b): Coupling paths between antennas m and n at receiving mode.

3.2.1 The Effects of Mutual Coupling in Antenna Arrays

The effect of mutual coupling between the nearby antenna elements in an antenna array it can be neglected if it is small. Otherwise, its effect should be considered because it effectively affects the overall performance of the antenna array. The mutual coupling between antenna elements of arrays is a critical issue that it should not be neglected in the MIMO antenna design procedure. Because it can lead to the incorrect foretelling of input impedance, distortion of the radiation pattern and degradation of efficiency. Furthermore, it can lead to serious deterioration in the whole performance. Recently decreasing size technology has become more critical since antennas have to

be closer to each other and this results high in the mutual coupling. Figure 3.2 presents the types of mutual coupling might occur in the antenna array [5].

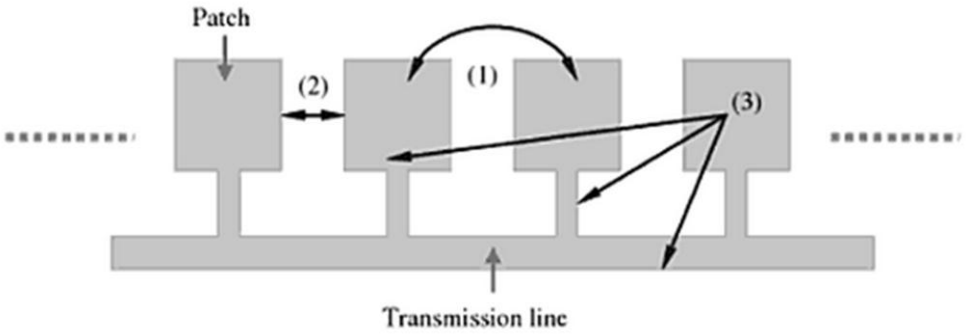

Figure 3.2 Types of coupling in microstrip antenna arrays.

(1) Free radiation and surface wave coupling between the antenna elements,
(2) Fringing field coupling between the nearby antenna elements,
(3) Coupling the antenna element and the feed network (transmission line) of the antenna array structure.

The serious effect of mutual coupling can be defeated by optimizing array architecture through exploitation the ground structures and optimizing impedance matching networks. At the point when a similar element is put among the other elements in the array, the boundary condition isn't the same as that of the single element alone. It can be controlled by every one of the elements of the array. The impact of mutual coupling is severe if the element spacing is small. The mutual coupling will change the characteristics of antenna array as shown below [14, 46]

1. Change the radiation pattern of the antenna array,
2. Change in the array manifold (the received element voltages),
3. Change the input impedance (matching characteristic) of the antenna elements.

The mutual coupling between the antenna elements is because of the induced current on one antenna in light of the other antenna. These induced currents are emerging as a result of:

1) Near Field Coupling Due to Other Nearby Antennas

The near-field coupling is emerging when an antenna is set in the near-field district of another antenna. The near-field coupling up to high levels in the cases when the antennas print on dielectric substrates has a very low permittivity. Coupling space-

waves dominate and show strong coupling when antennas are placed nearby to each other [47, 48].

2) The Common–Ground Current, Surface Waves

The surface wave produces the impact of reductions to the amplitude of the input signal before propagating across the air. Surface waves likewise present spurious coupling between the closely antenna elements. This impact produces extreme distortion in the performance characteristic of microstrip filters in light of the fact that excited surface waves decrease the isolation in the stop bands. Surface waves obtaining the outer boundaries of an open MAS structure reflected and diffracted by the edges. The diffracted waves give an extra commitment to radiation, which corrupting the antenna design by raising the side lobe and the cross-polarization levels. Surface wave influences are generally undesired for circuits and antennas, so it must be mitigated as much as possible.

3.2.2 Reduction The Mutual Coupling Effect

Sufficient isolation between the elements of the array is necessary for diversity and MIMO systems. The coupling between antennas reduces their efficiencies, where the power that would usually be radiated is captured by the other nearby antenna. Several techniques have been introduced to decrease the mutual coupling impact between the antenna elements in MIMO arrays [14, 46]:

1- Increasing the distance between the antenna elements,
2- Adding slits in the ground plane or a ground plane divided by slots,
3- Changing the positioning of radiating elements (parallel, orthogonal),
4- Changing both the positioning and spacing between the resonators,
5- Adding decoupling structures (such as MTM structures) between the antenna elements that change the electrical properties, thus mitigating the mutual coupling and improve the isolation between antennas.

3.3 MTM Theory

In the recent decades, attention has been ripped in MTM structures in the field of electromagnetic and antenna design. The MTM is an unnatural material (artificial) with unique electromagnetic macroscopic features having negative relative ε and μ. These two properties (ε, μ) have a great importance where they determine how the

material interacts with electromagnetic radiation. The material can be classified according to their ε and μ into four regions as shown in Figure 3.3. The first region I is where the ε and μ are both positive. This region is most examined and explored, where most of the exploratory material behaves. The single negative region, which is region II (where ε is negative) and region IV (where μ is negative) that impede the signal. The region III is one of the least explored areas, and this is where the MTM found. When both ε and μ are simultaneously negative, it is having a negative refractive index (NRI) or left-handed material (LHM). This relation can be given through Maxwell's formula for refractive index [49]:

$$n = \pm\sqrt{\mu\varepsilon} \tag{3.1}$$

Materials that available in this region are not promptly accessible in nature. Furthermore, the metallic structure of periodic array that printed on substrates is also recognized artificially as MTM [22,31].

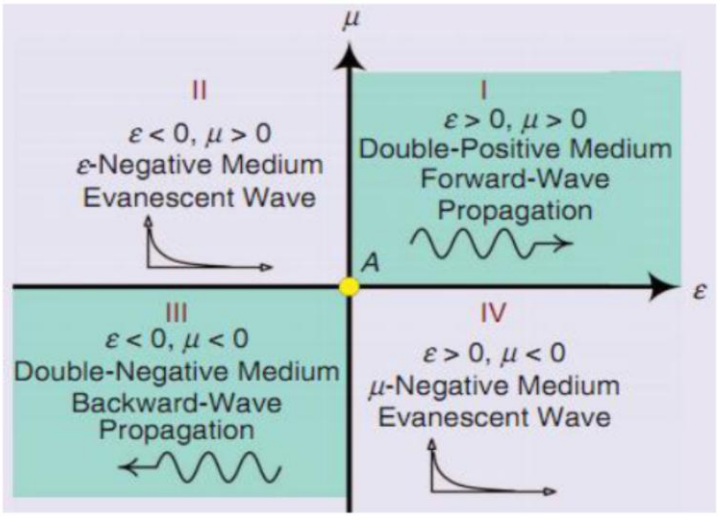

Figure 3.3 The diagram of (ε-μ)
which explains the material classifications

An antenna designed utilizing MTM can be classified as MTM antennas. Antenna designs combining MTM can improve the power of an antenna. The applicability of MTM has enhanced the performance and novel functionalities of the traditional antennas.The antenna array has turned out to be a standout amongst the most energizing uses of MTM because of its effective contribution to improving antenna performance. Master advantages of MTM antennas are a small scale of antennas, high gain, high directivity and highly efficient [23].

3.3.1 MTM Structures

The mutual coupling influences may consider one of the major challenges in multiple antenna systems. There are different types of MTM structures discussed in the literature that have been employed to enhance the performance of antenna array by reducing the mutual coupling between antenna elements such as EBG substrate, DGS, SRR, and CSRR. As listed below, a brief description of these MTM structures along with their operational principles [27] are given;

3.3.1.1 EBG Structure

EBG structures are repeated geometrical arrangements might be dielectric, or metallic inclusions or seldom a combination of both, which has specific features such as high impedance surface. These MTM structures dose not uphold the surface waves; this feature can be exploited in the MIMO antenna array to decrease the mutual coupling influence between the antenna elements. The feature of EBG that depicts the prohibited behavior of electromagnetic waves in the specific frequency band and possibility propagation in other regions. These blocked frequency bands are alluded to as prohibited bands or often known as band gaps. The frequently of EBG structure can be in one, two or three dimensions. The repeated configuration of these MTM structures can yield rise to stop band and pass band in the electromagnetic transmission spectrum along with the direction of periodicity. Thus, the frequencies in stop band are firmly reflected, whereas the frequencies in the passband are spread without fading or attenuation [18, 23].

Embed the EBG structure between the array elements leads to suppressing the mutual coupling among them by smothering the surface wave propagation. In this context, the EBG structure can be placed between the antenna structures above the substrate as shown in Figure 3.4. Usually, the fringing fields of the antenna are not influenced by EBG structures, which makes the resonant frequency of the antenna array keep unchanged [25]. Repeated EBG structures lead to a decrease the surface waves within the specific frequency band. As a result of this, the mutual coupling becomes weak, hence the performance of the antenna array is enhanced.

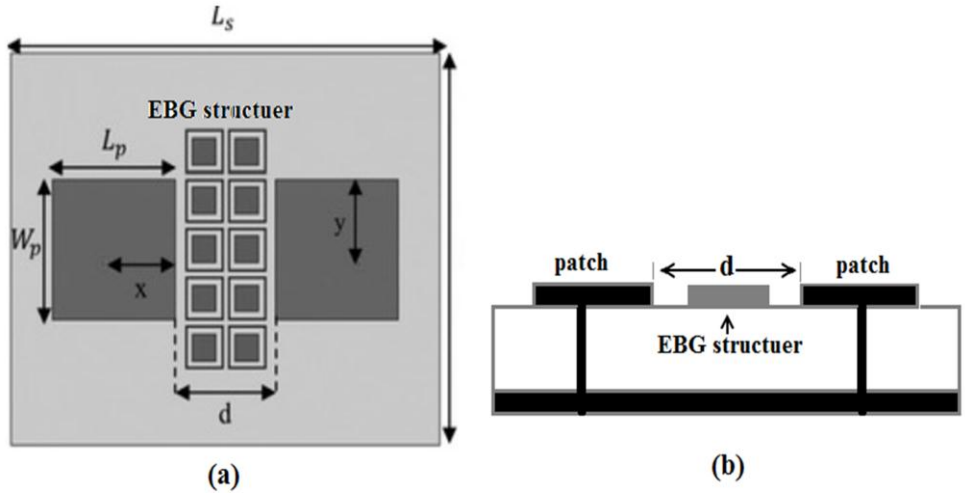

Figure 3.4 Insertion EBG structure between the antenna elements above the substrate (a) Tope view (b) Side view.

3.3.1.2 DGS

DGS is a technique in which the ground plane metal of a microstrip circuit is deliberately altered to improve the performance. The name for this procedure means merely that a "defect" has been located in the ground plane, which is generally supposed to be an approximation of an infinite, perfect-conducting current sink. In other words, DGS is obtained by etching the ground plane layer with a specific geometric shape leads to disturbing the current distribution of the patch. According to this disturbance, the microstrip patch characteristics will be changed, such as capacitance (C) and inductance (L) (any defect occurs in the ground plane layer of the microstrip patch can give rise to increasing effective capacitance and inductance).

DGS technology provides more options in microwave circuit design and can be employed in a wide range of applications such as filter design, couplers, and dividers. For antenna applications, DGS is used for antenna size reduction and mutual coupling reduction in antenna arrays [26, 27, 30].

a. DGS Unit

Research has shown that there is two effective method to exploit the properties of DGS, which are, DGS unit and repeated DGS. An assortment of geometric shapes that etched in the ground plane layer has been listed in the literature. In Figure 3.5, it is shown that an assortment of attached shapes involving the spiral head, arrow head-slot and "H" shape slots and so on.

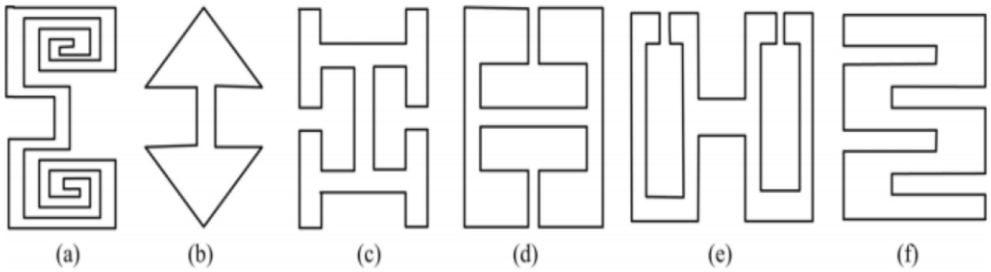

Figure 3.5 Different DGS geometries: (a) spiral head, (b) arrowhead-slot, (c) "H" shape slots, (d) a square open-loop with a slot in middle section, (e) open-loop dumbbell and (f) inter-digital DGS [3].

b. Periodic DGS

DGS Periodic structures for planar transmission lines have drawn the attention due to their wide applicability in microwave circuits and antenna design. Periodic refers to the repetition of the physical structure. Transmission lines in a periodic structure with a finite pass and rejection band as low-pass filters. With repeated DGS unit in the ground plane, the depth and *BW* of the stopband for DGS circuit are turned based on the number of periods. To get the desired results of repeated DGS, there are some points to be taken into consideration such as the shape of DGS, the space between the repeated DGS units, and the distribution of the assorted DGSs on the ground plane. As obvious in Figure 3.6, there are two classes of periodical DGS; the first one is horizontally periodic DGS (HPDGS); the second one is vertically periodic DGS (VPDGS) [23].

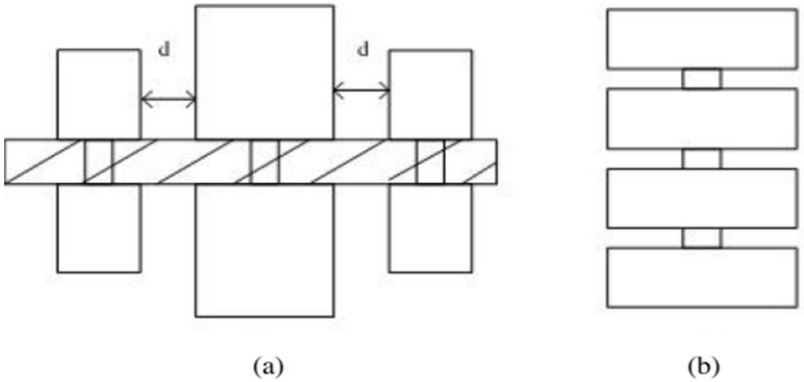

Figure 3.6 Periodic DGS: (a) HPDGS, (b) VPDGS .

3.3.1.3 SRR/CSRR

In MTM, different geometrical configurations have proposed and attracted attention for their unique electromagnetic properties. SRR is one such structure, which composes the essential part of LHM-MTM. SRR-MTM are made of two concentric rings separated by a gap, both having splits at opposite sides as shown in Figure3.7. The magnetic dipole is generated by the circulating current. It produces magnetic properties. The current circulation occurs in a metallic contour leading to increasing magnetic flux. If two metallic contours are placed adjacently coupling between these two contours occurs which shows capacitance between them leading to a sufficient net increase in the permeability [50]. Based on this concept, this type of artificial magnetic media needs a careful control of the SRR orientation relative to the incident wave besides the efficient SRR design, otherwise, the electromagnetic response is significantly more complicated. Several analytical models are used to study and analyze the resonant property in the SRR structures, and investigate their impact on mutual coupling [31, 32].

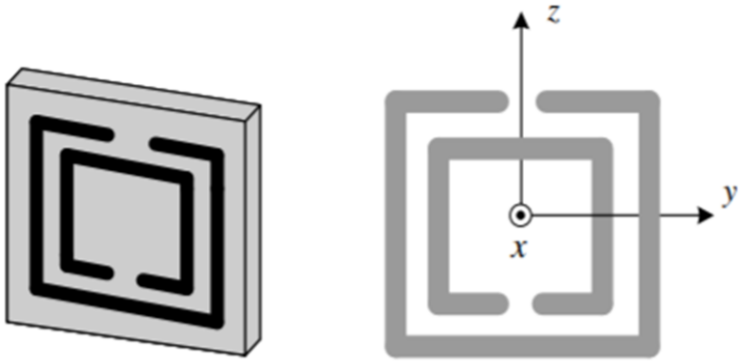

Figure 3.7 The SRR unit cell

3.3.2 Nicolson Ross Weir (NRW)

As previously mentioned, the MTM has negative ε and/or negative μ. The Nicolson-Ross-Weir (NRW) is a method for investigating the characteristic properties of MTM structures. In other words, the NRW is algorithm or tool that transforming the scattering parameters from the simulation or experimental into electrical and magnetic characteristics which are ε_r and μ_r respectively. In the NRW method [51], the S- parameter is:

$$\Gamma = x \pm \sqrt{x^2 - 1} \tag{3.2}$$

where: $x = \frac{S_{11}^2 - S_{21}^2 + 1}{2S_{11}}$ (3.3)

As a step to obtain the right root, *x* is must be in the form of scattering parameter. Here the magnitude of the reflection coefficient must be less than one $|\Gamma| < 1$.

The relative complex permeability is recast in the form:

$$\mu_r = \frac{\lambda_{0g}}{\Lambda}\left(\frac{1+\Gamma}{1-\Gamma}\right) \tag{3.4}$$

Where: $\lambda_{0g} = \frac{\lambda_0}{\sqrt{1-(\lambda_0/\lambda_c)^2}}$, $\Lambda = \frac{\lambda_0}{\sqrt{\varepsilon_r \mu_r - (\lambda_0/\lambda_c)^2}}$ (3.5)

λ_0: the free-space wavelength, λ_c: the cutoff wavelength

By using (3.4) to extract from (3.5) yields relative complex permittivity:

$$\varepsilon_r = \frac{\lambda_0^2\left(\frac{1}{\Lambda^2} + \frac{1}{\lambda_c^2}\right)}{\mu_r} \tag{3.6}$$

CHAPTER 4

EVALUATION OF DIVERSE CONFIGURATIONS OF MIMO MICROSTRIP ARRAY ANTENNA DESIGN

The methodology for implementation of this research includes firstly, a various types of microstrip antennas have been introduced that are being used as part of the design of two closely MIMO antenna systems. Secondly, several types of innovative decoupling structures have been proposed, without an appropriate mathematical approach, the design of such structures is based on trial-and-error [52]. Then has been placed between the antenna elements to suppress the mutual coupling and enhancement the isolation. The analysis of the ECC, DG, total efficiency and Voltage Standing Wave Raito (VSWR) are presented, to assess the performance of the MIMO systems. Finally, to certify the validity of the designs, all models have been fabricated, then the outcomes have been compared.

In this research, we used Computer Simulation Technology Microwave Studio (CST MWS) software 2016 for simulation of antenna and to find out the results. This work is supported by the Scientific and Technological Research Council of Turkey (TÜBİTAK) under Project No. 114E495.

4.1 Mutual Coupling Reduction of E-Shaped MIMO Antenna With Matrix of C-Shaped Resonators

In this design, E-shaped MIMO microstrip antenna systems operating in WLAN and WiMAX bands (5-7.5 GHz) are proposed with enhanced isolation features. The systems are comprised of two antennas that are placed parallel and orthogonal to each other, respectively. According to the simulation results, the operating frequency of the MIMO system is 6.3 GHz, and mutual coupling is below -18 dB in a parallel arrangement, whereas they are 6.4 GHz and -25 dB, respectively, in the orthogonal arrangement of the MIMO system is 6.3 GHz, and mutual coupling is below -18 dB in a parallel arrangement, whereas they are 6.4 GHz and -25 dB, respectively, in the

orthogonal arrangement. The 2x3 matrix of C-Shaped Resonator (CSR) is proposed and placed in the middle of the antenna elements over the substrate, to mitigate the mutual coupling and improve the isolation between the antennas. More than 30 dB isolation between the array elements is achieved at the resonant frequency for both of the configurations. The essential parameters of the MIMO array such as mutual coupling, surface current distribution, ECC, DG, and the total efficiency have been simulated to verify the reliability and the validity of the MIMO system in both parallel and orthogonal configuration. The experimental results are also provided and compared for the mutual coupling with simulated results. An adequate match in the middle of the measured and simulated results is achieved**.**

4.1.1 Antenna Design and Decoupling Structure

4.1.1.1 Antenna Design

Since the goal is to deal only with the mutual coupling mechanism, a simple MIMO system consisting of two E-shape monopole antennas have been chosen to demonstrate the capability of the approach in this thesis. The antennas are placed in parallel and operating between 5 and 7.5 GHz is proposed as shown in Figure 4.1 (a). The size of each antenna is chosen such that the system resonates at 6.3 GHz, providing an impedance bandwidth of 34.42% as shown in Figure 4.1 (b). The antennas are placed on FR4 substrate having dielectric constant ε_r= 4.3 with a loss tangent of 0.025 and thickness h =1.6 mm. The separation between the antenna elements is d=0.42 λ_o (where λ_0 is the free-space wavelength at 6.3 GHz). All other dimensions are given in Table 4.1.

A prototype of this antenna system is shown in Figure 4.2. It is tested by using an HP8720D network analyzer. Figure 4.3 shows the comparison between simulated and measured S-parameters' results of the proposed MIMO system. It is noticed that there is little difference between the simulation and experimental results. This difference can be considered acceptable as long as its effect on the resonant frequency is not high and the frequency band does not shift much. The discrepancies are mostly due to the insertion loss of SMA connectors, surrounding environment that influences on wave reflection, or the fabrication tolerances. As can also be observed from Figure 4.3, the coupling is about 18 dB in simulation and 16 dB in measurements. To reduce this coupling and increase the isolation, the CSRs, whose design procedure will be explained in the next section, are used.

Table 4.1 The dimensions of the parameters of the MIMO antenna

Parameter	Ws	Ls	W1	W2	Wf	L1	L2	L3	Lf	a	b	c	c1	g	d
Dimension (mm)	100	41	19	11	3	11	20	11	10	9	11	10	2	2	20

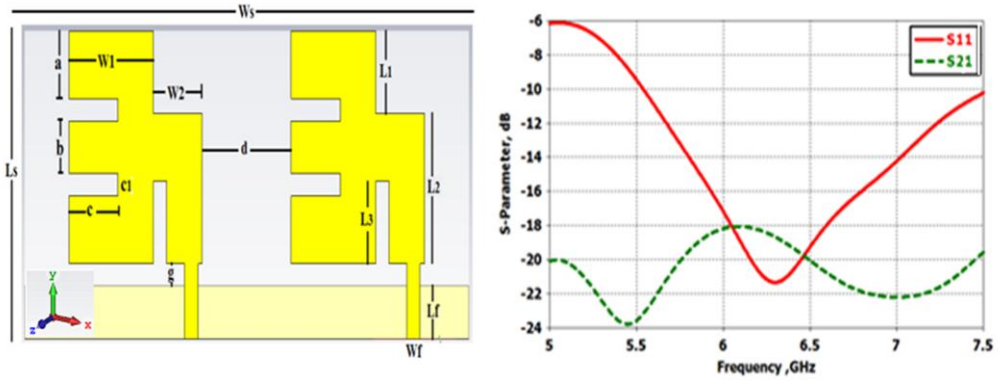

a b

Figure 4.1 a)The proposed MIMO system, b) S-Parameters.

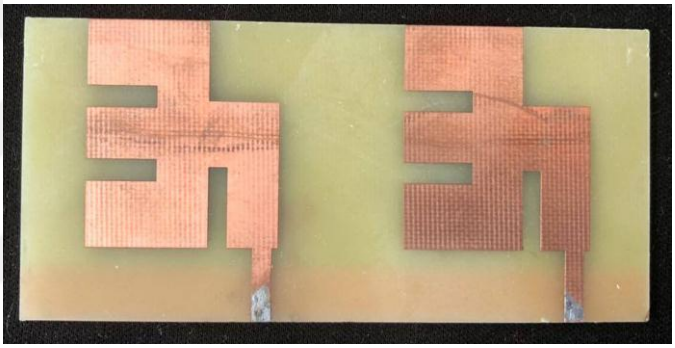

Figure 4.2 Fabricated antenna.

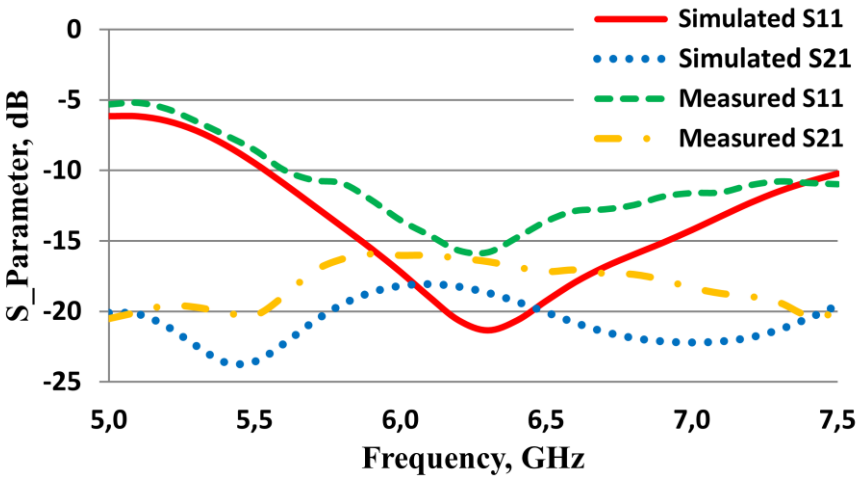

Figure 4.3 Comparison between the simulated and the experimented S-parameter results.

4.1.1.2 Analysis of the Unit Cell

Figure 4.4 (a) shows the 3D view of the geometrical proposed unit cell of CSR. The CSR unit cell can be modeled by an equivalent circuit using a capacitor and an inductor element. In this case, the gap in CSR can be represented by a capaitor C while the C-shaped strip can be represented by the inductor L as shown in Figure 4.4(b). C_m denotes the coupling to the next element of the array of CSRs. The dimensions of the unit cell are given in Table 4.2. The model of the structure is first designed and tested on an FR4 substrate with a relative dielectric constant of 4.3 and a thickness of 1.6 mm as shown in Figure 4.5 (a).

It is obvious that the placement of a sheet of resonators of infinite extension between the two antennas is not possible. Therefore the designed structure consisting of a 2x3 matrix of CSR is studied. To investigate the characteristic properties such as the effective ε and effective μ of this matrix, the NRW method (previously explained in chapter three) is used. The results are provided in Figure 4.5 (b), and it is observed that 2x3 matrix of CSR structure exhibits negative ε and negative μ in the frequency band of interest around the operation frequency. So this structure can be considered as a DNG medium. This MTM property of the 2x3 matrix of CSR structure has the ability to suppress the surface waves and the space waves (which are considered to be two significant sources to enhance the coupling between the closely antennas), by impeding wave propagation in the space between the MIMO antenna elements.

Table 4.2 Dimension of unit cell

Parameter	L	Rin	Ro	g	h
Dimension (mm)	8	1.8	3	3.6	1.6

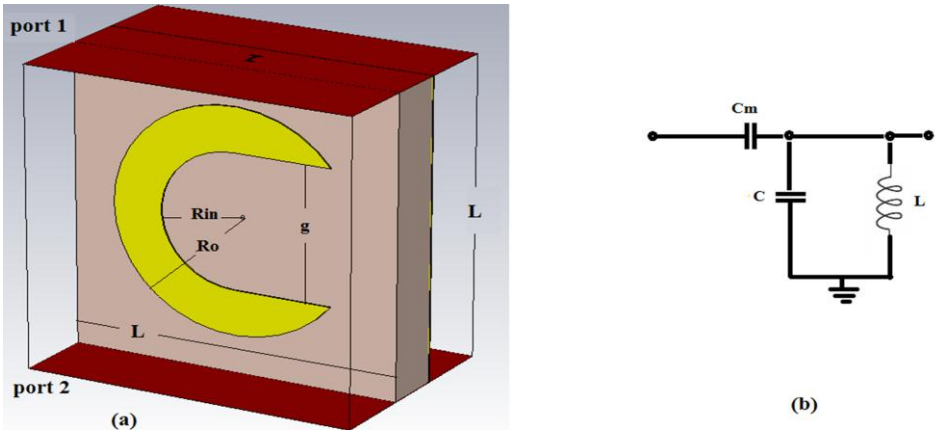

Figure 4.4 The unit cell of CSR structure.(a) 3D view of the CSR. (b) Equivalent circuit of the CSR.

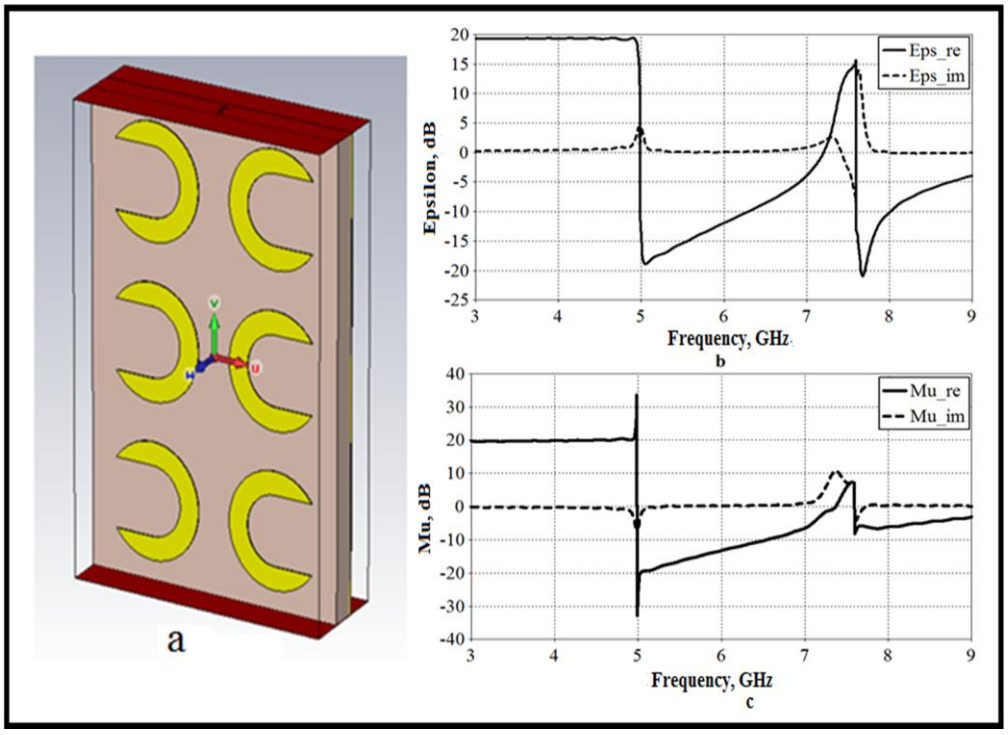

Figure 4.5 a) 2x3 matrix of MTM–CSR, b) effective permittivity, c) effective permeability.

4.1.2 Measurements and Results

4.1.2.1 Parallel Configuration

In this section, the proposed decoupling technique is utilized to enhance the isolation in the middle of MIMO antennas by placing a 2x3 matrix of the CSR structure as shown in Figure 4.6 (a). The CSR matrix can block the surface waves inside the substrate of the antenna and guide them in another direction by creating an indirect signal with the additional coupling path that reverses the signal going straightly from element to element. It is known that if the two waves have comparable amplitudes, then the two waves add up destructively resulting in the suppression of mutual coupling [53]. It is evident from the simulation results in Figure 4.6 (b) that the proposed technique achieves a reduction in mutual coupling and results in an isolation of 30 dB with an improvement in the isolation about 12 dB at the resonant frequency.

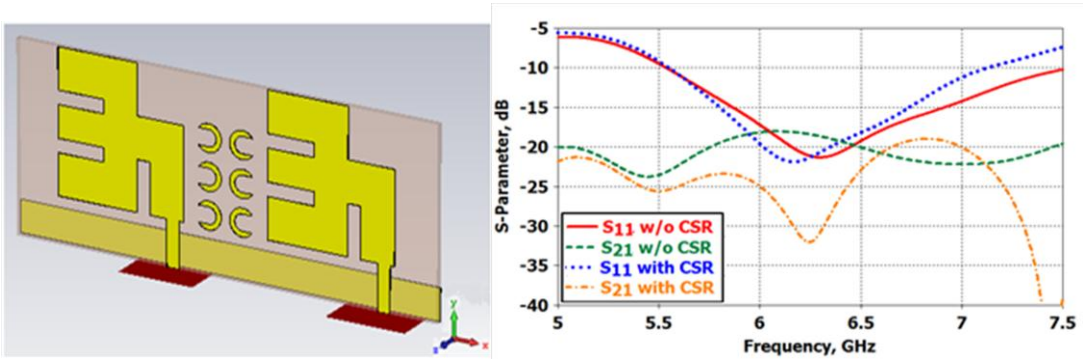

a b

Figure 4.6 a) MIMO System antennas with CSR matrix structure, b) Simulated S-parameters with & without CSR matrix structure.

The prototype of the antenna system is printed as displayed in Figure 4.7. The comparison between the measured S-parameters of the offered MIMO system with and without MTM-CSR matrix structure is shown in Figure 4.8, and it is observed that there is an improvement in S_{21} with the MTM-CSR matrix structure from 16 dB to 26 dB. Figure 4.9 shows the simulated and measured S-parameters with the MTM-CSR matrix of the proposed MIMO system, where there is a good match between the results [34].

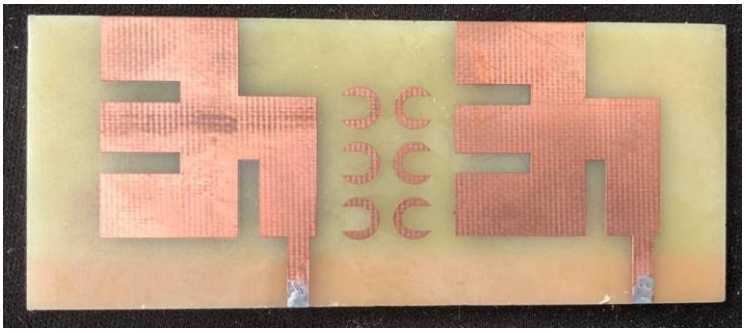

Figure 4.7 Fabricated antenna.

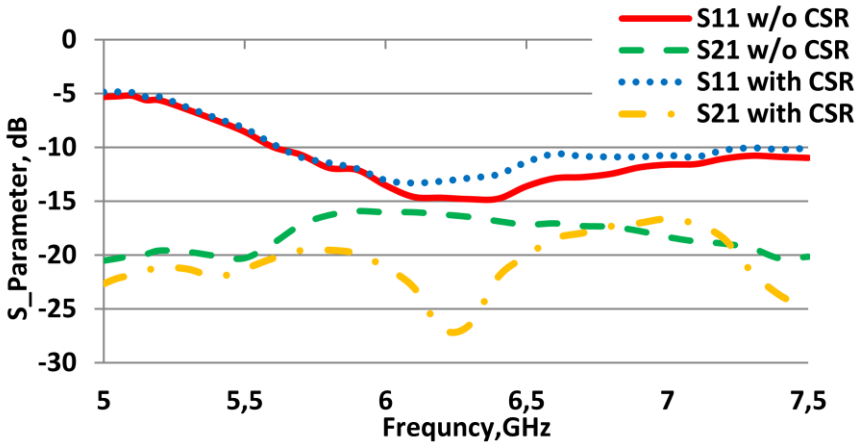

Figure 4.8 Comparison between measured S-parameters of the proposed MIMO system with and without CSR matrix structure.

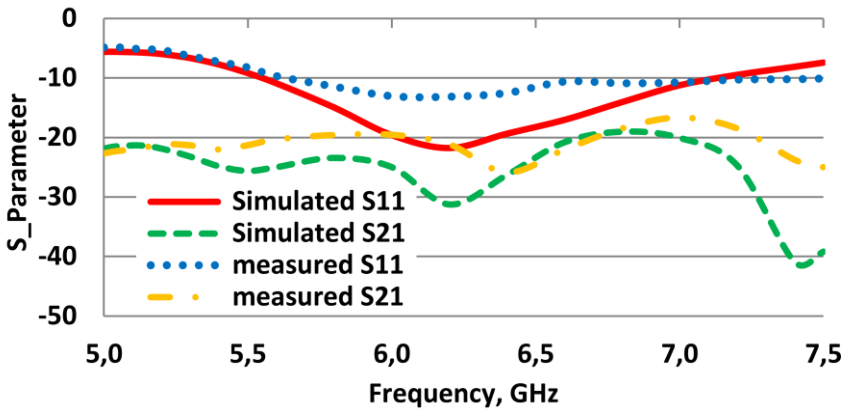

Figure 4.9 Comparison between simulated and measured S-parameters with the CSR matrix of the proposed MIMO system [34].

The influence of decoupling can be observed by the surface current plots on the MIMO system without CSR matrix structure. High surface current can be seen on the patch antenna on the right side while the left patch is excited as shown in Figure 4.10 (a). The surface current is suppressed by the introduction of CSR matrix structure in the middle of antennas as shown in Figure 4.10 (b). The surface current caused by mutual coupling is reduced by adding the MTM decoupling structure.

ECC is a metric that affords essential knowledge about the performance of the array for MIMO systems. The lower the correlation, the higher data throughput can be supported by the MIMO antenna. Generally, it is viewed as that antenna with a correlation coefficient under 0.3 has the ability to provide a rich diversity performance. The ECC can be calculated from S-parameters as given in Eq (2.17). The ECC is calculated for MIMO system, without and with MTM-CSR matrix structure and is plotted in Figure 4.11. From the plot, it can be noted that the ECC is under 0.0001, which means there is a good isolation between the two antennas.

The DG is an extra critical parameter must be considered when evaluating the MIMO performance. Through which the reliability of the MIMO system is determined. The DG has been calculated using the Eq (2.19). The higher the value of diversity, indicating the better isolation and vice versa. As observed from Figure 4.12, there is an improvement in the DG with MTM-CSR matrix. The DG of the proposed system with MTM-CSR matrix approaches about 9.99 dB within the frequency band.

Finally, Figure 4.13 describes the simulated total efficiency of the MIMO array when the antennas are in the parallel configuration in the absence and presence of the decoupling structure MTM-CSR matrix. It is apparent that the total efficiency shows

an improvement within the operating frequency band of the antennas with the decoupling structures.

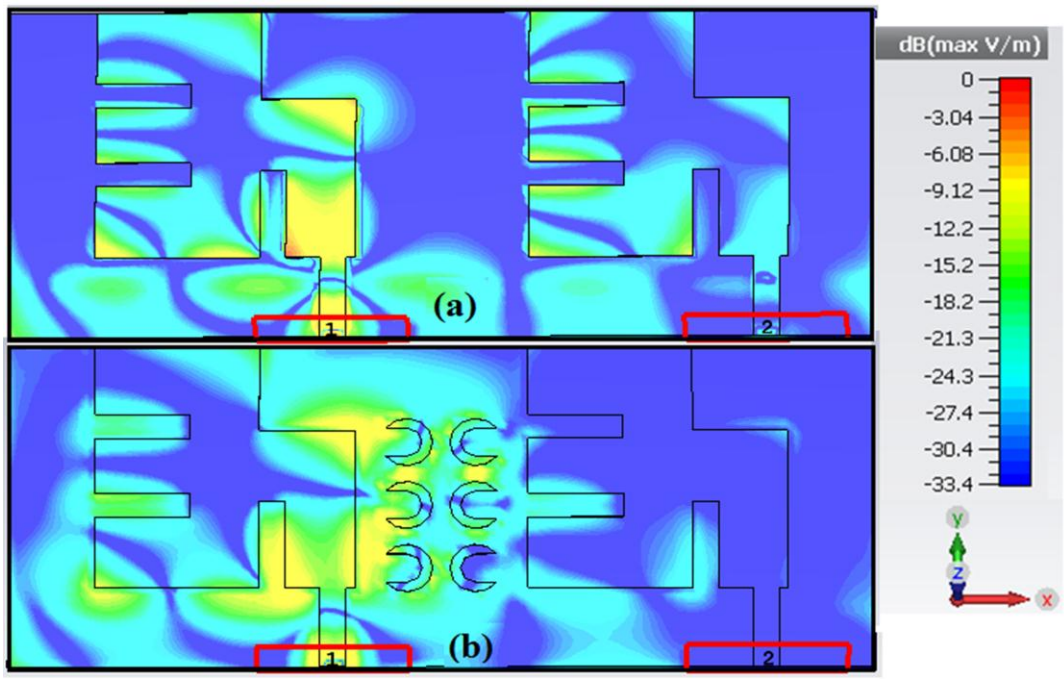

Figure 4.10 The surface current distribution (a) without CSR matrix structure (b) with MTM-CSR matrix structure.

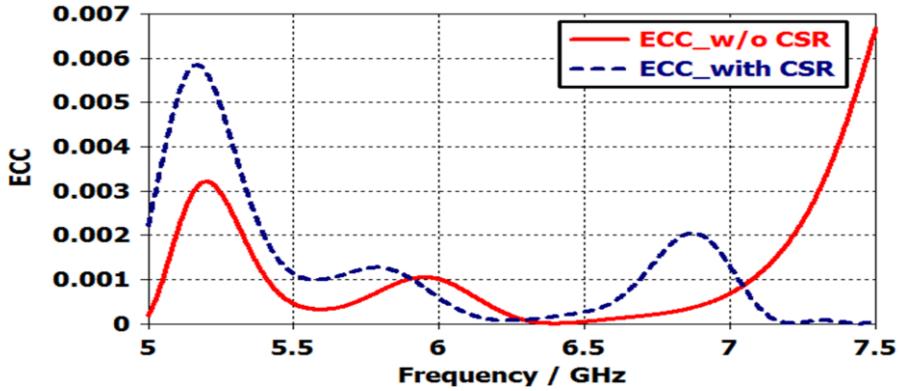

Figure 4.11 ECC of MIMO system without and with MTM-CSR matrix

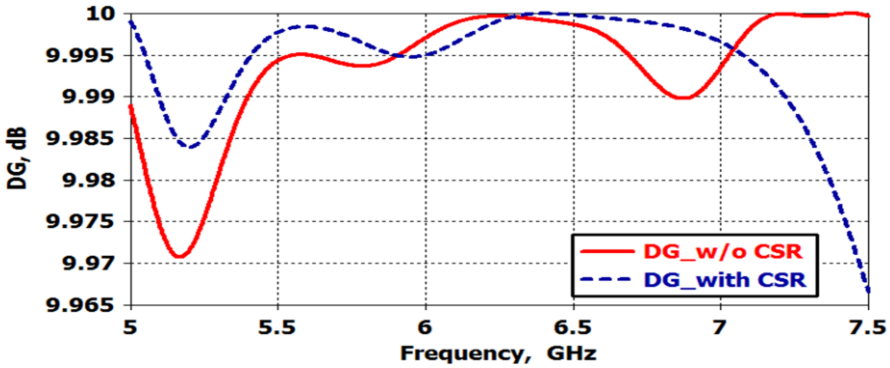

Figure 4.12 DG of the MIMO system with and without MTM-CSR matrix structure

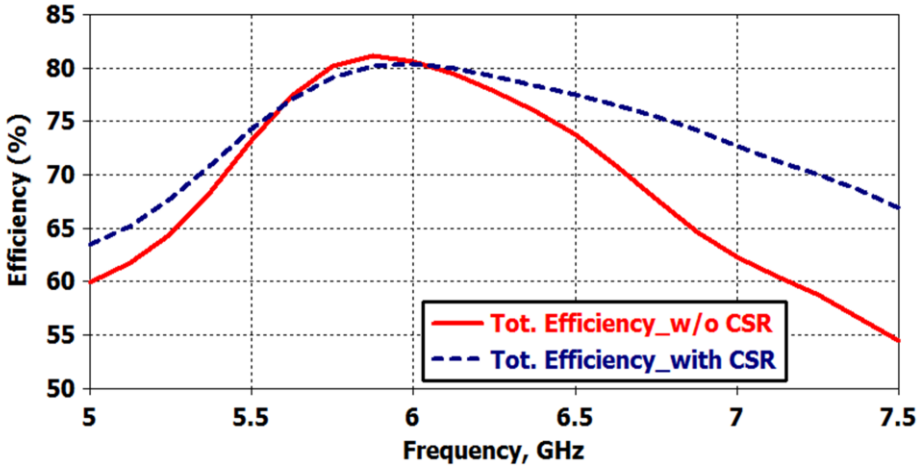

Figure 4.13 Simulated total efficiency of whole MIMO system with and without MTM-CSR matrix structure

4.1.2.2 Orthogonal Configuration

The performance of a MIMO system can also be improved by using the antennas with orthogonal configuration. In order to study this concept, the antenna elements are orthogonally placed on the same substrate as given in Figure 4.14(a). However, after performing a parametric study and running several simulations, the optimum size (Lg x Wg) of separate ground planes are chosen as 7×50 mm^2, and the ideal separation (d) between the antenna elements is 18 mm. The same 2×3 matrix of MTM-CSR is placed between the antennas as shown in Figure 4.14(b).

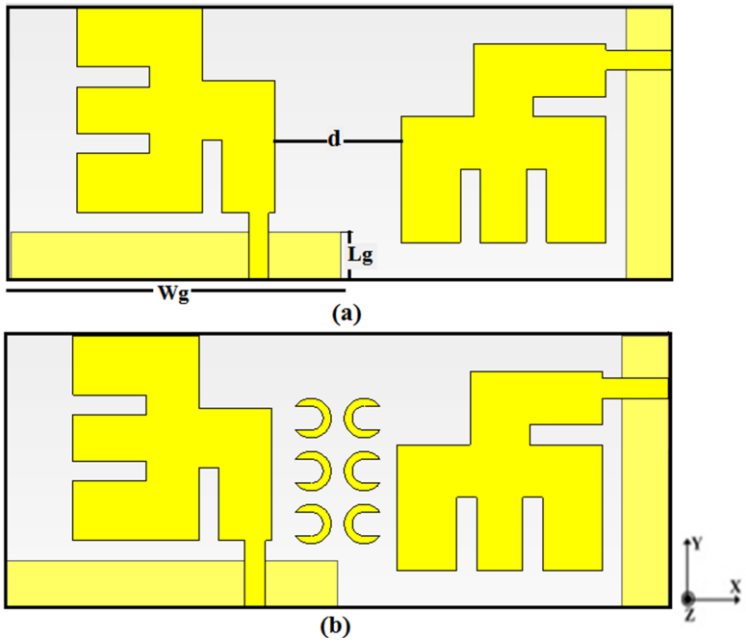

Figure 4.14 The proposed MIMO system in orthogonal configuration a) without CSR matrix structure, b) with CSR matrix structure

Figure 4.15 presents the simulation results for the S-Parameters with and without the MTM-CSR matrix structure. The mutual coupling without CSR matrix structure is now about 26 dB and appears to be lower than that of the structure in Figure 4.1(b). As seen from this figure, the proposed technique achieves a reduction in mutual coupling up to 30 dB, which improves the isolation between antenna elements.

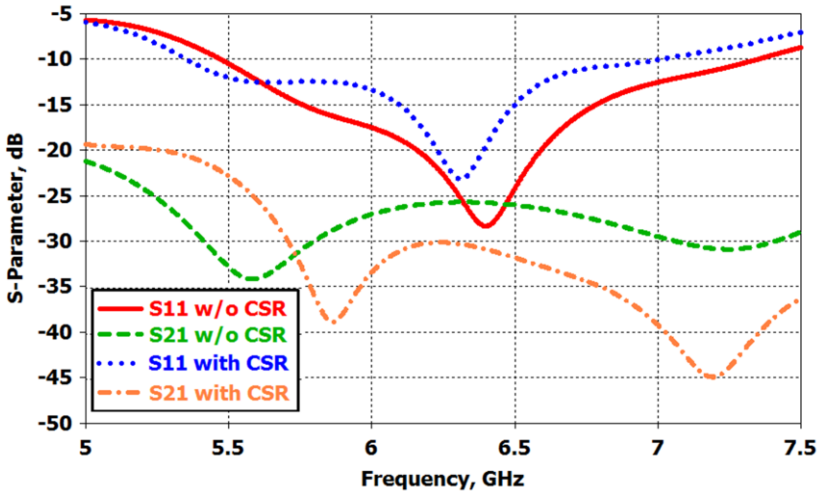

Figure 4.15 Comparison between simulated S-parameters with and without CSR matrix structure.

Figure 4.16 shows the MIMO system in an orthogonal configuration with and without CSR structure. Figure 4.17 shows the comparison between the experimental S-parameters with and without CSR structure, and Figure 4.18 shows the simulated and experimental S-parameters with CSR structure. It's seen that there is a good match between the results.

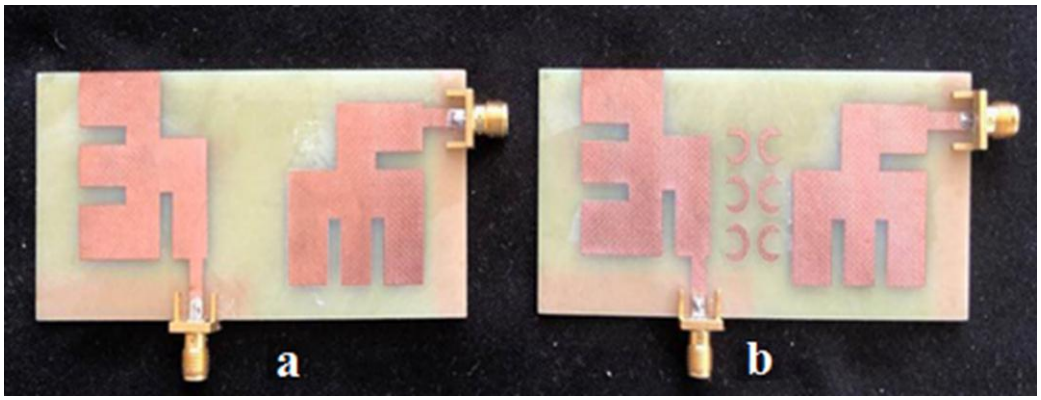

Figure 4.16 Fabricated antenna in orthogonal configuration a) without CSR structure and (b) with CSR structure

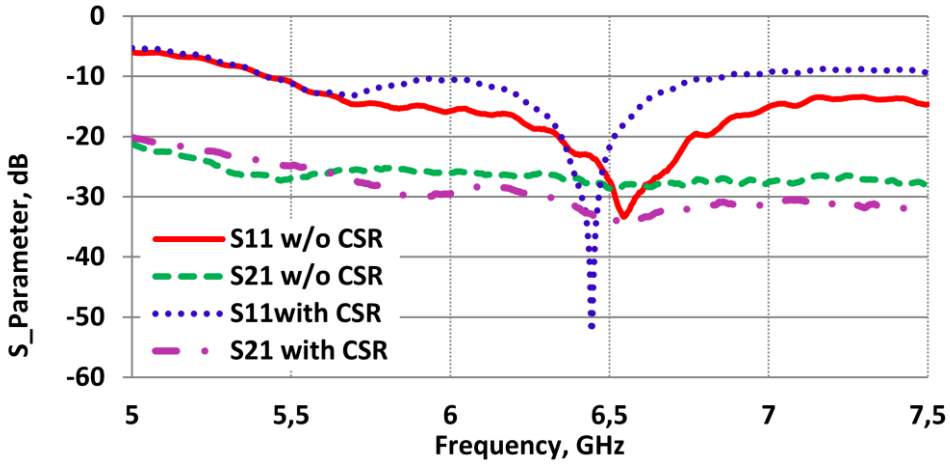

Figure 4.17 Comparison of the measured S-parameters of the modified MIMO system with and without CSR structure.

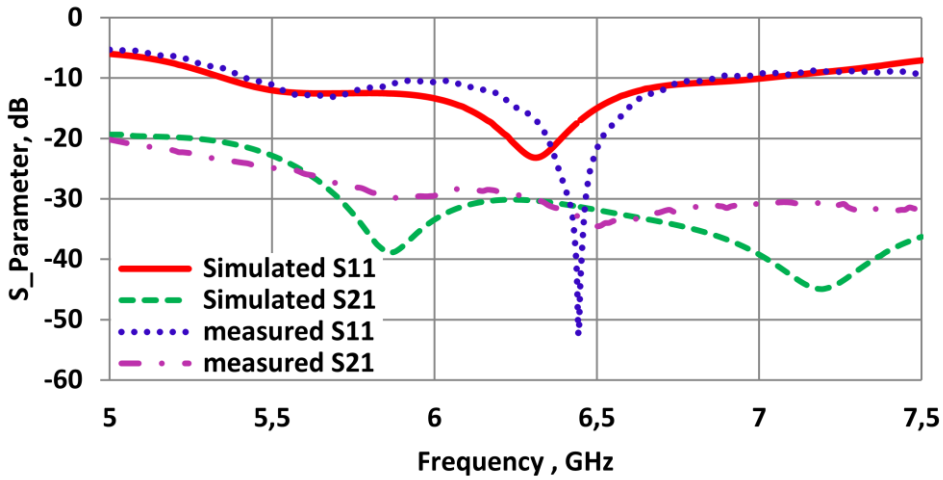

Figure 4.18 Comparison of the experimanted and simulated S-parameters of the modified MIMO system with CSR structure.

By investigating the surface current distribution, the mechanism of CSR matrix structure can be more understandable. The mutual coupling between the two antenna elements in a MIMO array is related to the current direction that flows on the surface of the antennas. If the current flows in the same direction on the adjacent sides of both the antennas, the mutual coupling increases. Likewise, if the currents are in the opposite path, the induced mutual coupling is suppressed. The surface waves can clearly be observed in Figure 4.19 (a) without CSR matrix structure. Figure 4.19 (b) shows that the induced surface current can be suppressed on the other element, which decreases the mutual coupling when the CSR matrix is added between antenna elements.

To evaluate the orthogonal MIMO system performance in terms of correlation and reliability, The ECC and DG were calculated. Figure 4.20 shows the ECC with and without MTM-CSR matrix. It is evident that ECC lower than 0.001 in both cases, it is pretty good, while Figure 4.21 shows the DG. It is clear that the DG reaches 9.99 in both cases (with and without MTM-CSR matrix) within the frequency band. This confirms that the maximum DG is obtained when the ECC is zero. Hence, the system could be classified as a high-efficiency system with good diversity performance.

Figure 4.22 demonstrates the simulated total efficiency of the MIMO array when the antennas are in an orthogonal configuration with and without decoupling structure MTM-CSR matrix. It is clear that the total efficiency exhibits an enhancement across the operating frequency band of the MIMO system with the proposed decoupling structures.

To examine the influence of the decoupling structure on the radiation pattern of the antennas. The left patch was excited, and the right patch was terminated with 50-Ω impedance in Figure 4.1, Figure 4.6, and Figure 4.14 (a) and 4.14 (b). The proposed MIMO system is placed in *x-y* Plane. Figure 4.23 illustrates the simulated E-plane and H-plane of the radiation pattern of the E-shaped MIMO system in a parallel configuration with and without placing CSR matrix structure between the antennas. Finally, the radiation pattern of the proposed system in the orthogonal configuration for the left and the right E-shaped MIMO antennas are shown in Figure 4.24. It is observed that the decoupling structure has little effect on the radiation pattern of the antenna system, which is the desired result.

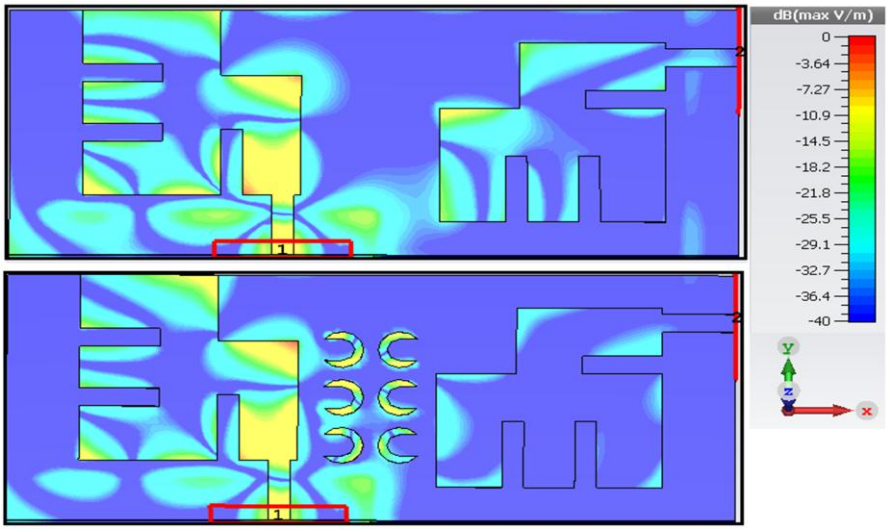

Figure 4.19 Surface current distribution (a) without CSR matrix structure (b) with CSR matrix structure.

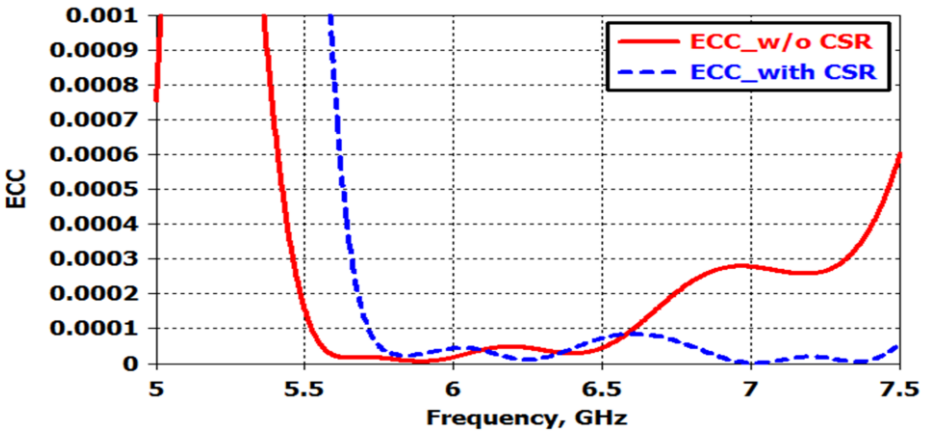

Figure 4.20 ECC of orthognal MIMO system without and with MTM-CSR matrix

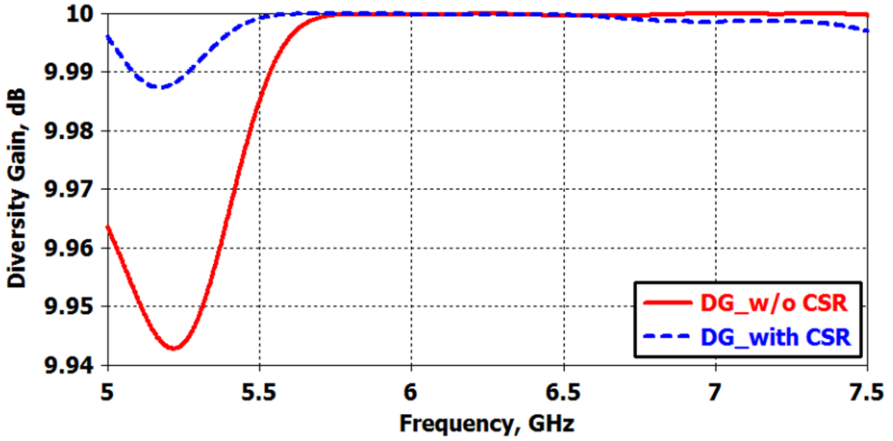

Figure 4.21 DG of the orthognal MIMO system with and without MTM-CSR matrix structure

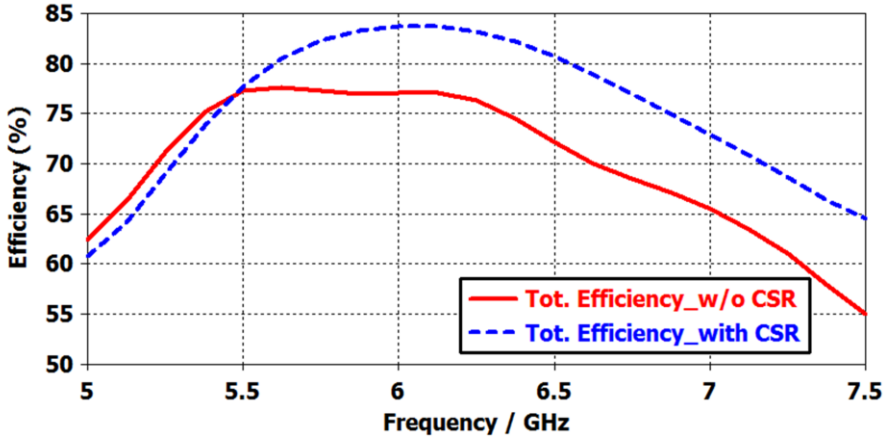

Figure 4.22 Simulated total efficiency of whole MIMO system with and without MTM-CSR matrix structure

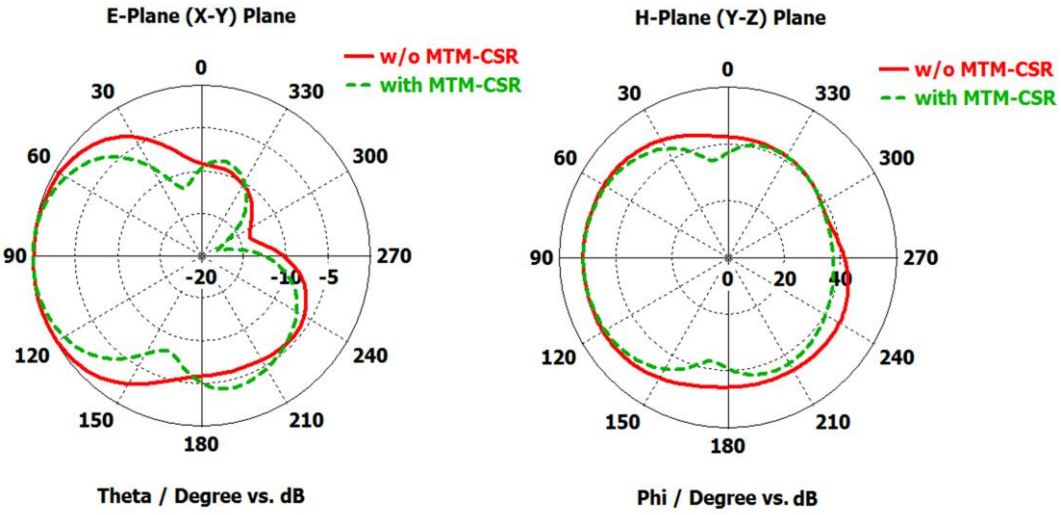

Figure 4.23 Radiation pattern of the E-shaped MIMO system in parallel configuration a) E-Plane, b)H-Plane

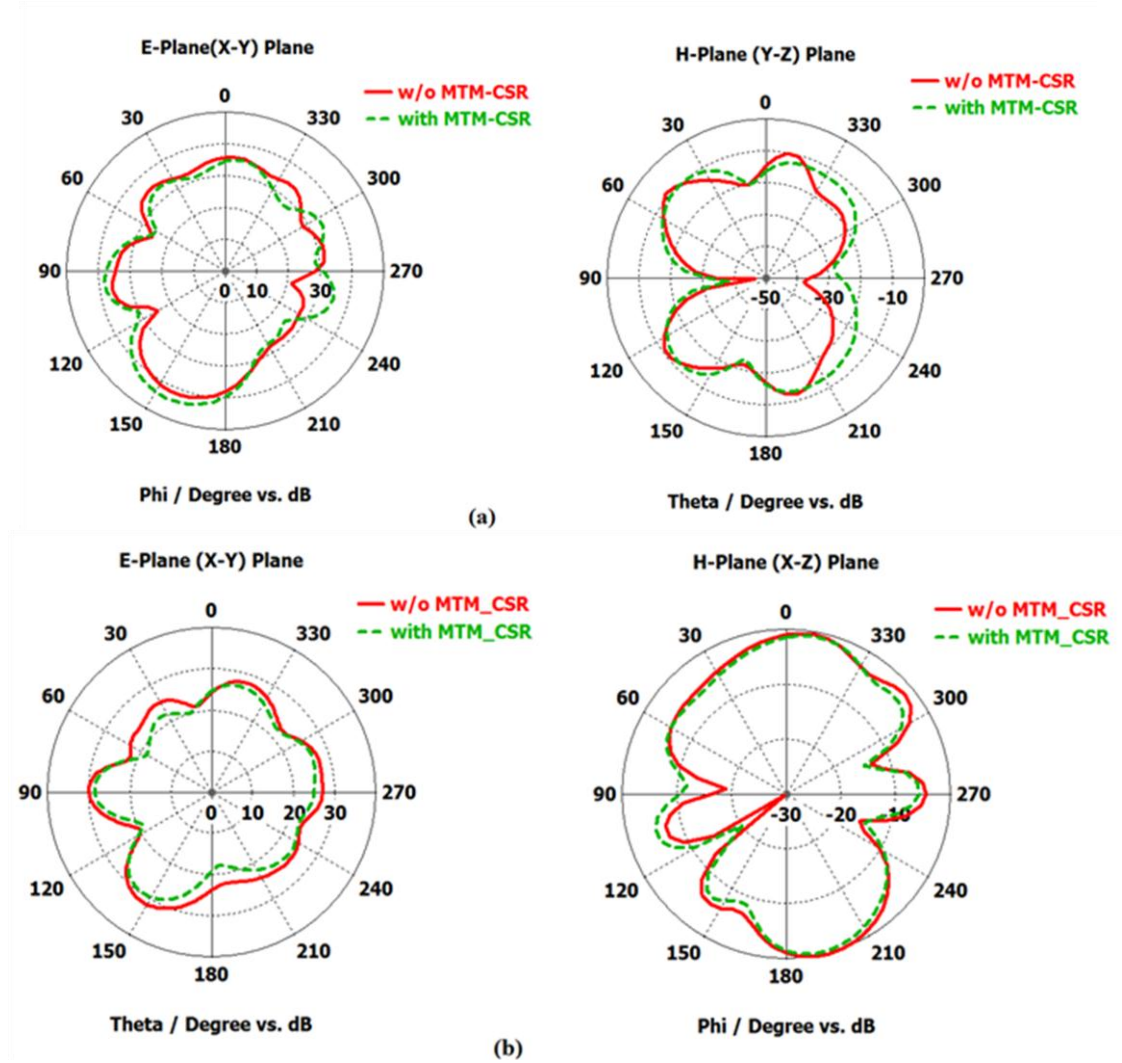

Figure 4.24 Radiation pattern of the E-shaped MIMO antenna system in orthogonal configuration: a) E-Plane and H-Plane for left, and b) E-Plane and H-Plane for right E-shaped antenna.

4.2 Mutual Coupling Suppression Between Closely Spaced MSA by Method of Ladder-Shaped Conducting Wall (LSCW)

To suppress the mutual coupling between two closely MSAs, a novel ladder-shaped conducting wall structure (LSCW) has been proposed and presented in this section. This structure consists of two ladder shaped strips of copper printed on an FR-4 dielectric substrate. It is inserted in the middle of the MSAs, and also some part of LSCW surrounds a portion of each antenna. The developed compact MIMO system has a compact size of 50x25 mm^2, and dual-band design resonates at 4.45 GHz or 10.3 GHz frequencies depending on the dimensions of LSCW structure. It can be used in many wireless applications in C (4-8 GHz) band or X (8-12 GHz) band. The value of VSWR $\leq$ 1.5 for both resonant frequencies. Also, the diversity performance, such as the ECC, DG, and the total efficiency are calculated and compared. A prototype is fabricated, and the measured mutual coupling shows that the isolation between the antenna ports has been enhanced about 50 dB at 4.45 GHz and 40 dB at 10.3 GHz.

4.2.1 Geometry of LSCW Decoupling Structure

A proposed LSCW decoupling structure, inserted between the two microstrip patch antennas is shown in Figure 4.25. The patches are operating at 4.45 GHz; they are printed on an FR-4 substrate having dielectric constant ε_r = 4.3 with a loss tangent of 0.025 and thickness h=1.6 mm. The edge to edge distance between the MSAs system is taken as d = 8mm (merely 0.118 λ_0). All other dimensions are given in Table 4.3. The patches are fed with 50-Ω coaxial probes. The feed position is optimized so as to achieve the best impedance matching at the resonant frequency which is then connected to a 50 Ω SMA connector.

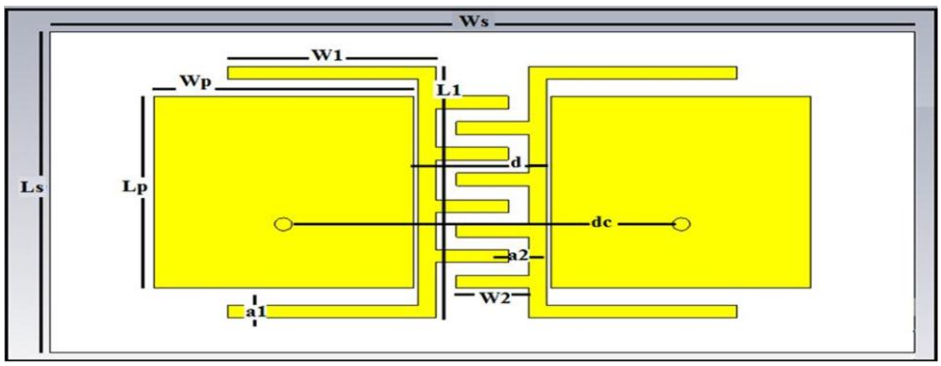

Figure 4.25 Designed antenna elements with proposed LSCW structure.

The LSCW is a copper symmetrical shape consists of two bars with the periodic rows look like a ladder shape surrounding the perimeter of each antenna, printed on the substrate. The prototype of this antenna system was produced in the research laboratories of the Iskenderun Technical University, Turkey, where it was manufactured by the LPKF circuit board plotter as shown in Figure 4.26. The physical realization of the antenna system without and with LSCW structured are described in Figure 4.27. Finally, the measurements were carried out using the N5234A Vector Network Analyzer (N5234A VNA). This is a measuring tool that can be used to measure scattering parameters as a function of frequency. The first step is to make sure that the VNA is specified to work over the frequency range (5-7.5) GHz. Once we know the network analyzer is suitable, we can move on. Next, calibration of the VNA is required. We will take the cables that we are using for probes (that connect the VNA to the antenna) and follow a simple procedure so that the effect of the cables (which act as transmission lines) is calibrated out. To do this, typically the VNA will be supplied with a load which contains a matched load 50 Ω, an open circuit load and a short circuit load. After the calibration procedure is finished, now, connect the VNA to the antenna under test, and set the frequency range interested in on the VNA. In this case, the VNA transmits a small amount of power to the MIMO antenna and measures how much power is reflected back to the VNA. Then, it can plot the measured S-parameters as shown in Figure 4.28. Measurements were conducted in the research laboratories of the Iskenderun Technical University, Turkey.

Table 4.3 Dimensions of the parameters of the MSAs system

Parameter	Ws	Ls	Wp	Lp	W1	W2	L1	a1	d	dc
Dimension (mm)	50	25	15	15	12	4.2	19.6	1	8	23

Figure 4.26 LPKF circuit board plotter that produced the antenna system.

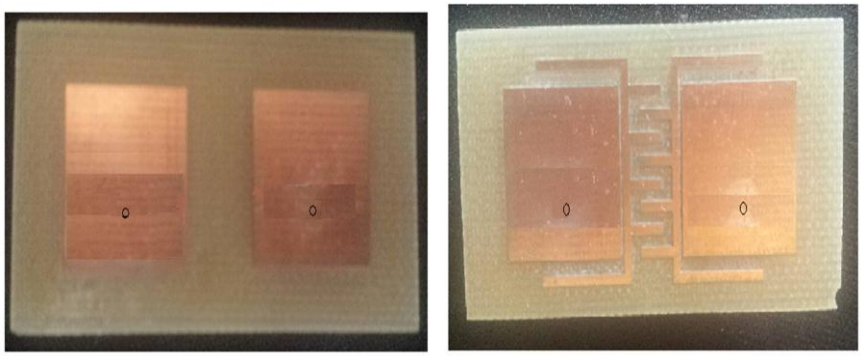

Figure 4.27 Fabricated antenna (a) without LSCW structure (b) with LSCW structure

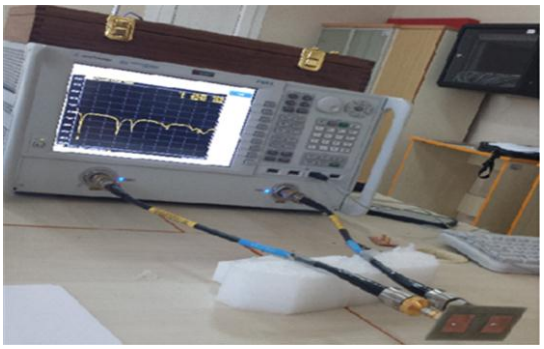

Figure 4.28 Measurement setup for the fabricated antenna system

4.2.2 Simulated Results

A. Mutual coupling and Isolation

In this section, to analyze the performance of the proposed LSCW decoupling structure by inserting it between the MSAs and surrounding the perimeter of each antenna. Figure 4.29 shows the simulated and measured S_{11} and S_{21} comparisons between MSAs with and without the proposed LSCW structure.

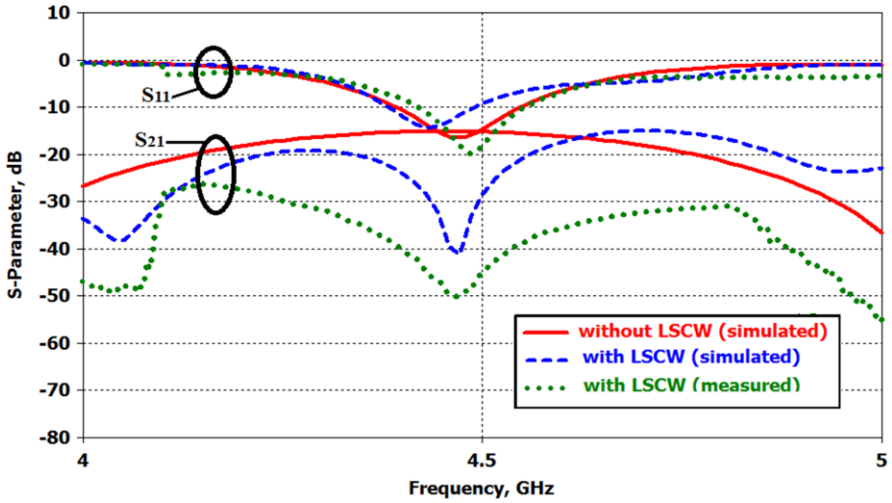

Figure 4.29 Simulated and measured S-parameters with & without LSCW structure.

From Figure 4.29, it can be observed the S_{21} is reduced from −15 to −41 dB at the resonant frequency 4.45 GHz. This means that by introducing the proposed LSCW structure between the antennas, provides a significant improvement in isolation. Furthermore, the S_{21} is below than −20 dB in the operating band (S_{11} lower −10 dB).

B. Surface Current Distributions

Figure 4.30 (a) shows the current distributions on antenna patches when MSAs are placed on the substrate without LSCW structure; it is clear that a huge current is induced on the coupled antenna element on the right side when the antenna on the left side is energized. Huge mutual coupling is created between the two antenna elements. After the proposed LSCW structure is inserted in the middle of the two patch antenna, the current induced in the MSA is significantly suppressed as shown in Figure 4.30 (b), which explains the reason why mutual coupling is suppressed by the proposed LSCW.

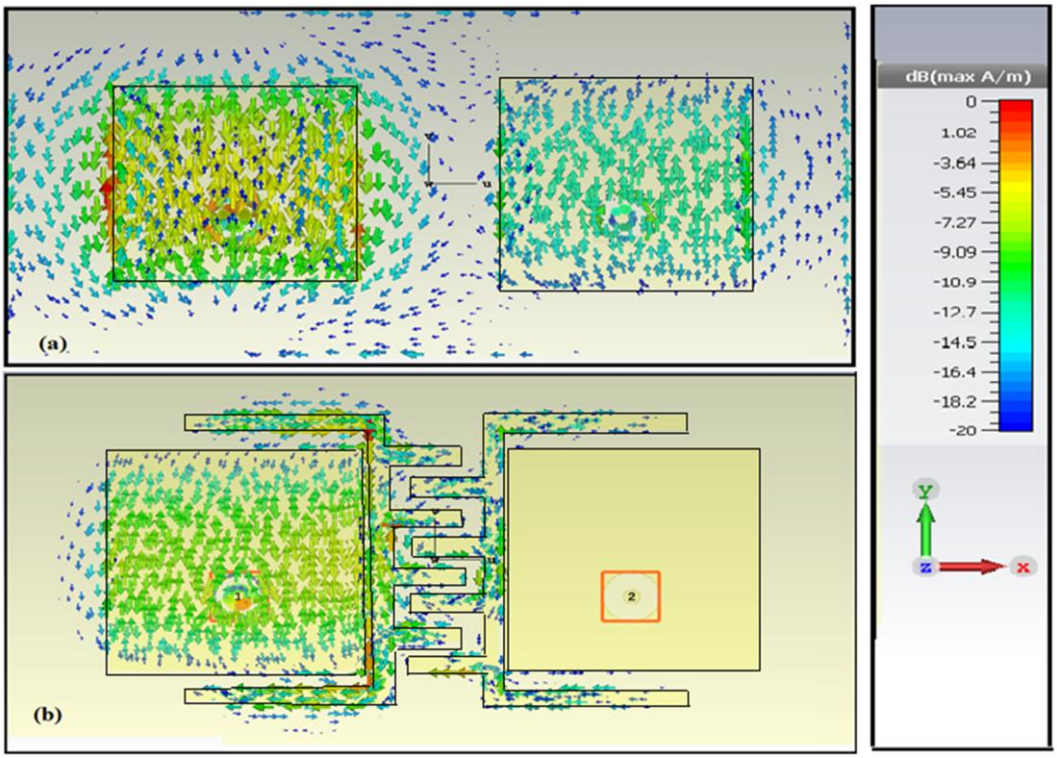

Figure 4.30 Surface current distributions at 4.45 GHz
a) without LSCW structure b) with LSCW structure

C. VSWR

The variation of VSWR of the MSAs system according to the frequency with and without the proposed LSCW structure is shown in Figure 4.31. It is observed that the value of VSWR ≤ 1.5 at resonant frequency 4.45 GHz.

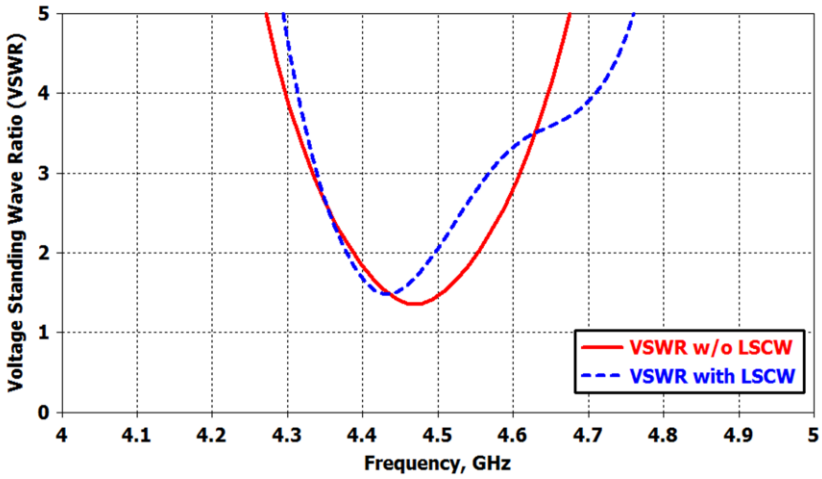

Figure 4.31 Simulated VSWR at 4.45 GHz with and without LSCW structure

D. Diversity Performance

Diversity performance is the critical merit of the MIMO antenna system for mobile communication. A various of typical parameters that commonly used to depict the diversity performance of the MIMO system in a wireless communication system. The most critical parameters that have been used in this section are ECC, DG, and the total efficiency.

The ECC is calculated for both of the MSAs systems using the scattering parameters obtained by measurements and is plotted in Figure 4.32. From the plot, it is evident that at the resonant frequency, the ECC is very low, which highlights the high level isolation between the antennas in the MIMO system. The obtained ECC value at the resonant frequency for the MIMO array system without decoupling structure is 0.00025 and with LSWC structure between the antennas is 0.000078, these quantities are small compared to the ECC value obtained in [10], which is around 0.005.

There is a definite growth in the DG with LSCW as observable from Figure 4.33. The DG of the proposed system with LSCW reaches about 9.89 dB within the frequency band, while the diversity gain of the MIMO system without LSCW is 9.6 dB at the starting off the bandwidth frequency at 4.36 GHz and reduces about 9.55 dB at 4.51 GHz at the end of the bandwidth frequency. Finally, Figure 4.34 describes the simulated total efficiency of the MIMO array in the absence and presence of the LSCW structure. It is clear that the total efficiency shows improvement within the operating frequency band of the antennas with the LSCW

structure. 4.92% antenna efficiency enhancement from 43.63% to 48.55% is obtained by employing the proposed LCSW.

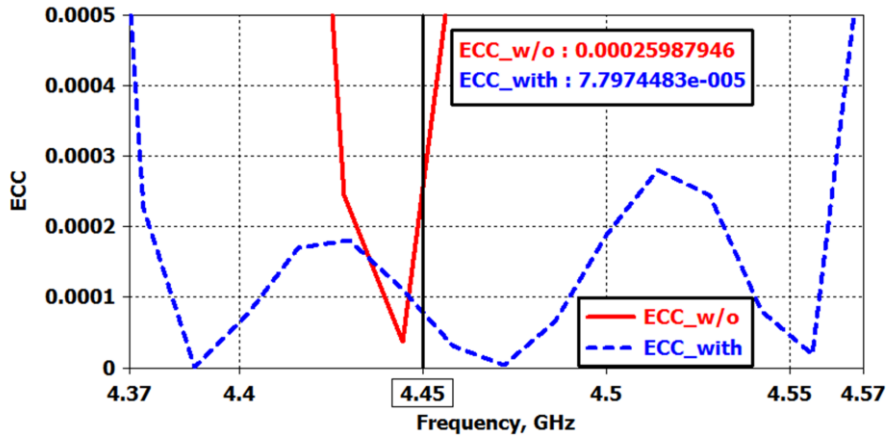

Figure 4.32 ECC of MSAs at 4.45 GHz with and without LSWC structure

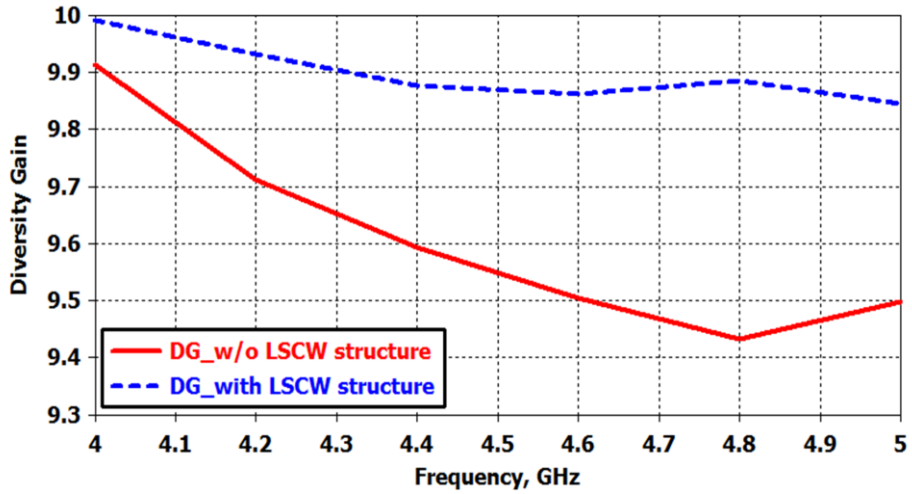

Figure 4.33 DG of MSAs at 4.45 GHz with and without LSWC structure

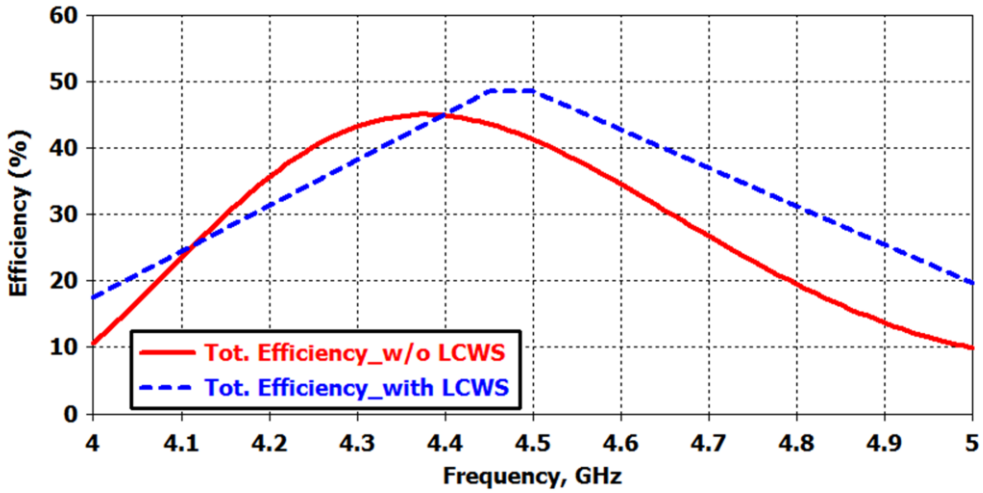

Figure 3.34 Simulated total efficiency of whole MIMO system with and without LSWC structure

e. Radiation Pattern

Simulated polarization 2D radiation patterns of the MIMO system in the E-H planes (x-z and y-z planes) with and without LSCW structure are shown in Figure 3.35, for the case when the 1st patch antenna is excited, and the 2nd patch antenna is terminated with a 50 Ω. It has been noted that the proposed MIMO antenna has a linear polarization, a directive pattern with a moderate side lobe level. In addition, there is no significant difference between the simulated lobe patterns. This suggests that the proposed LSCW structure can be safely used for mutual coupling suppression without altering the radiation characteristics of the antennas.

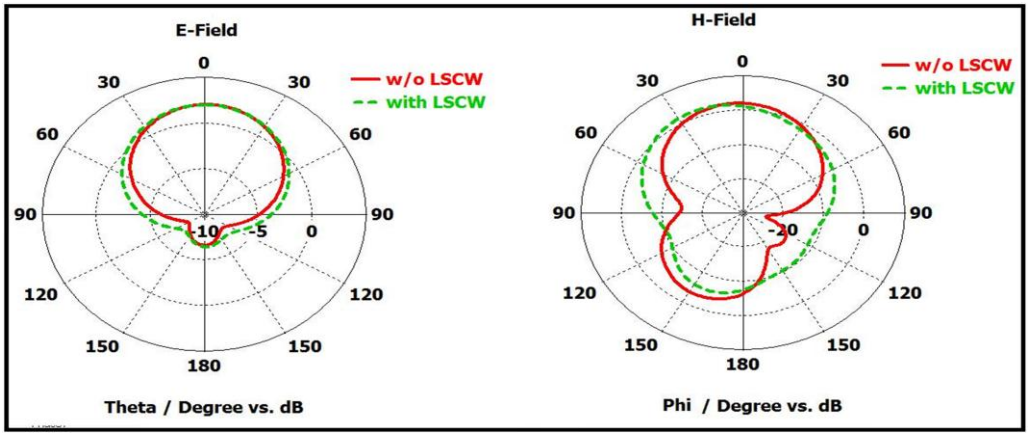

Figure 4.35 Radiation patterns on E-plane and H-plane

4.2.3 Parametric Study

Parametric investigations of LSCW structure are found through parameters sweeps and optimization. The mutual coupling between the patches is influenced by the conducting wall length (W1, L1) which surrounds the edge of each antenna, and the length of periodic row (W2) of the LSCW structure. Figure 4.36 plots S-parameters versus frequency for various W1 sizes from 0 to 16 mm, holding the other dimensions constant. Figure 4.38 shows S-parameters for multiple values of L1 from 18.8 to 21.2 mm, while the other dimensions are constant. In Figure 4.37, S-parameters have been obtained by varying the value of W2 from 4 to 5 mm and fixed the other dimensions. In this design, by means of parameter sweep and optimization, W1, W2 and L1 are adjusted to 12, 4.2, 19.6 mm respectively to give maximum isolation between the patches and to reduce the mutual coupling S_{21} to -41 dB at the resonant frequency 4.45 GHz while maintaining the overall mutual coupling less than −20 dB in the operating band.

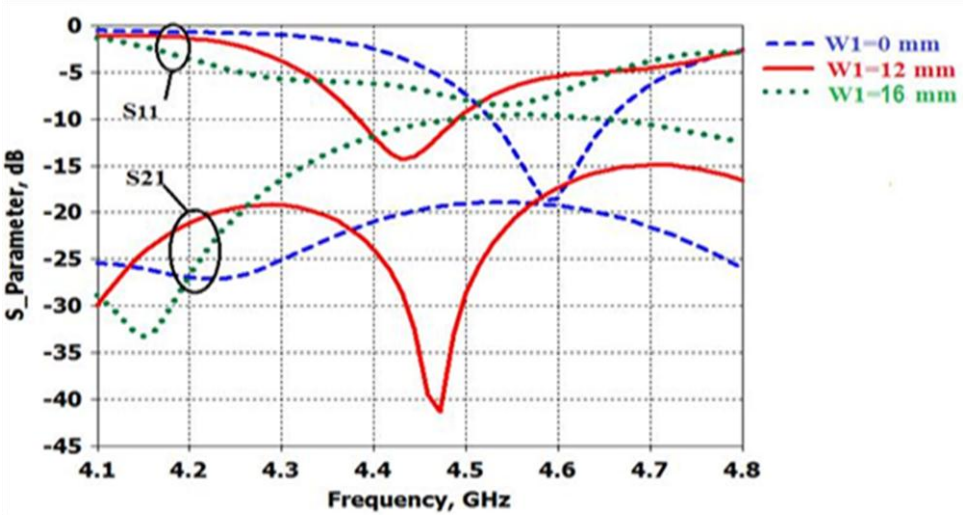

Figure 4.36 S-parameters for various length W1 of LSCW

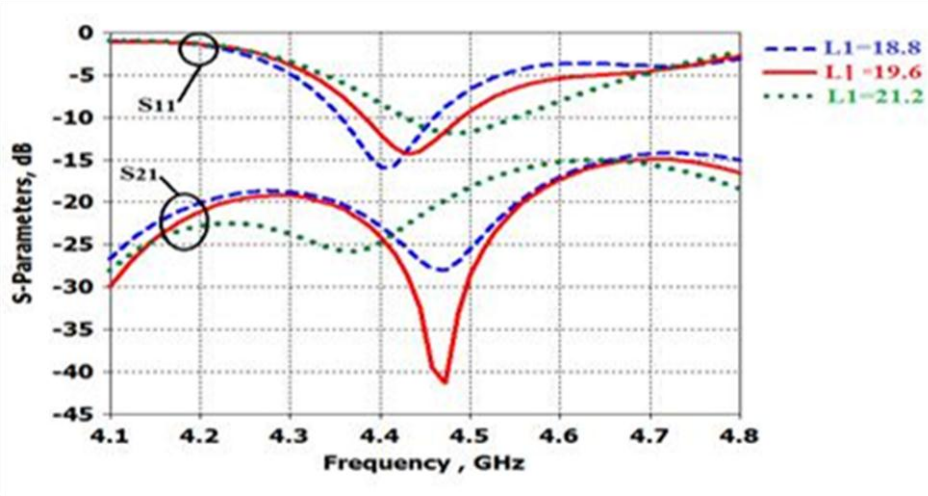

Figure 4.37 S-parameters for various length L1 of LSCW

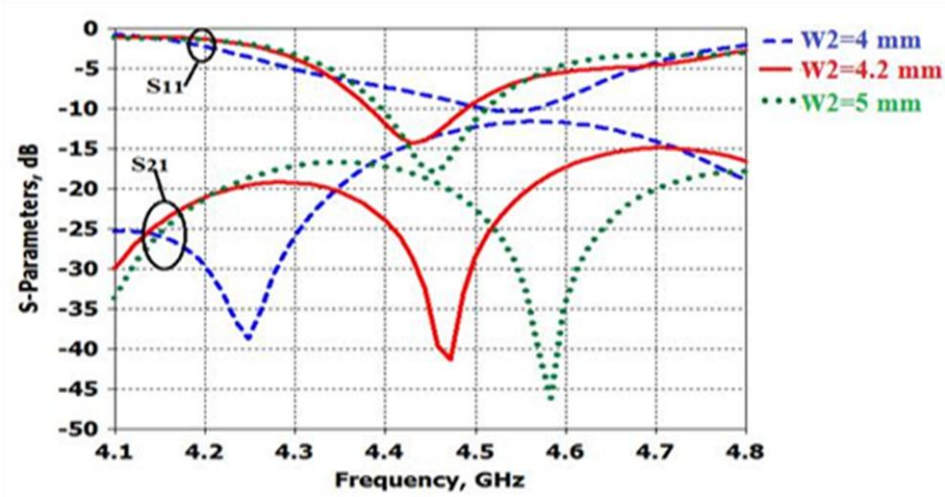

Figure 4.38 S-parameters for various length W2 of LSCW.

On the other hand, if the dimensions of W1, W2 and L1 are adjusted to 16, 5, 21.2 mm, respectively, as shown in Figure 4.39 (a), we can get maximum isolation between the patches and reduction in mutual coupling S_{21} from (-14.4 to -37) dB at

the resonant frequency 10.3 GHz. This antenna is compatible with radiolocation applications in X-band (8–12 GHz).

The picture of the fabricated prototypes is depicted in Figure 4.39 (b). Figure 4.40 shows the comparison between the simulated and experimental S-parameters with and without the proposed LSCW structure. It's seen that there is a good match between the results.

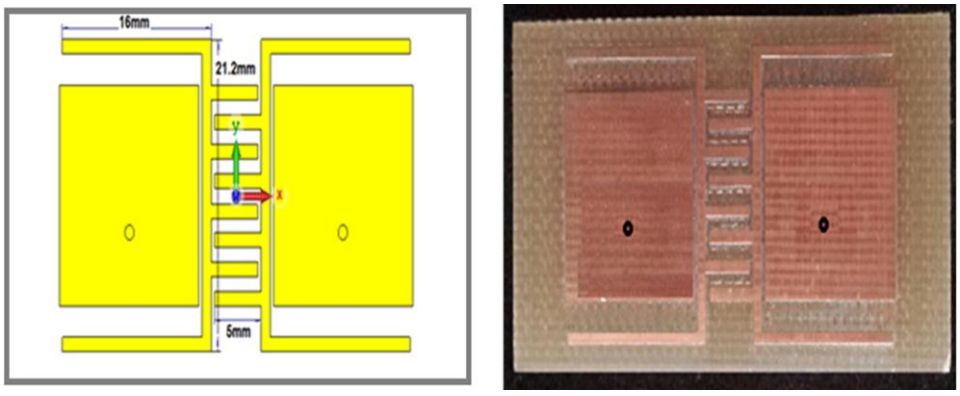

(a) (b)

Figure 4.39 a) The proposed MIMO system at 10.3 GHz,
b) Fabricated antenna

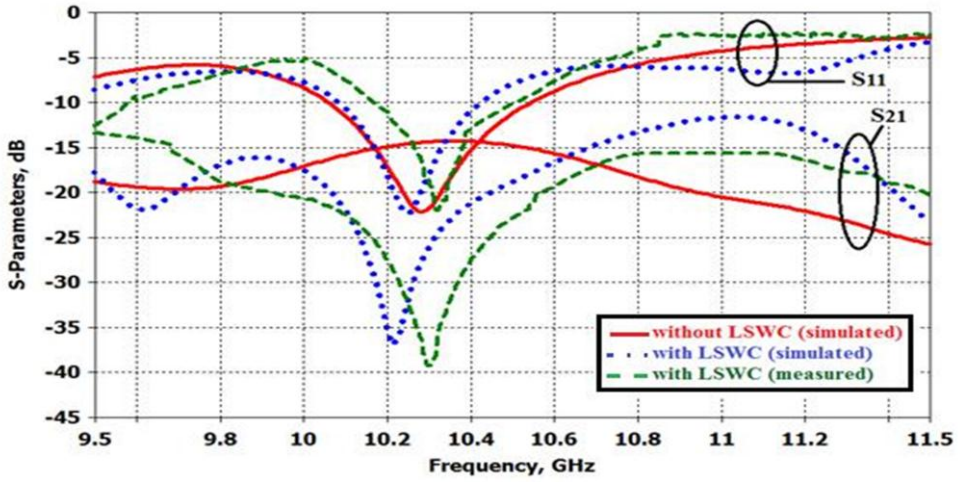

Figure 4.40 Simulated and measured S-parameters with & without LSCW structure at resonant frequency 10.3 GHz.

The surface current is suppressed by the introduction of LSCW structure in the middle of antennas when the 1st patch antenna is excited as shown in Figure 4.41. It is evident that the isolation between MSAs have been improved when the proposed LSCW structure is presented. Figure 4.42 shows the VSWR of proposed antenna. It is clear that the value of VSWR $\leq$ 1.5 around the operating frequency 10.3 GHz. The ECC and DG were estimated for MSAs system with and without LSCW structure. The ECC for MSAs systems is plotted in Figure 4.43. It can be deduced that the

ECC lower than 0.0001 at the resonant frequency in both cases, it is pretty good, whereas Figure 4.44 depicts the DG. It is obvious that the DG approached 9.99 in both cases (with and without LSCW structure) at the resonant frequency 10.3 GHz. This demonstrates the most extreme DG is gotten when the ECC is almost zero. Finally, Figure 4.45 illustrates the 2D radiation patterns in E-H planes (x-z and y-z planes) of the designed MIMO antenna at 10.3 GHz. It is evident that the overall shape of the radiation patterns of the MIMO array was not significantly affected when executing the LSCW structure between the two antennas.

Figure 4.41 Surface current distributions at 10.3 GHz with LSCW structure

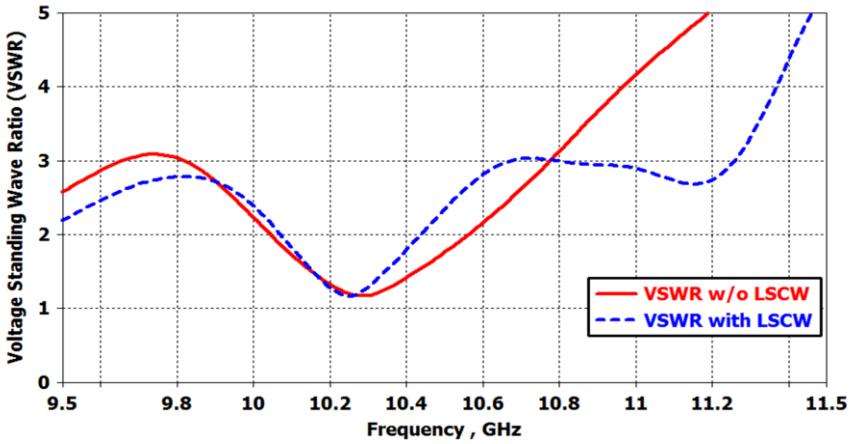

Figure 4.42 Simulated VSWR at 4.45 GHz with and without LSCW structure

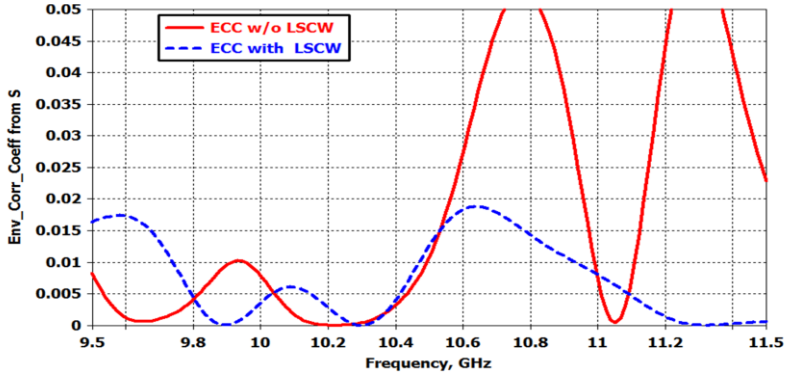

Figure 4.43 ECC of MSAs at 10.3 GHz without and with LSWC structure

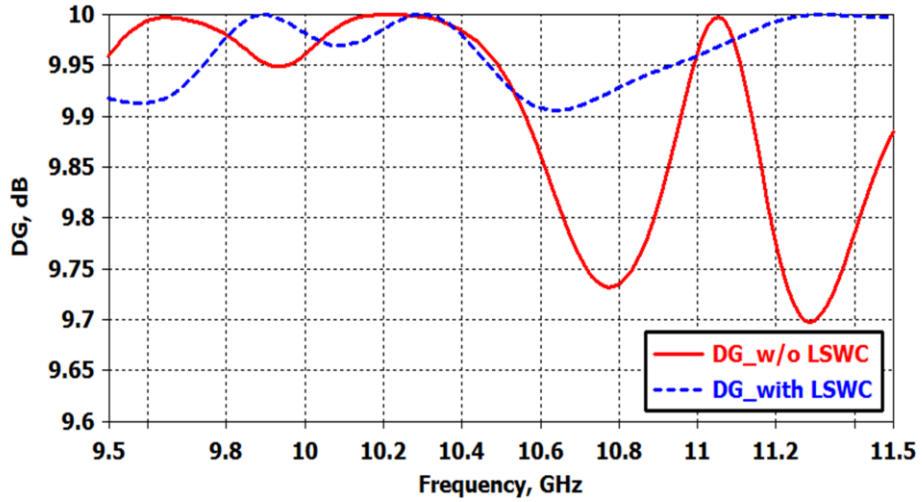

Figure 4.44 DG of MSAs at 10.3 GHz without and with LSWC structure

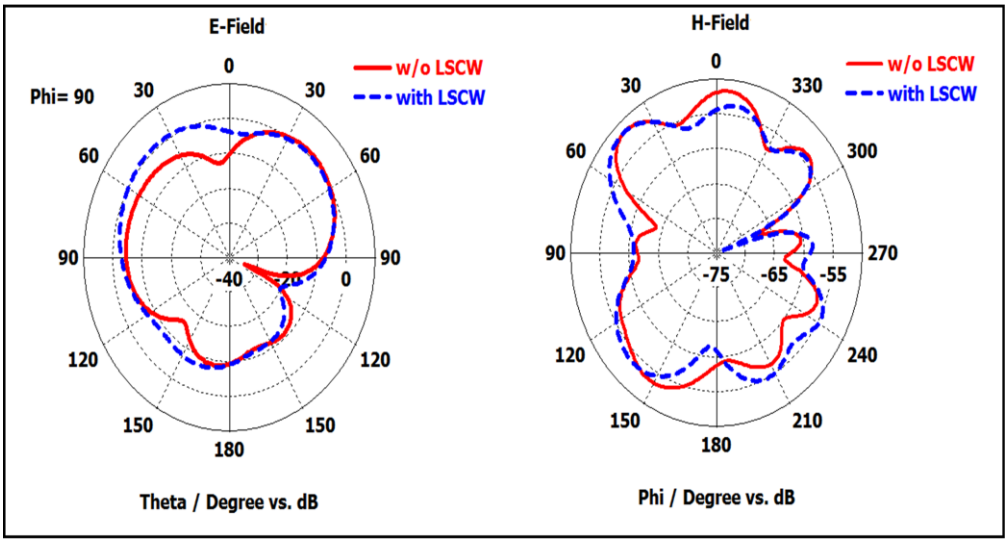

Figure 4.45 Radiation patterns on E-plane and H-plane

Comparing the performance of the prototype MIMO antenna with that of previously proposed designs in the literature are depicted in Table 4. It is evident from Table 4 that the proposed decoupling structures (LSCW) lead to better isolation enhancement with a shorter edge to edge separating distance between the two antennas and smaller size of the array.

Table 4.4 Comparison between the proposed array and other designs from the literature

Paper	Approach	Frequency, f_o (GHz)	Edge to Edge Spacing (mm)	Enhancement in S_{21} at f_o (dB)	DG	Size of the Array (mm^2)
[24]	double-size EBG plus rectangular DGS	2.6 & 5.7	13.3	20 & 5	-	10.6x67.2
[28]	S-shaped periodic DGS	2.75	23	40	-	70x80
[29]	C-shaped resonator & C-shaped slot DGS	2.78 & 4.12	7	18 & 10	-	75x60
[33]	SCCSRR metastructure	3.7	13.8	14.6	-	44.1 x74.19
[34]	2 × 3 matrix of C-shaped	6.3	20	30	9.99	100x41
This Design	ladder-shaped conducting wall structure (LSCW)	4.45 & 10.3	8	50 & 40	9.87 & 9.99	50 x 25

4.3 Mutual Coupling Suppression Between Two Printed Monopole Arrays Using Spiral Defected Ground Structure (SDGS)

A novel compact monopole array with SDGS is designed to mitigate the mutual coupling and enhancement the isolation. The proposed SDGS composed of spiral square slots etched from the extending ground plane. Antenna system operating from 4 -7 GHz is recommended for wireless applications in C band. The edge to edge separation between the antennas is taken as $0.3\lambda_o$ at 5 GHz. With a view to evaluating the reliability and diversity performance of the proposed MIMO system, the critical parameters such as mutual coupling, surface current distribution, ECC, DG have been simulated. A good compatible have been obtained between the simulation and the experimental results, with employing of the SDGS, the measured mutual coupling of the array has been reduced efficiently exceeded 50 dB.

4.3.1 Antenna Design

The architecture of the proposed MIMO system is demonstrated in Figure 4.46. The two antennas are a printed monopole antenna, operating around 5 GHz; this operating band is suitable for many wireless applications in C band (4 to 8 GHz). The antennas are placed on FR4 substrate having dielectric constant $\varepsilon_r = 4.3$ with a loss tangent of 0.025 and thickness h=1.6 mm. The edge to edge distance between the antennas in the MIMO system is taken as d = 18 mm (merely 0.3 λ_0). The resonant antenna behavior is optimized for the extending ground plane dimension at

21 mm. The gap (g) between the radiating antenna elements and the edge of ground plane influences the impedance bandwidth. Therefore g is optimized at 1 mm. The overall dimension of the proposed MIMO antenna system is of $70 \times 70 \times 1.6$ mm^3.

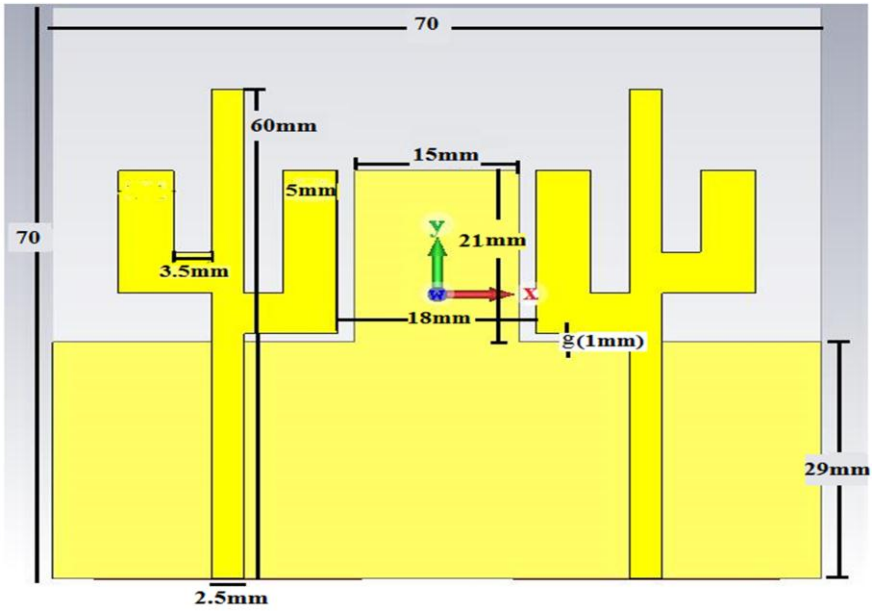

Figure 4.46 The proposed MIMO system

The simulated S-parameters of the proposed MIMO system are shown in Figure 4.47. The MIMO system provides S_{11} around 17 dB at the resonant frequency. In this research, the primary goal is to focus on the S_{21}, where it was found to be −10 dB around the resonant frequency.

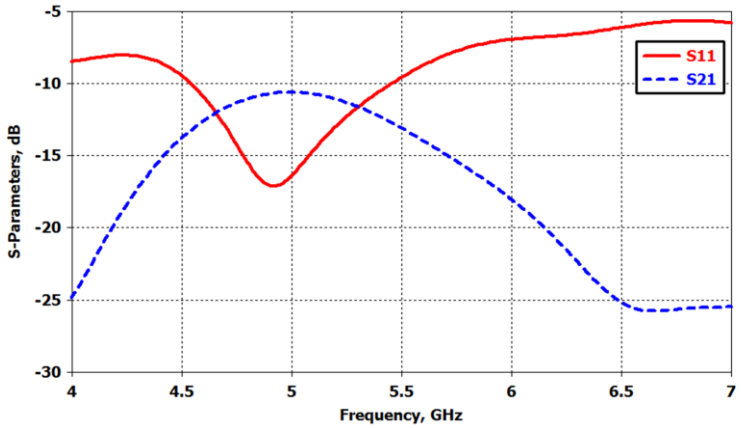

Figure 4.47 Simulated S-parameters of the proposed MIMO.

4.3.2 Antennas System Performance

4.3.2.1 Mutual Coupling and Isolation

The proposed SDGS structure is etched in the extended ground plane of the monopole array. The final optimized structure and dimensions are depicted in Figure 4.48. The simulated S-parameter with and without the SDGS are shown in Figure 4.49, to measure the mutual coupling effect; the S_{21} among the printed monopoles is specified. It is notable that the proposed SDGS contribute to a marked increase in the isolation of from -10 to -48 dB. Meanwhile, etching SDGS out from the ground plane leads to slightly shift the resonant frequency. This is because of the etched SDGS, and the monopole antennas are in a proximity which creates the slow-wave effect and disturbs the impedance matching, occurring in the frequency shift from 4.9 GHz to 5.2 GHz [48, 54]. In order to verify the results that achieved from simulations, a prototype MIMO antenna was manufactured. The measurements are carried out using the Agilent N5234A. The fabricated prototype and measurement set up of the developed antenna system are shown in Figure 4.50 and Figure 4.51 respectively, the setup and calibration details were mentioned in section 4.2.1. The comparison between measured and simulated S-parameters of the two monopole array are shown in Figure 4.49. From Figure 4.47, the developed antenna system gives isolation of 10 dB between the two antennas. In this section, by observing Figure 4.49; it can be noticed that the coupling coefficient S_{21} of the array with the SDGS exceeded 50 dB. The SDGS contributed to the enhancement of the isolation about 40 dB. Thereby, With this result, the necessary condition is achieved that the mutual coupling between the two array elements is to be below than -20 dB for best performance of the MIMO system in the range of C band. This configuration improves the isolation between the two antennas by making the ground plane itself provides the filter impact. This impact can provide a lower mutual coupling between the antennas through suppressing surface wave propagation. However, etching SDGS out from the ground plane shifts the resonant frequency somewhat. This shifting can be because of the deficiency in the fabrication procedure which cannot be avoided entirely.

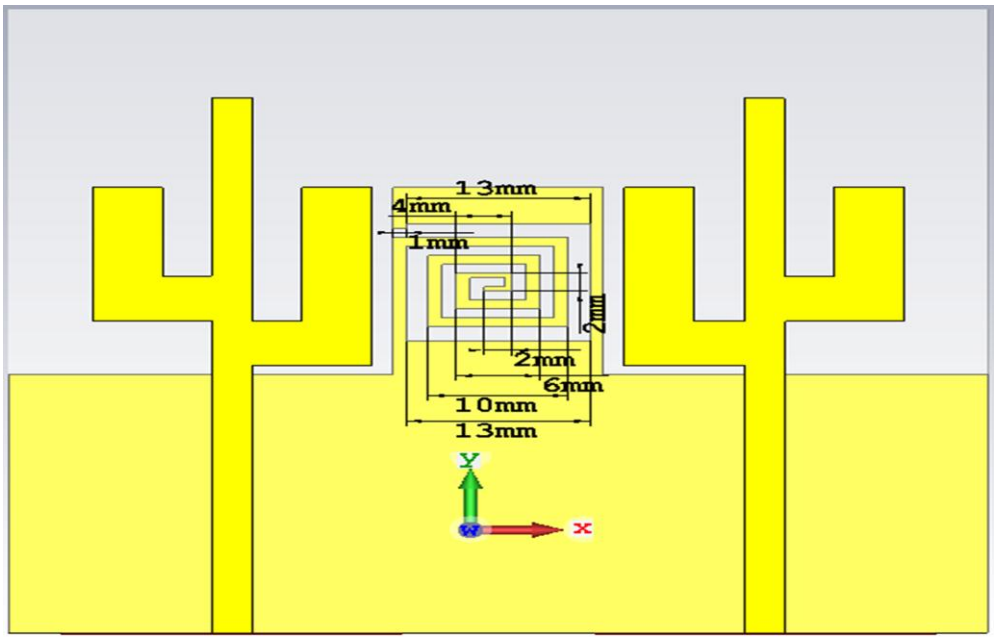

Figure 4.48 The MIMO system with SDGS.

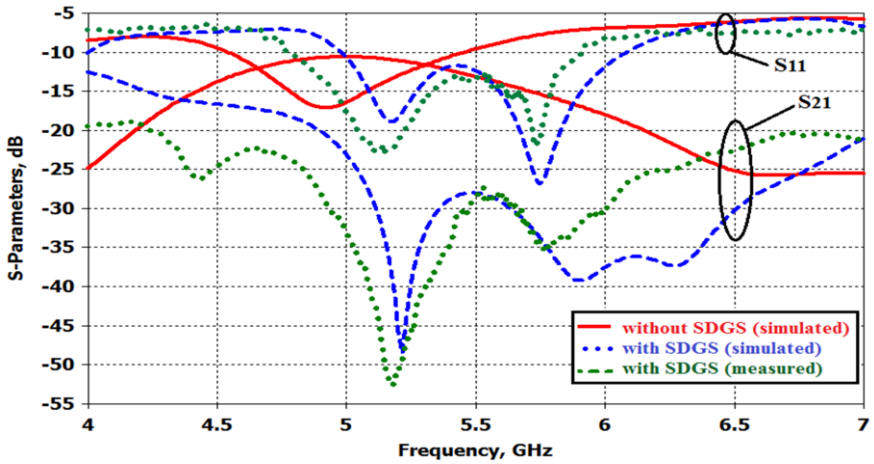

Figure 4.49 Simulated and measured S-parameters with & without SDGS.

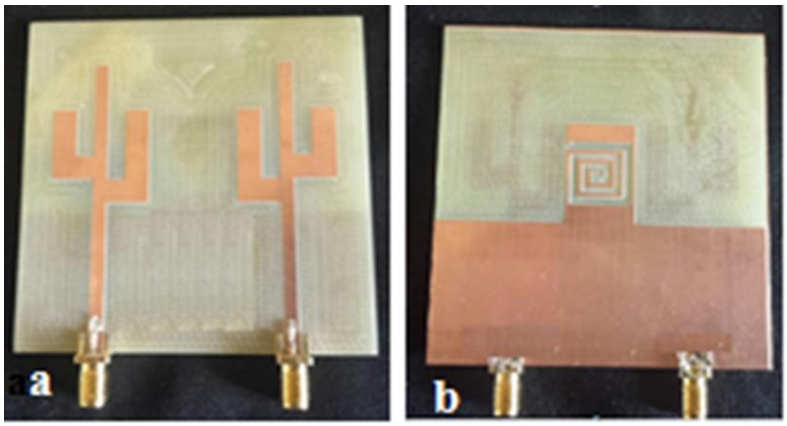

Figure 4.50 The fabricated prototype of the printed array with SDGS section.(a) the top view; (b) the bottom view.

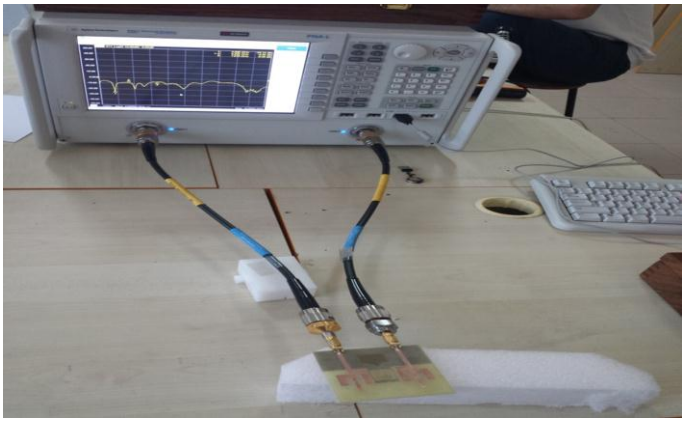

Figure 4.51 Measurement setup for the fabricated antenna system

4.3.2.2 Surface Current Distributions

The surface current distributions on the antenna elements and the ground plane layer for the situation in which 1st antenna (number 1) is energized whereas the 2nd antenna (number 2) is terminated with a 50-Ω load are shown in Figure 4.52. It is evident that the impact of SDGS on the isolation; without SDGS, high surface currents are induced on the 2nd antenna, while when it exists, only weak surface currents are induced on the 2nd antenna. In other words, the coupling current on the ground plane produced by surface waves and space waves is progressively reduced when the SDGS has been etched in the ground plane.

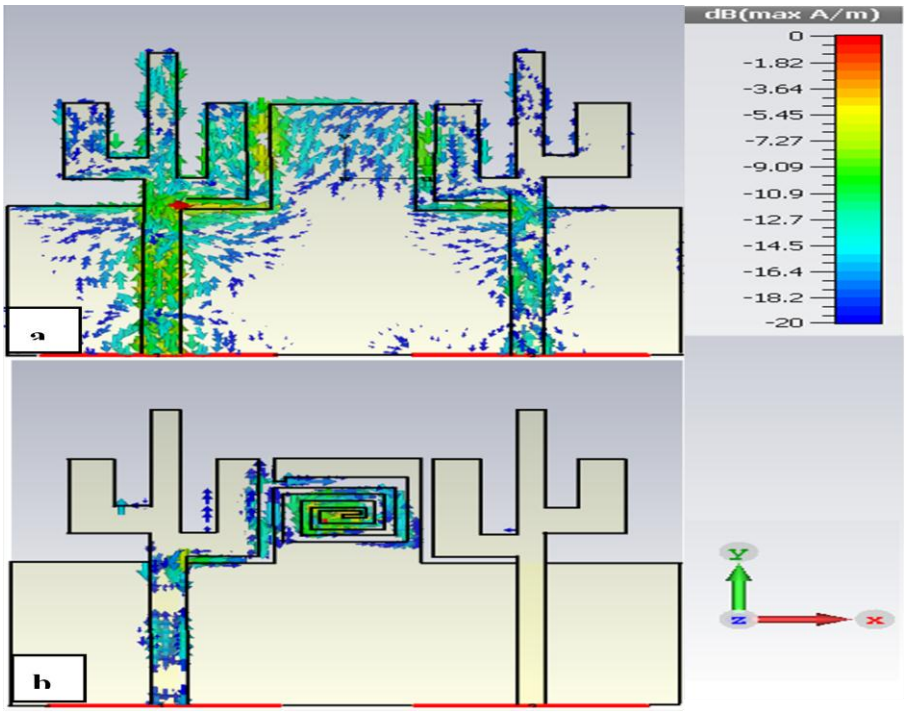

Figure 4.52 Surface current distributions with SDGS.

4.3.2.3 Diversity Performance

The diversity performance of the proposed MIMO system is described in terms of the ECC, DG, and total efficiency. Figure 5.53 shows the plot of ECC over the frequency range. Generally, it is viewed as that antenna with a correlation coefficient under 0.3 has the ability to provide a rich diversity performance [13]. From the plot, it is clear that the ECC for the proposed MIMO array is 0.001 that is quite suitable.

There is a definite improvement in the DG with SDGS, as observed from Figure 5.54. The DG of the proposed system with SDGS reaches about 9.99 dB within the frequency band, while the DG of the MIMO system without SDGS equals 9.76 dB at the starting off the bandwidth frequency at 5 GHz and rises about 9.99 dB at 6.1 GHz at the end of the bandwidth frequency.

The next diversity parameter is total efficiency. For the proposed MIMO system the total efficiency with and without SDGS is plotted in Figure 4.55. It is obvious that the total efficiency increases within the operating frequency band of the MIMO antenna with the proposed SDGS structure. About 22% antenna total efficiency enhancement from 55% to 77.18% is obtained by employing the proposed SDGS.

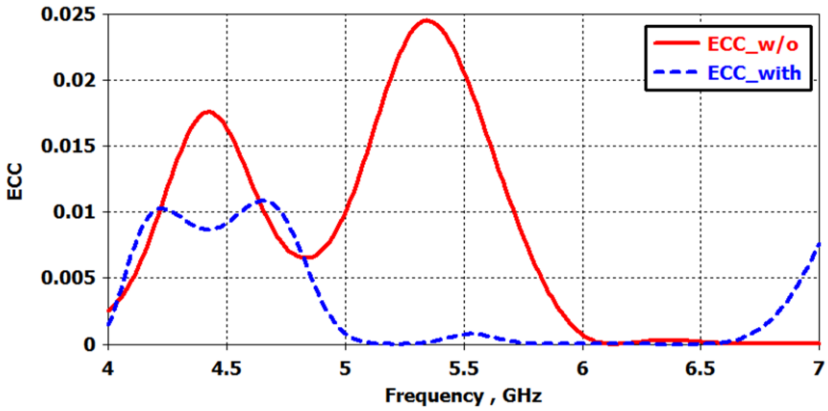

Figure 4.53 ECC of printed monopole array without and with SDGS

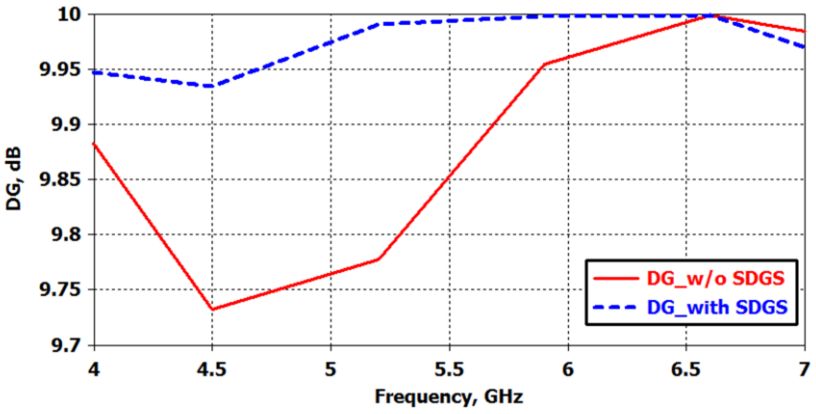

Figure 4.54 DG of printed monopole array without and with SDGS.

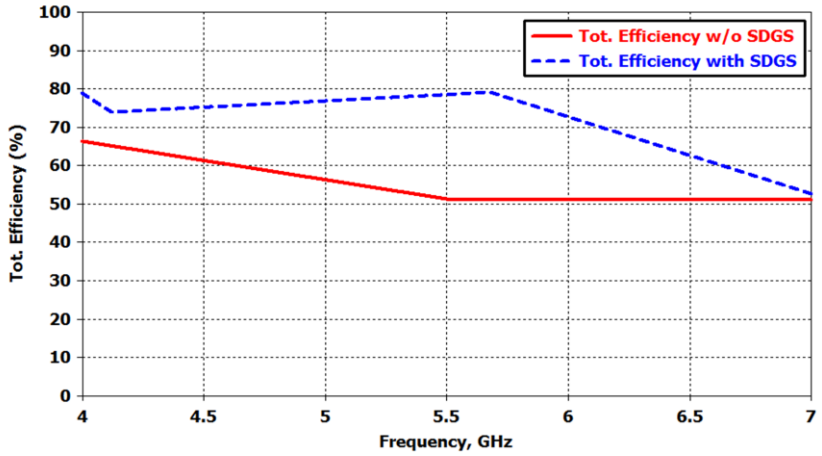

Figure 4.55 Simulated total efficiency of whole antenna system with and without SDGS section

4.4 Isolation Improvement of Dual-Band Planar Compact MIMO Monopoles Using Metamaterial Structure

A systematic design of planar MIMO monopole antennas with markedly mutual coupling suppression depending on the MTM concept is presented. The design performed by MTM resonator, inserted in the space in the middle of the two antenna elements. The basic concept is that the MTM structure acts as a small MTM sample, thus affording an active means of dominating the electromagnetic wave propagation that contributes to suppressing mutual coupling. The proposed configuration accomplishes extensively high levels of isolation between the two antenna elements, without mainly influencing the simplicity and planarity of the MIMO antenna. The results show that the proposed antenna can provide dual-band operation between 6.2-6.727 and 8.85–9.57 GHz to achieve 6.5/9.25 GHz frequencies for VSWR less than 2, can be widely used for WiMAX applications. The measured results prove that the isolation in the middle of the antenna ports has been enhanced about 40 dB and 19 dB respectively at the two operating frequencies with the presence of the proposed MTM structure. The ECC is below 0.05 and DG is almost 10 for all two bands.

4.4.1 Antenna Design

The planar MIMO array that has been chosen geometrically as simple as possible. It's composed of two standard microstrip-fed planar monopoles as seen in Figure 4.56; they are mounted on a FR-4 substrate having dielectric constant ε_r = 4.3 with a loss

tangent of 0.025 and thickness h = 1.6 mm. The edge to edge distance between the two antenna elements is taken as 20 mm.

A prototype of this antenna system is shown in Figure 4.57. The measurement set up of the developed antenna system is shown in Figure 4.58 (the setup and calibration details were mentioned in section 4.2.1). The comparison between the simulated and measured S-parameters results of the proposed MIMO system are shown in Figure 4.59. From the simulated results for the S-Parameters (reflection coefficient S_{11} and mutual coupling S_{21}), it is obvious that the antenna exhibits two resonances around 6.5 and 9.25 GHz. It is also noticed that the magnitudes of the mutual coupling S_{21} are about -20 dB and -19 dB at the two operating frequencies, respectively. Comparison of the experiment and the simulation results presents a good match. The mutual coupling from the measurements is higher compared to the simulation at 6.5 GHz. This serves the purpose of our study to improve the mutual coupling and enhancement the isolation depending on metamaterial properties as explained in the next section.

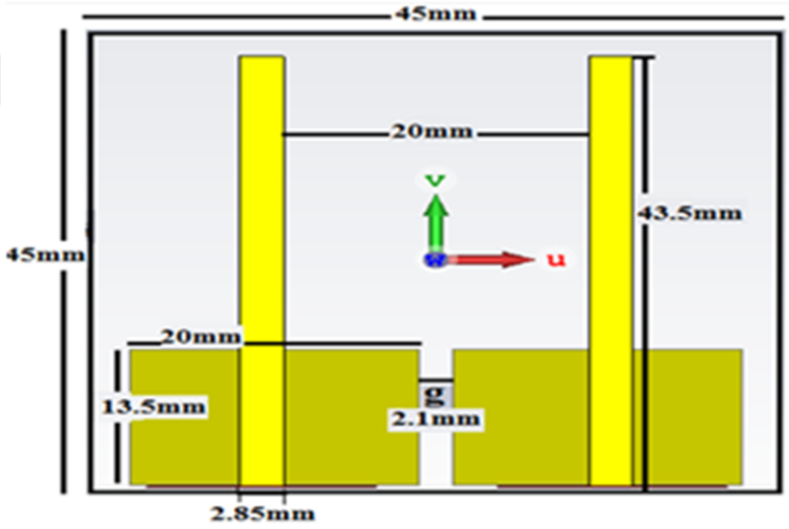

Figure 4.56 The proposed MIMO system.

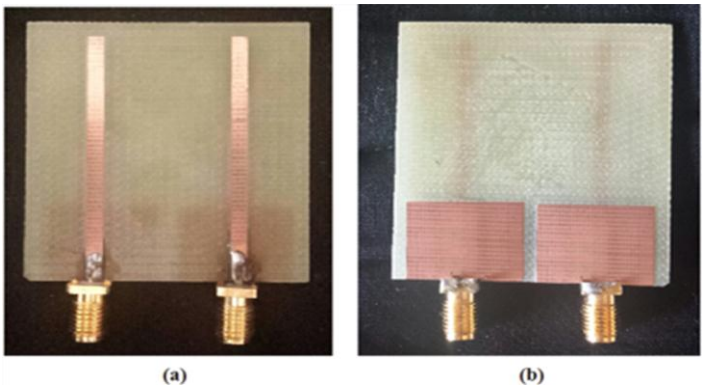

Figure 4.57 A prototype of the fabricated antenna
a) top view b) back view.

Figure 4.58 Measurement setup for the fabricated antenna system.

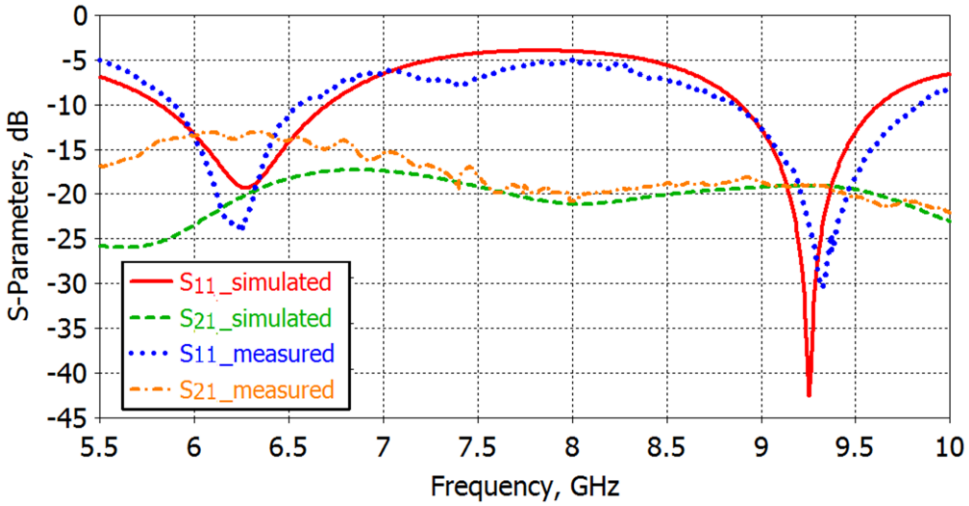

Figure 4.59 Comparison between the simulated and the measured S-parameters results

4.4.2 Analysis of MTM Resonator

The next step requires the design of the resonator structure have metamaterial properties to be placed between the antennas to suppress the mutual coupling and enhance the isolation of MIMO systems.

Figure 4.60 shows the geometrical configuration of the proposed MTM structure. The Nicolson-Ross-Weir (NRW) method is used to determine the effective permittivity ε and permeability μ using measurements of the S_{11} and the S_{21}. Albeit different kinds of resonators could be utilized for this reason, we have picked this structure. In this manner, with the proposed structure a time-varying magnetic field vertically mounted on the ring's surface leads to excites the surface currents depending on the resonant properties of the MTM structure, then create a magnetic field that may either oppose or enhance the incident field, thus resulting in positive or negative effective μ and/or ε [15]. The MTM structure geometric parameters should be carefully selected to appear the properties of a small MTM sample. Figure 4.61

shows the double negative properties (negative ε and negative μ) of the proposed MTM structure in the frequency band of interest around the operation frequency. In other words, it shows a wideband metamaterial behaviour.

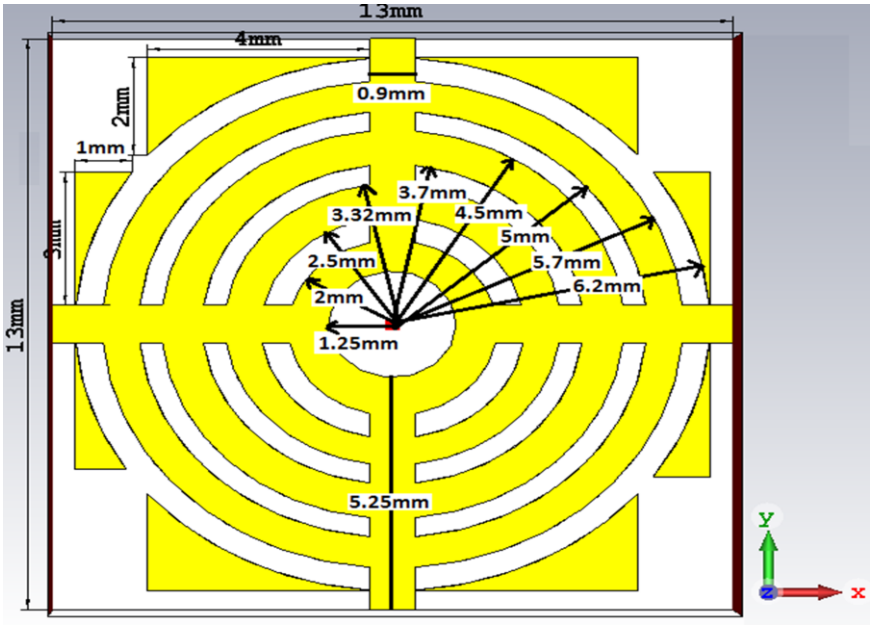

Figure 4.60 Perspective view of the MTM structure.

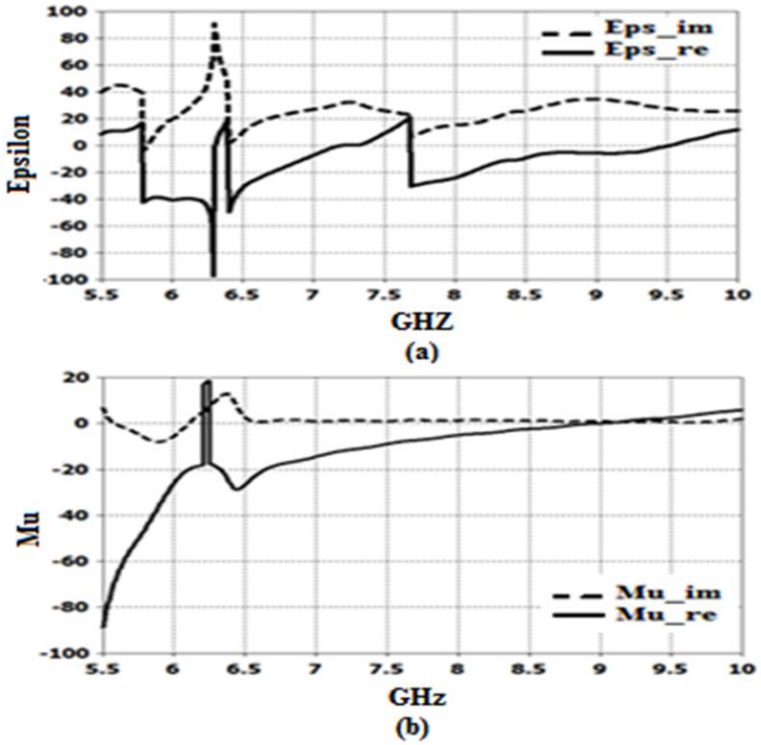

Figure 4.61 a) permittivity, b) permeability

4.4.3 MTM-Enhanced MIMO Antennas

In this section, the proposed decoupling technique is utilized to enhance the isolation of a MIMO system by placing MTM structure in the middle of the elements of the MIMO antennas, as shown in Figure 4.62 (a). Figure 4.62(b) illustrates the simulated S_{11} and S_{21} of antenna elements with and without the proposed MTM structure. It is clear that the port isolation is increased by 14 dB at the lower frequency 6.25GHz and about 16 dB at the higher frequency 9.25 GHz.

The prototype of the MIMO antenna system is printed as shown in Figure 4.63. Figure 4.64 illustrates the simulated and experimented S-parameters with the MTM structure of the proposed MIMO system. It can be seen that the simulation results agree well with the measurement results, although with a slight frequency shift. It is also noticeably shown in the figure that the experimented mutual coupling has been decreased about 34 dB at 6.25 GHz and 11 dB at 9.25 GHz.

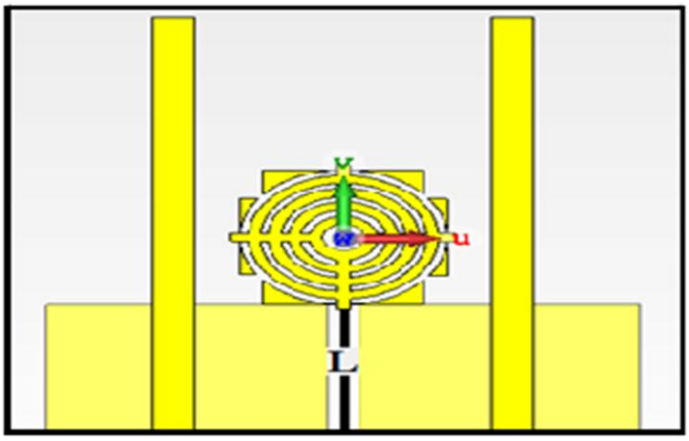

(a)

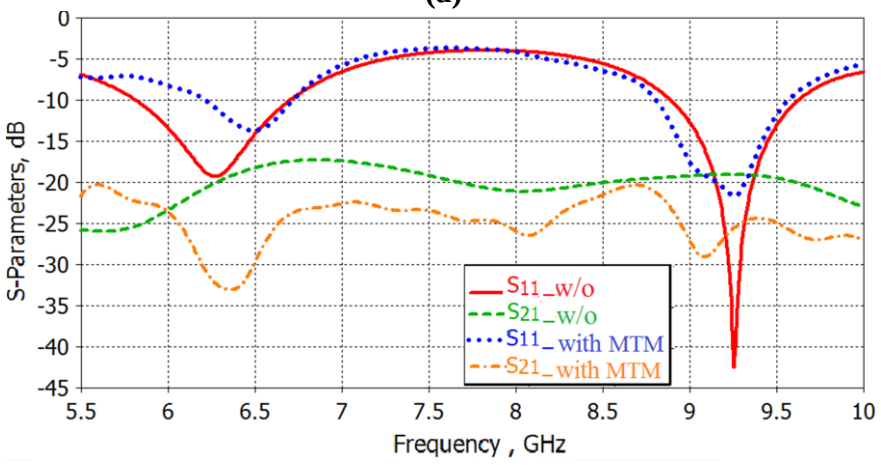

(b)

Figure 4.62 a) MIMO System with MTM structure.
b) Simulated S-Parameters with & without MTM structure.

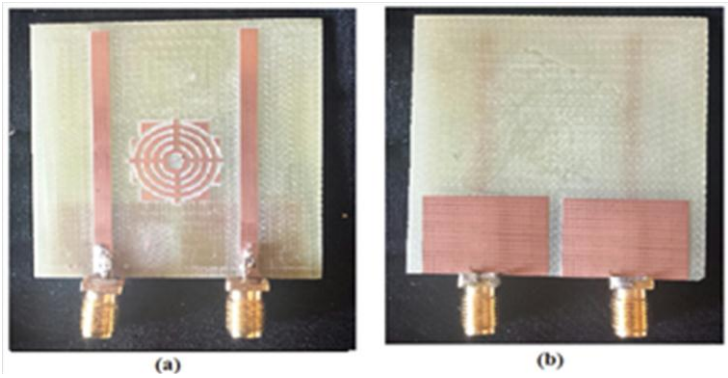

Figure 4.63 A prototype of fabricated antenna a) top view b) back view

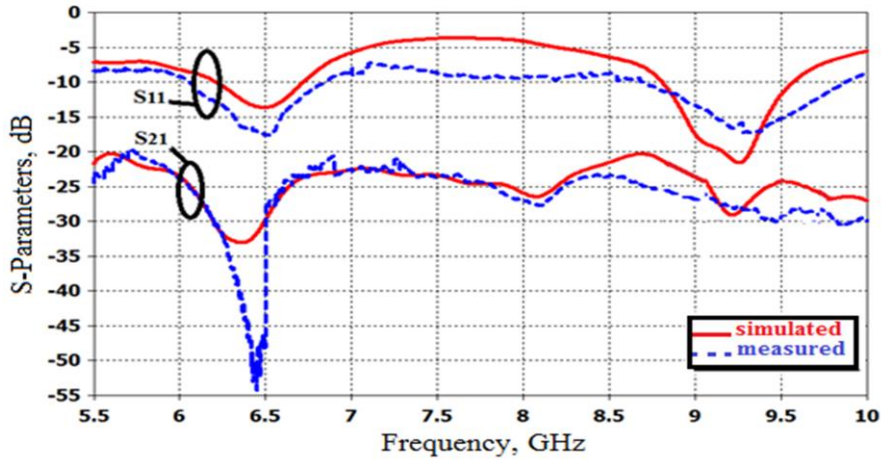

Figure 4.64 Simulated and expreimented S-parameters with MTM.

4.4.3.1 Parametric Study

Parametric investigations of MTM structure are found through parameters sweeps and optimization. The mutual coupling between the monopoles antenna is influenced by the distance (L) from the lower edge of the MTM structure to the lower edge of the substrate. Figure 4.65 shows S-Parameters versus frequency for various values of (L) from 0 to 19 mm. From the figure, it is evident that the proportionate position of the MTM structure does affect on S_{11} and the S_{21} of the MIMO System. When L = 13 mm, the achieved enhancement in port isolation is more than 34 dB and 11 dB at the 6.5 GHz and the 9.25 GHz, respectively as shown in Figure 4.62(b).

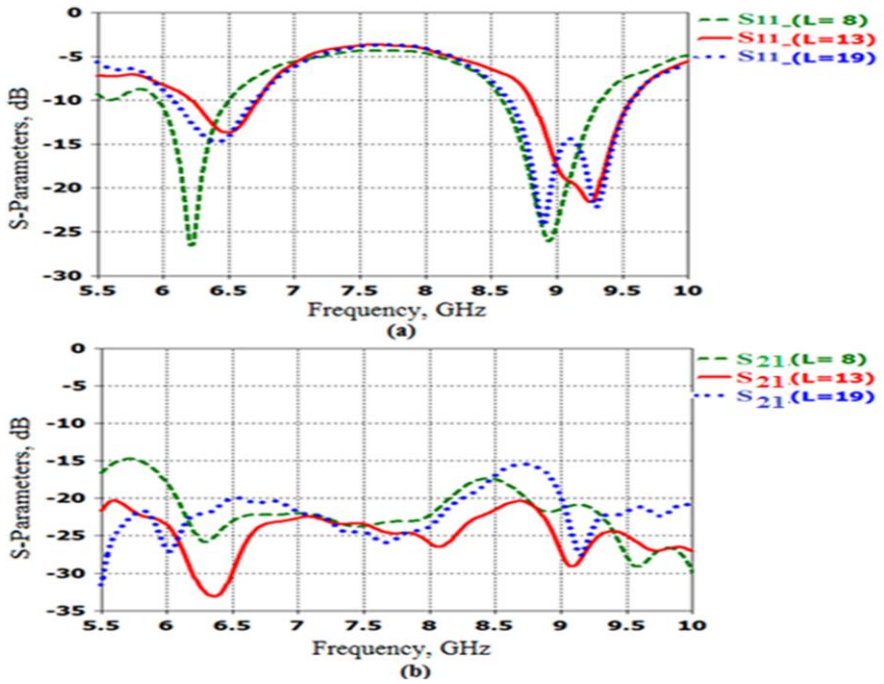

Figure 4.65 Parameter for various distance of (L), a) S11, b) S21

4.4.3.2 Current distribution

In order to have a clear conception of the propagation mechanism that responsible of mutual coupling, the current distribution on MIMO array at 6.5 and 9.25 GHz had been investigated as shown in Figure 4.66 and Figure 4.67 receptively. In the case in which 1st antenna (left side) is excited while the 2nd antenna (right side) is terminated with a 50-Ω load. It is obvious that the isolating effect of the MTM structure; without it, great surface currents are induced on the 2nd antenna, while when it introduced, just weak surface currents are induced on the 2nd antenna at both frequencies 6.5 and 9.25 GHz.

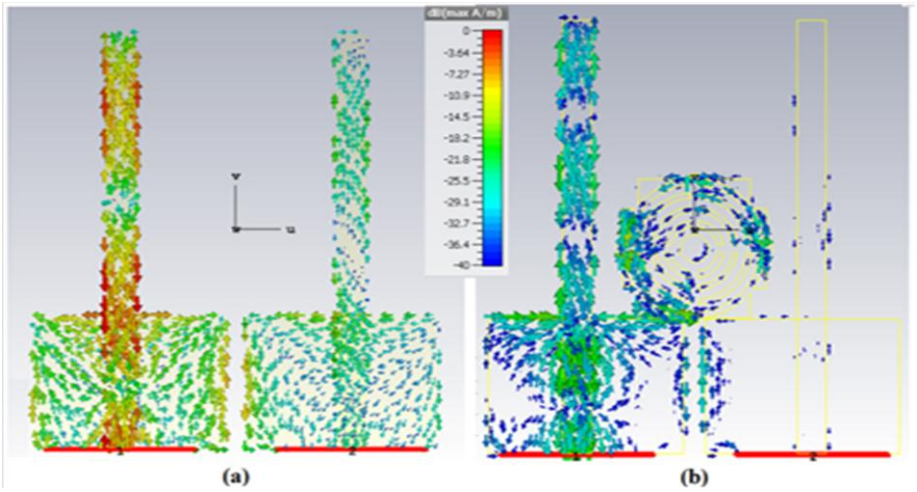

Figure 4.66 Current distribution at 6.5 GHz a) without MTM structure, b) with MTM structure.

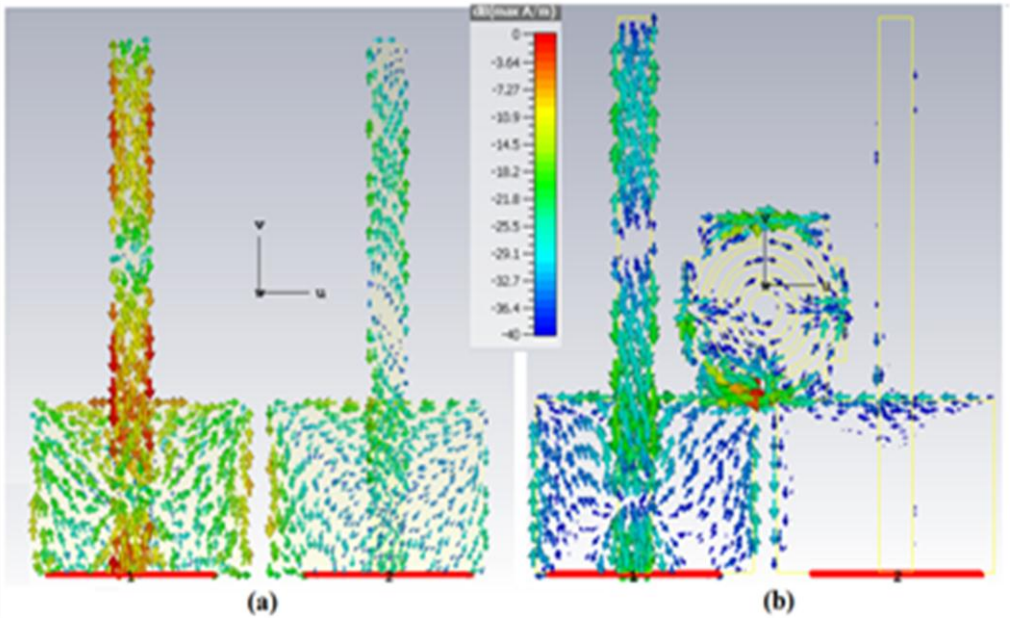

Figure 4.67 Current distribution at 9.25 GHz a) without MTM structure, b) with MTM structure.

4.4.3.3 Diversity performance

ECC is plotted in Figure 4.68, with and without MTM structure between the antennas. It can be observed that the ECC is very low at the tow resonant frequencies (6.25 and 9.25) GHz, which indicates the good isolation in between the two antennas in the MIMO system can be achieved. Moreover, it which means that the antenna array has good spatial diversity and is suitable for MIMO applications. From Figure 4.69, it is obvious that the DG of the proposed MIMO system with MTM has been improved.

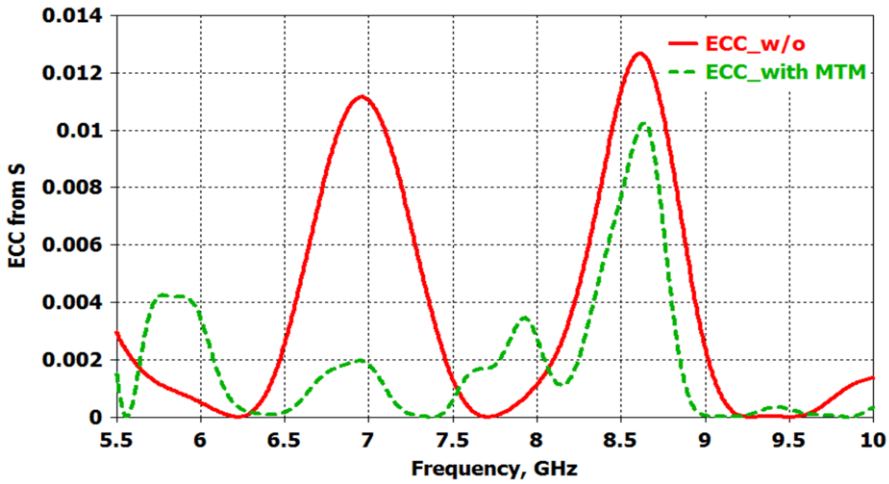

Figure 4.68 ECC of MSAs without and with MTM structure.

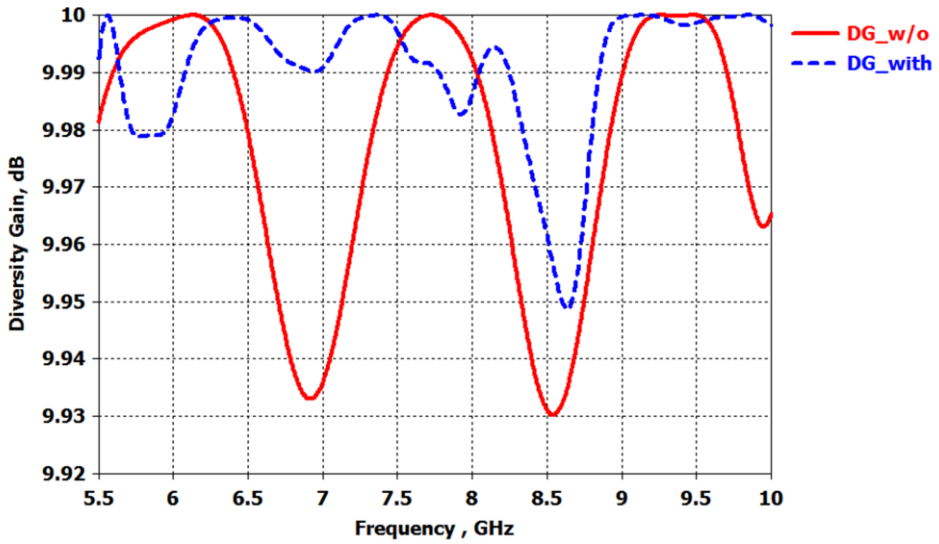

Figure 4.69 DG of MSAs without and with MTM structure.

4.4.3.4 VSWR

The simulated VSWR of the antenna with and without MTM structure is shown in Figure 4.70. As a comparison, the MIMO antenna without MTM structure at resonant frequency (6.25 and 9.25) GHz with the VSWR less than 2. For the proposed antenna with MTM structure. The two bandwidths for the VSWR below 2 are 5.78-6.74 and 8.85–9.65 GHz.

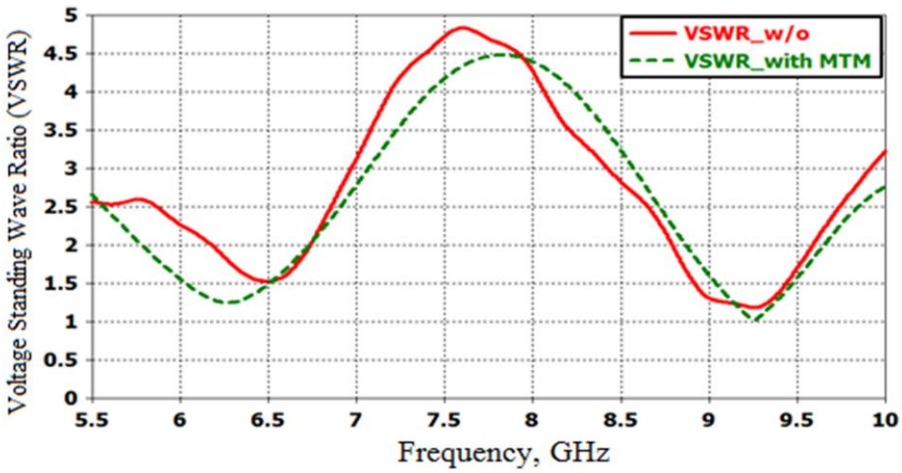

Figure 4.70 Simulated VSWR of the antennas with and without MTM structure

4.5 Mutual Coupling Reduction of MIMO Array Using Periodic T-Shaped DGS Structure

This section presented the design of a two-element microstrip MIMO array with PDGS to mitigate the mutual coupling between the two array elements at 3.3 GHz using coaxial probe feed technique. Three periodically T- Shaped DGS are etched in the ground plane in the middle of the two elements in the array to impede the propagation of surface waves between them.

The distance from edge to edge of two patches is 16 mm. The analysis of the ECC, DG, and total efficiency is presented to validate the performance of MIMO system. The MIMO system obtained an isolation about 28 dB and ECC of less than 0.003 with the frequency band. Good compatibility exists between the simulated and the experimental results.

4.5.1 Microstrip MIMO Antenna

The antenna system formed from two radiating rectangular patches printed on a common FR4 substrate, a dielectric constant of 4.3, a dielectric loss tangent 0.025, of thickness 1.6 mm and size of 72×44 mm^2, whereas the space in the middle of them was optimized to 16mm as depicted in Figure 4.71 (a). The fabricated antenna is shown in Figure 4.71 (b). The antenna system using coaxial probe feed technique. The feed position is optimized so as to obtain the best impedance matching at the resonant frequency which is then connected to a 50 Ω SMA connector. Figure 4.72 shows the measured and simulated scattering parameters (S_{11} and S_{21}) of the microstrip MIMO antenna. From the displayed simulated results, it is evident that the MIMO system is operating at 3.3 GHz at which the S_{11} reach to 30 dB. On the other hand, it is observed that the isolation S_{21} is about 16 dB at the operating frequency. From the experimental results, can note that the S_{11} almost 42 dB and S_{21} is 15 dB. Good compatibility is achieved between the simulated and the experimented results.

The total electric field inside the substrate is illustrated in Figure 4.73 (a). It is obvious that the electric field of the 1st antenna element can cross the 2nd antenna element which enhances the mutual coupling between them. Additionally, Figure 4.73 (b) shows that the surface current between the two antennas is at the high level. Consequently, the DGS filter which that will demonstrate in the following section is designed to offer a stop band at 3.3 GHz which is the desired antenna resonant

frequency. Accordingly, mutual coupling between the two antennas is expected to be suppressed.

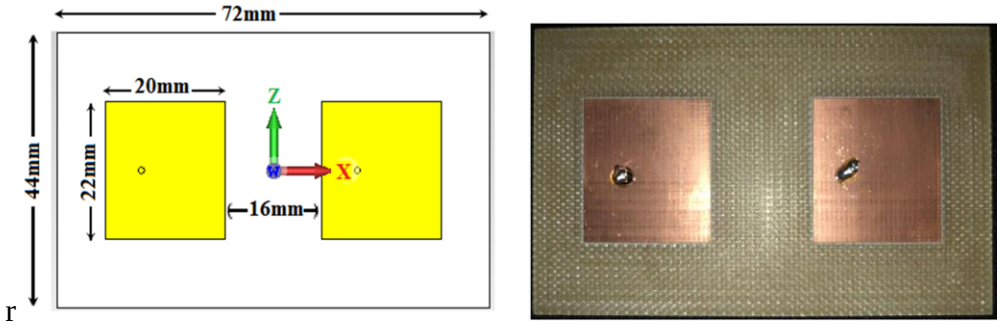

a b

Figure 4.71 (a) The microstrip MIMO array.
(b) Picture of the fabricated MIMO array.

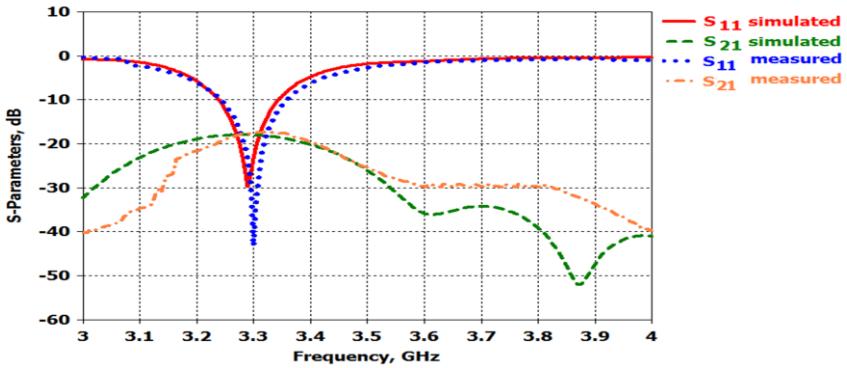

Figure 4.72 S-parameter of the simulated and the experimented results the MIMO system.

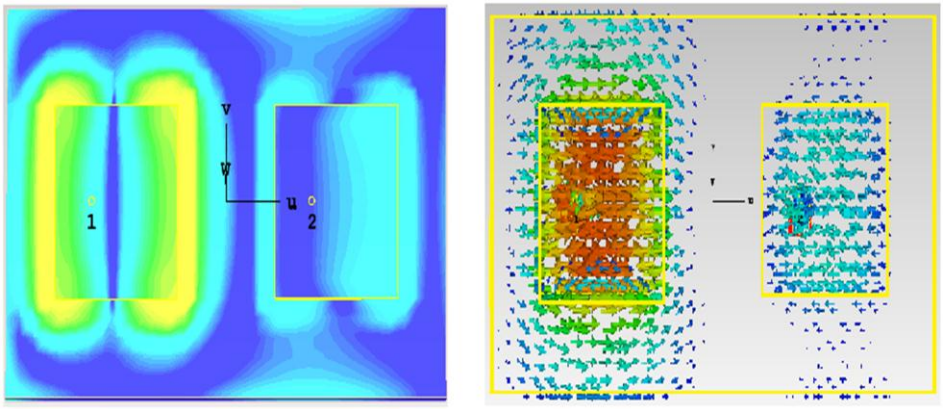

a b

Figure 4.73 (a)Total electric field inside the substrate.
(b) Surface current distrbution.

4.5.2 T-Shaped DGS Resonator

T-Shaped DGS resonator etched on the ground plane excited by 50 Ω microstrip transmission line as shown in Figure 4.74. The DGS was designed by using T-

Shaped on substrate FR4, a dielectric constant of 4.3, a dielectric loss tangent 0.025, and thickness 1.6 mm. All other dimensions are given in Table 4.4 The equivalent circuit model for this DGS is the LC tank circuit shown in Figure 4.75. The Simulated S-Parameters response of the DGS is shown in Figure 4.76. There is an attenuation pole near 3.3 GHz in the field simulation result. For verifying the Double-Negative properties of the proposed MTM-DGS, NRW technique [8] has been used for obtaining the values of μ and ε as shown in Figure 4.77.

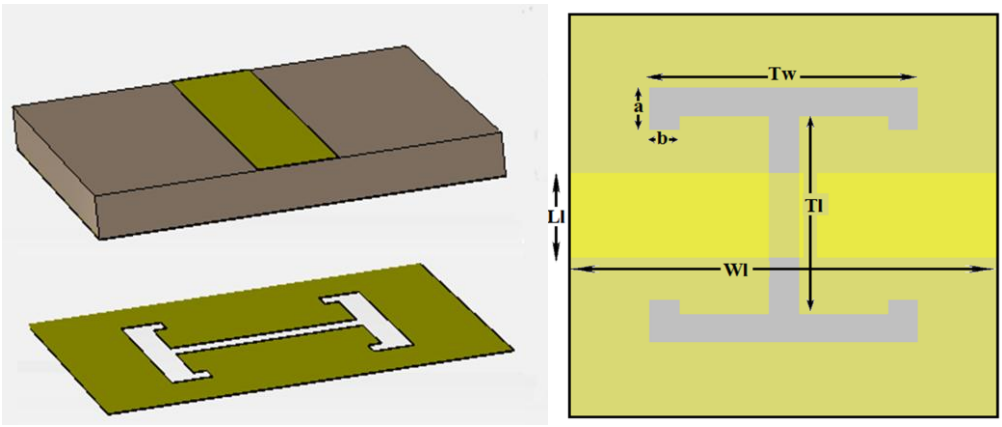

a b

Figure 4.74 (a) 3D view of the T-Shaped DGS resonator. (b)front view

Table 4.4. Dimensions of T-Shaped DGS

Parameter	W1	L1	Tw	Tl	a	b
Dimension (mm)	15	3	9	7	1.5	1

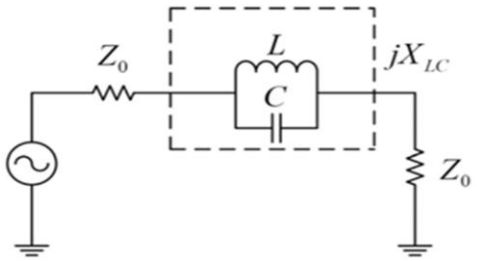

Figure 4.75 LC equivalent circuit, where the dotted box shows the DGS. Section.

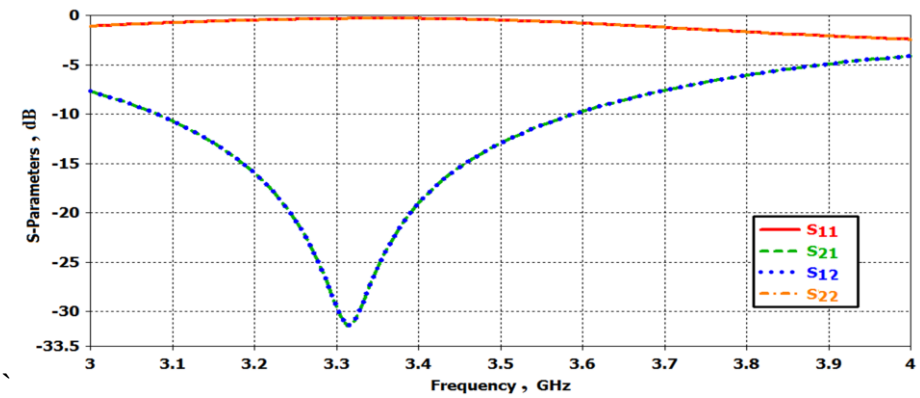

Figure 4.76 S-Parameter for the T-shaped DGS Section.

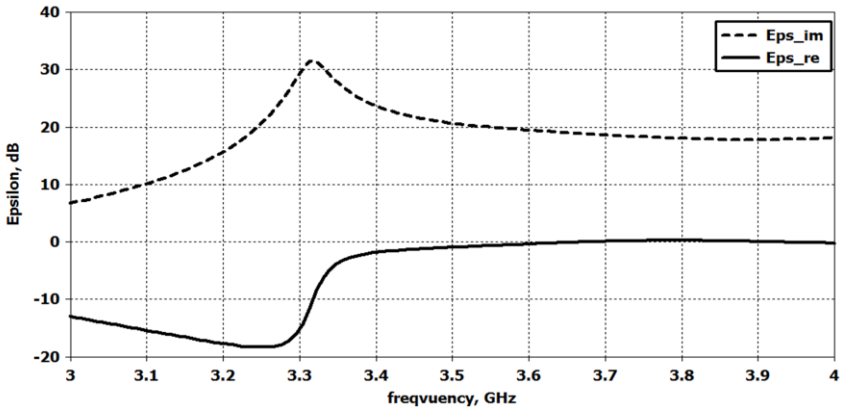

a

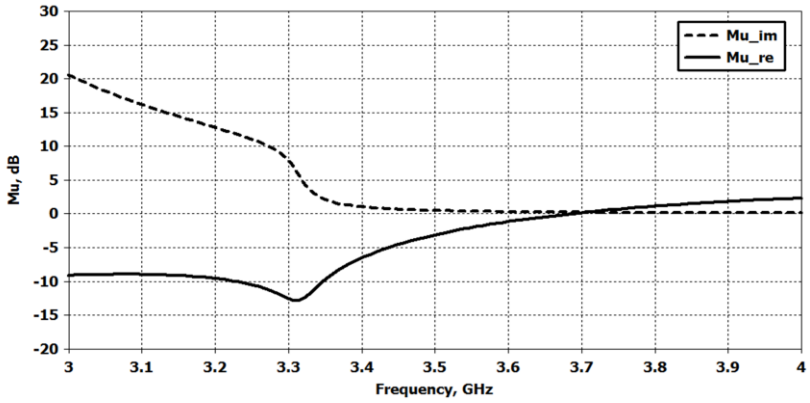

b

Figure 4.77 (a) effective permittivity, (b) effective permeability

4.5.3 Prop

The microstrip patch antenna arrays are suffering from low performance because of the high mutual coupling that it caused by surface waves. Due to the ability of DGS to disturb the shield current distribution in the ground plane of microstrip patch antenna which in turn leads to suppressing the mutual coupling impact. To achieve maximum coupling reductions, a three periodic T-shaped DGSs has been optimized, etched on the ground plane and sandwiched in the middle of the two antenna elements. Also, the optimal values for both distances S1 and S2 are set to 3.623 and 0.5 mm respectively to get the best results, as shown in Figure 4.78. For verifying the validity of the design, hardware has been fabricated on the PCB as demonstrated in Figure 4.79. The antenna parameters like S_{11} and S_{21} are measured by the N5234A network analyzer (the setup and calibration details were mentioned in section 4.2.1). Figure 4.80 depicts the setup which is used for antenna parameters measurement. The measured and simulated S-Parameters of the proposed MIMO system are shown in Figure 4.81. From the simulated results, it can see that the resonant frequency of the MIMO system is marginally shifted from 3.3 to 3.335 GHz. The reason for this

deviation was due to the existence the DGS structure which affects the current distribution in the ground plane, which can influence the antenna electrical length and consequently the resonance frequency. On the other hand, the mutual coupling S_{21} is decreased from 18 to 30 dB during the DGS structure is employed. Besides, the measured results show that the prototype MIMO system operates at 3.34 GHz, approximately, with almost S_{11} is 22 dB and S_{21} around 70 dB. Figure 4.82 illustrated the visualization surface wave distribution with the presence the T-shaped DGS. It is obvious that the DGS blocks most of the field from crossing to the 2^{nd} antenna element, which indicates that the mutual coupling of the MIMO system is reduced. In another word, the T-shaped DGS contribute to mitigating the surface waves propagating on the air-dielectric interface. The space waves, which is one of the important sources for enhanced coupling, are also mitigated by the T-shaped DGS, as they catch and transform the space waves to the surface current. To verify the diversity performance of the MIMO antenna, ECC, DG and the total efficiency have been calculated. A comparison of the ECC of the MIMO system with and without DGS is shown in Figure 4.83. It is evident that the ECC of the MIMO antenna less than 0.1 without and with DGS, while the ECC of the proposed MIMO antenna less than 0.02 within frequency band. Figure 4.84 illustrates the DG of the MIMO antenna with and without DGS. It is obvious that the DG of the MIMO system with DGS is best of without it. The DG of the MIMO system with DGS reaches around 9.99 dB within the frequency band.

The next diversity parameter is total efficiency. For the proposed MIMO system the total efficiency with and without TDGS is plotted in Figure 4.85. It is obvious that the total efficiency increases within the operating frequency band of the MIMO antenna with the proposed TDGS structure.

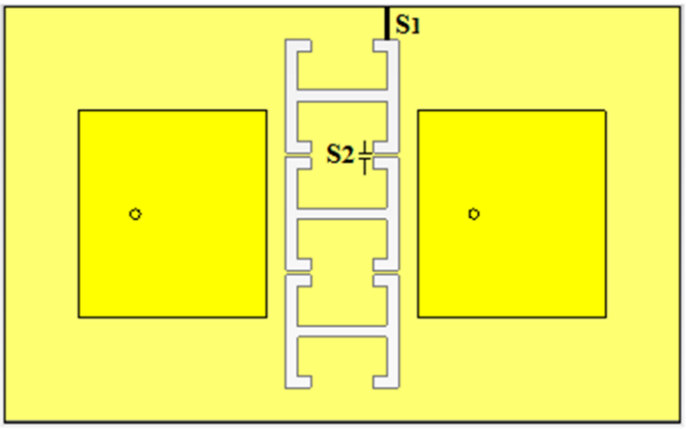

Figure 6.78 Back view of the proposed MIMO system with T-shaped DGS

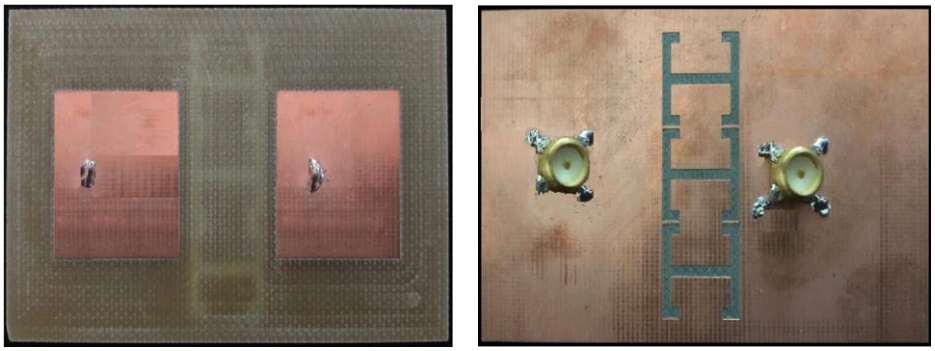

a b

Figure 6.79 A photograph of the fabricated MIMO system.
(a) front view (b) back view

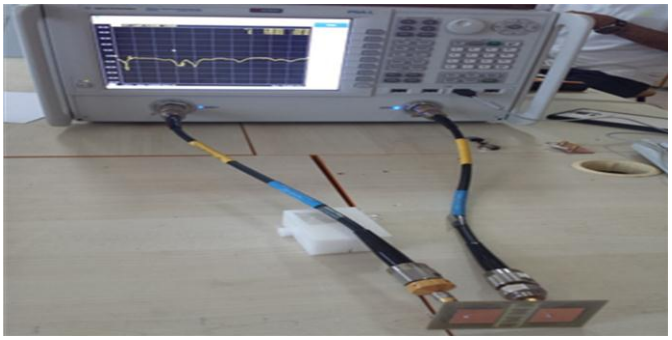

Figure 4.80 Setup for measurement of antenna parameters

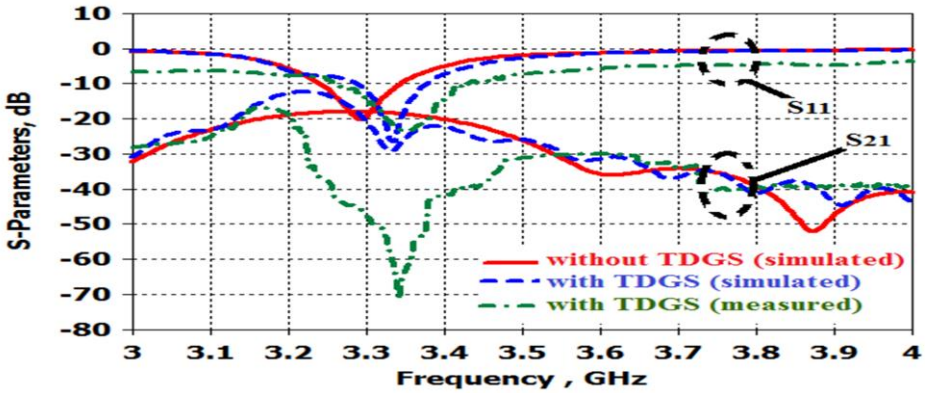

Figure 4.81 S-Parameter of the simulated and the experimented results of the proposed MIMO system.

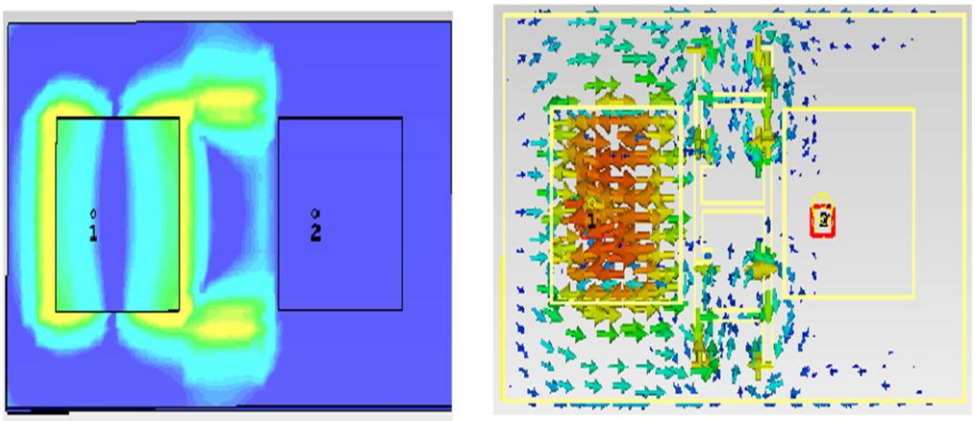

a b

Figure 4.82 (a) Total electric field inside the substrate.
(b) Surface current distrbution

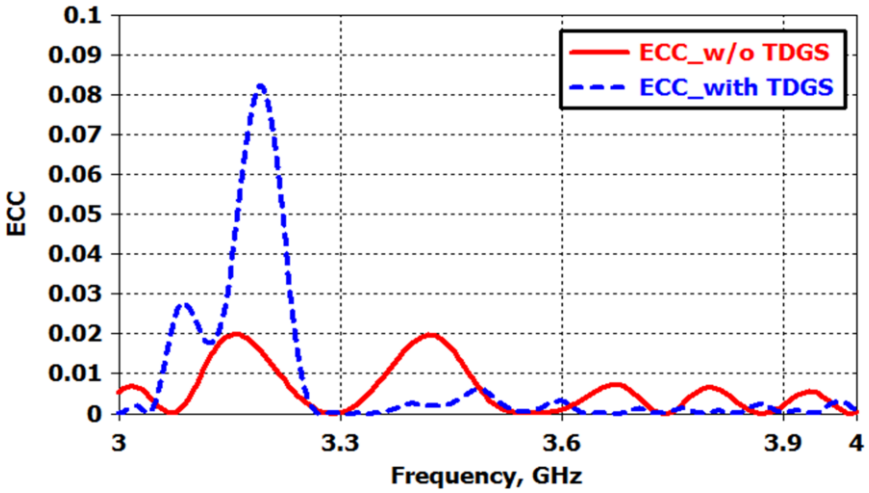

Figure 4.83 ECC of the MIMO antenna with and without TDGS.

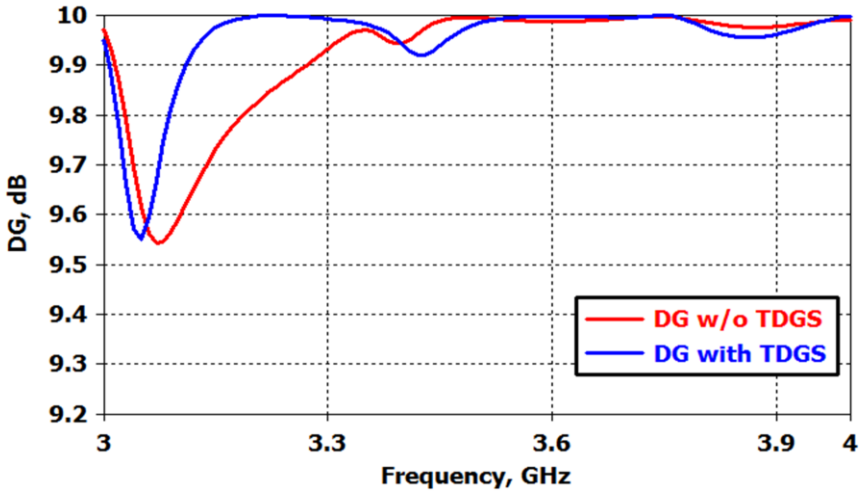

Figure 4.84 DG of the MIMO antenna with and without TDGS

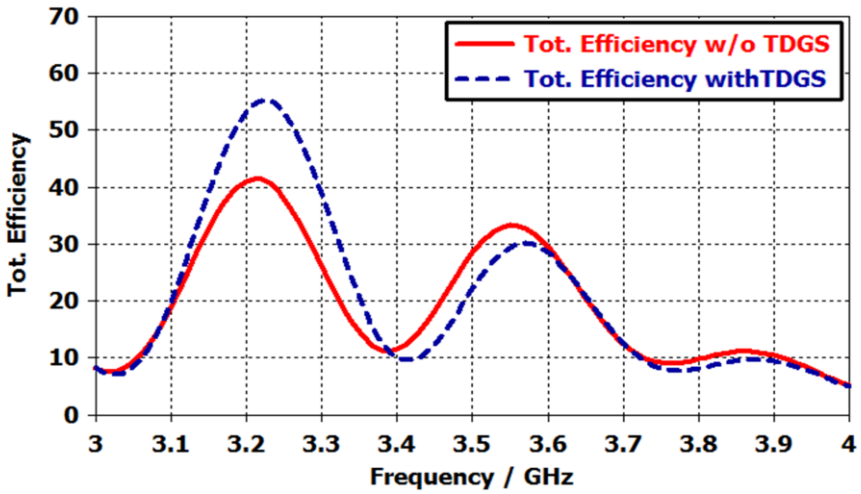

Figure 4.85 Simulated total efficiency of whole antenna system with and without TDGS section

CHAPTER FIVE

CONCLUSIONS AND SCOPE FOR IMPROVEMENT

5.1 Conclusions

This dissertation introduced design and analysis of five different geometrical configurations of microstrip MIMO arrays based on various decoupling structures, to obtain high-performance microstrip antenna arrays better than the conventional systems. Fabrication of the prototypes were made to verify the simulation results.

In the first design, a two E-shaped antenna MIMO system suitable for WLAN and WiMAX applications is proposed. The coupling reduction has been achieved by printing a 2x3 MTM-CSR matrix in the middle of array elements. This MIMO antenna system resonates at 6.3 GHz with an impedance bandwidth of 34.42% in the range of frequencies from 5.5–7 GHz. The isolation of MIMO antennas with EBG structures is shown to improve about 12 dB, whereas it is improved in orthogonal arrangement around 6 dB and maintaining the overall mutual coupling less than −20 dB in the operating band.

In the second design, a novel conducting wall isolation structure to suppress the mutual coupling between closely spaced MSAs is presented. The developed antenna system resonates at 4.45 or 10.3 GHz depending on the dimensions of LSCW structure that used. The analysis of the ECC and DG are presented to evaluate the diversity performance of the MIMO antenna. A prototype has been fabricated and assessed to attest the authenticity of the proposed structure; this prototype achieved the high isolation of about 50 dB between two MSAs at 5.2 GHz and 40 dB at 10.3 GHz and maintaining the overall mutual coupling less than −20 dB in the operating band. The proposed LSCW decoupling structure can be used in various microstrip array applications, including the MIMO systems and it can be used in many wireless applications in C or X band.

In the third design, the mutual coupling suppression of a printed monopole array by employing compact SDGS has been presented. To verify the validity of the proposed monopole array with the SDGS structure, a prototype has been fabricated and measured. This prototype obtained enhancement the isolation of about 50 dB in the middle of two MIMO antenna around 5.2 GHz and reduction the overall mutual coupling less than −20 dB in the operating band. Good compatible has been accomplished in the middle of the circuit simulation and empirical results. With the etching SDGS in extending ground plane, the mutual coupling of the monopole array has been suppressed efficiently at the resonant frequency. The analysis of the ECC and DG are presented to evaluate the diversity performance of the MIMO antenna. Enhanced the isolation between the two ports, makes the array appropriate for applications in MIMO wireless communication systems in C band.

In the fourth design, a dual-band planar compact monopole antenna array with a novel metamaterial structure is presented. Because of its unique design as compared to previous MTM structures, when the proposed MTM structure has been sandwiched in the middle of the two monopoles, it eliminates the effect of two significant coupling sources which are the space wave and the near-field coupling. The proposed MIMO system can provide dual-band operation in the middle of the ranges 6.2-6.727 and 8.85–9.57 GHz at 6.5/9.25 GHz. The measured results show that the isolation in the middle of the antenna ports has been enhancement about 40 dB and 19 dB respectively at the two operating frequencies with the presence of the proposed MTM structure.

In fifth design, suppression of mutual coupling is achieved by using T-shaped DGS structure. The MIMO antenna is designed to work at frequency 3.3 GHz for WiMAX application. The separation in the middle of the edges of the two elements has been achieved to be only 16 mm (0145 λ_o). The analysis of the ECC and DG are presented to evaluate the diversity performance of the MIMO system. Besides, it has also been verified that the T-shaped DGS structure satisfies DN feature within the operating frequency band. The measured results are introduced to evident the enhancement in isolation between MIMO antenna ports about 70 dB, and ECC equals 0.000048 at 3.34 GHz. Good compatibility has been achieved between the simulated and the experimental results.

5.2 Suggestion for Future Work

Finally, the following topics are useful for additional investigation:

- In this dissertation, different configurations of 1×2 array have been used. This work can be extended to more number of antenna element array such as four-element MIMO array for increased channel capacity in high data-rate applications.

- The designs can be more improved in terms of fundamental parameters such as type of substrate, dielectric constant, and the thickness of the substrate.
- In future also, as per requirement, many new antenna shapes can replace the conventional shapes. There are many shapes in the field of microstrip patch antenna. A design of slots on the patch element and making defected structure in the ground plane for improving the bandwidth as well as achieving the multiband operation.

RFERENCES

[1] Fang, G. D. (2010). Antenna theory and microstrip antennas. U.S.A: Taylor and Francis Group, LLC,

[2] Deschamps, G. (1953). Microstrip Microwave Antennas. The Third Symposium on The USAF Antenna Research and Development Program University of Illinois, Monticello Illinois. 18-22.

[3] Garg, R, Bhartia, P, bahl, I. and Ittipiboon, A. (2001). Microsrtip Antenna Design Handbook, London: Atrech House.

[4] Balanis, C. A. (2005). Antenna Theory Analysis and Design. 3rd Edition . New Jersey: A John Wiley & Sons, INC.

[5] Kumar , G, Ray, K. P. (2003). Broadband Microstrip Antennas. Boston . London: Artech House, INC.

[6] Carver, K, R, Mink, J, W. (1981). Microstrip Antenna Technology. *IEEE Transactions on Antennm as and Propagation,* **29**.2-24.

[7] Bharati, M. (2015). Effect on Efficiency Due to Variation of Patch Height of Rectangular Microstrip Patch Antenna. *IJAREEIE*, **4**.

[8] Gupta, K, T. (2009). Copper Interconnect Technology, chapter 2, Springer Science and Business Media.

[9] Mane, P, Patil, S, A, and Dhanawade, P, C, (2014). Comparative Study of Microstrip Antenna for Different Subsrtate Material at Different Frequencies. *International Journal of Emerging Engineering Research and Technology.* **2**.

[10] Elliott, S, R. (2003). Antenna Theory and Design. John Wiley & Sons. Inc,

[11] Bouras, C, J. (2006). Trends in Telecommunications Technologies. China: InTech.

[12] Kuhn, V. (2006). Wireless Communications over MIMO Channels. Germany: John Wiley & Sons Ltd.

[13] Sharawi, M, S. (2013). Printed Multi-Band MIMO Antenna Systems and Their Performance Metrics. *IEEE Antennas and Propagation Magazine.* **5.**

[14] Craeye, C., and González-Ovejero, D. (2011). A review on array mutual coupling analysis. Radio Sci. **46**, RS2012, doi:10.1029/2010RS004518.

[15] LUi, H, S, HUi, H, T, Leong, M, S. (2009). A Note on the Mutual-Coupling Problems in Transmitting and Receiving Antenna Arrays. *IEEE Antennas and Propagation Magazine,* **51**.

[16] Hui, H, T, Bialkowski, M, E. Lui, H, S. (2010). Mutual Coupling in Antenna Arrays. *Hindawi Publishing Corporation, International Journal of Antennas and Propagation.*

[17] Najamn, A, I, Duroc,Y, Leao J, F. (2009). A Novel Co-located Antennas System for UWB-MIMO Applications. *IEEE, Conference Location: San Diego.*

[18] Li, Z, Du, Z, Takahashi, M, Saito K. (2012). Reducing Mutual Coupling of MIMO Antennas With Parasitic Elements for Mobile Terminals. *Antennas and Propagation,IEEE Transactions*.**60**.

[19] Chi, G, Binhong, L, Qi, D. (2005). Dual band printed diversity antenna for 2.4/5.2 GHz WLAN applications,. *Microw.Opt.Technol.Lett,* **45**

[20] Indumathi, S. (2017). Isolation improvement of MIMO antenna for wideband applications. *IEEE. International Conference on Intelligent Computing and Control Systems. Conference paper. Madurai. India.*

[21] Zarrabi, R, B, Mansouri, Z. (2015). Investigation of EBG array performance on decreasing the mutual coupling and improve shield factor. *Journal of Electrical Systems and Information Technology.* **2** . 184–196.

[22] Kamiya, J, Shirota, K, Yagi, T, Nakazawa,T. (2012). Study of EBG Structures using Metamaterial Technology. *OKI Technical Review*.**79**.

[23] Li, Q, Feresidis, A, P, Mavridou, M, A. Hall, P, S. (2015). Miniaturized Double-Layer EBG Structures for Broadband Mutual Coupling Reduction Between UWB Monopoles. *IEEE Antennas and Propagation.* **63**.

[24] Tu, D, T, Hov, N, V, Son P, D, Yem, V, V. (2017). Design and Implementation of Dual-Band MIMO Antenna with Low Mutual Coupling using Electromagnetic Band Gap Structures for Portable Equipments. *International Journal of Engineering and Technology Innovation.***7**. 48 – 60.

[25] Toolabi, M, Sadeghzadeh, R, A, Moghadasi, M, N. (2016). Compact Meandered-Shape Electromagnetic Bandgap Structure Using in a Microstrip Array Antenna Application. *Microwave and Optical Technology Letters.* **58** .

[26] Arya, A, K, Kartikeyan, M, V, Patnaik, A. (2010). Defected Ground Structure in the perspective of Microstrip Antennas:A Review. *Frequenz.*

[27] Zulki, F, Y, Rahardjo, E, T. (2011). Compact MIMO Microstrip Antenna with Defected Ground for Mutual Coupling Suppression. *Progress In Electromagnetics Research Symposium Proceedings. Marrakesh. Morocco.*

[28] Wei, K, Li, J. Wang, L, Xing, Z, Xu, R. (2016). S-shaped periodic defected ground structures to reduce microstrip antenna array mutual coupling. *Electronics Letters,* **52**. 1288–122.

[29] Yu,Y, Yi, L, Liu, X, Gu, Z. (2016). Mutual Coupling Reduction of Dual-Frequency Patch Antenna Arrays. *ACES Journal.* **31**.

[30] Wei, K, Li, J, Y, Wang, L. (2016). Mutual Coupling Reduction by Novel Fractal Defected Ground Structure Bandgap Filter. *IEEE Transactions on Antennas and Propagation.* **64**.

[31] Chaires, J, Schumerth, D, Drawdy, C, Yang, W. (2015). Gain Incorporated Split-Ring Resonator Structures for Active Metamaterials. *Advances in OptoElectronics.* Article ID 247630.

[32] Lee,Y, Chung, H, Choi, J. (2010). Improving the Isolation of MIMO Antennas Using Split Ring Resonators. *Journal of The Korean Institute of Electromagnetic Engineering and Science*.**10.**

[33] Shafique, M, F, Riaz, L, Qamar, Z, Saleem, R, Khan, S, A. (2015). Coupling Suppression In Densely Packed Microstrip Arrays Using Metamaterial Structure. *Microwave and Optical Technology Letters.***57**.

[34] Alsultan, R, G, Yetkin, G. Ö. (2018). Mutual Coupling Reduction of E-Shaped MIMO Antenna with Matrix of C-Shaped Resonators. *International Journal of Antennas and Propagation,*. Article ID 4814176.

[35] Srivastava, D, K, Vihwvakarma, B, R, Saraswat, R, C. (2007). Investigation of Effect of Substrate Thickness and Permittivity of Rectangular Microstrip Antenna for Bandwidth Enhancement. *IET-UK International Conference on Information and Communication Technology in Electrical Sciences.* 970-973.

[36] Rayno, J, T, Sharma, S, K. (2012). Effect of Substrate Thickness on the Performance of a a Printed Planar Monopole Antenna (PMA). *IEEE. Antennas and Propagation Society International Symposium (APSURSI).*

[37] Balanis, C, A, Panayiotis, I, I. (2007). Introduction to smart antennas. United States: Morgan & Claypool Publishers.

[38] Zelst, A, V. (2003). Physical Interpretation of MIMO Transmissions. *In Proc. of the 10th Proceedings Symposium IEEE Benelux Chapter on Communications and Vehicular Technology in Benelux.*

[39] Diallo, A, Thuc, P, L. Luxey, C, Staraj, R. (2006). Enhanced diversity antennas for UMTS handsets. In *Proceedings of 1st European Conf. Antennas and Propagation*.

[40] Abelairas, J, P, Martín F. M. Techniques to reduce the Mutual Coupling and to improve the Isolation between antennas in a Diversity System, Aalborg University, 2009.

[41] Ganatsos,T, Siakavara, K, Sahalos, J, N. (2009). Mean Effective Gain Enhancement of Antenna Systems with EBG Ground Plane. *Proc. of the 3rd European Conference on Antennas and Propagation.* 3567-3571.

[42] Najam, A, I, Duroc, Y, Tedjini, S. (2012). Ultra Wideband - Current Status and Future Trends. InTech. ch.10.

[43] Douglas, M, G, Okoniewski, M, (1998). A Planar Diversity Antenna for Handheld PCS Devices. *IEEE Transactions on Vehicular Technology*. **47**.

[44] Mnati, M, J. (2013). Design and Performance Antenna Diversity for MIMO WiMAX Mobile Terminals. *International Journal of Soft Computing and Engineering (IJSCE).* **3.**

[45] LUi, H, S, Hui, H. T. and Leong, M, S. (2009). A Note on the Mutual-Coupling Problems in Transmitting and Receiving Antenna Arrays. *IEEE Antennas and Propagation Magazine,* **51**.

[46] Christina , A. Malathi, J, Thiripurasundari, D. (2016). Review on Isolation Techniques in MIMO Antenna Systems. *Indian Journal of Science and Technology.*

[47] Nikolic, M, Djordjevic, A, Neorai, A. (2005). Microstrip antennas with suppressed radiation in horizontal directions and reduced coupling. *IEEE Transaction on Antennas and Propagation.* **52**. 3469–3476.

[48] Qamar, Z, Park, H, C. (2014). Compact Waveguided Metamaterials for Suppression of Mutual Coupling in Microstrip Array, *Progress In Electromagnetics Research,* **149**. 183–19.

[49] Shalaev,V. (2007). Optical negative index metamaterials. Nature Photonics.

pp.41-48.

[50] Rui Yang, Yongjun Xie, Yang, X, and Wang, R. (2009). Fundamental modal properties of SRR metamaterials and metamaterial based waveguiding structures. *Optical Society of America*.**17**. 6101-6117

[51] Frasch, E, J, Rothwell, J, L, Ellison, S, M,. Chahal, P, and Ouedraogo, R, O. (2016). Analysis of the Nicolson-Ross-Weir Method for Characterizing the Electromagnetic Properties of Engineered Materials. *Progress In Electromagnetics Research*. **157**. 31–47.

[52] Kovács, P. (2010). Design and Optimization of Electromagnetic Band Gap Structures. Czech: Brno University of Technology.

[53] Bait-Suwailam, M, M, Siddiqui, O, F, Ramahi O, M. (2010). Mutual coupling reduction between microstrip patch antennas using slotted-complementary split-ring resonators. IEEE Antennas and Wireless Propagation Letters. **9**. 876–878.

[54] Hou, B, D, Xiao, S, Wang, B, Z, Jiang, L, Jiang, J. (2009). Elimination of scan blindness with compact defected ground structures in microstrip phased array. *IET Microwaves, Antennas and Propagation*. **3**. 269–275.

Vita

PERSONAL INFORMATION

Name and Surname: Raghad Ghalib AlSULTAN

Nationality: Iraq

Birthplace and date: 06-03-1974

Marital status: married

Phone number: 05398439981

Fax:

Email: raghad_ghalib2011@yahoo.com

EDUCATION

	Graduate school	**Year**
Master	University of Mousl/ Electrical Engineering	2004
Bachelor	University of Mousl	1997
High School	Khadija Al Kubra High School	1992

Work experience

	Place	**Enrollment**
2006-Present	Technical Institute-Mosul Electronic Department	Assistant teacher
2005-1998	Ministry of Health Engineering Workshop	Maintenance Engineer

PUBLICATIONS

Mutual Coupling Reduction of E-Shaped MIMO Antenna with Matrix of C-Shaped Resonators

FOREIGN LANGUAGE: Arabic, English and Little Turkish